

Mette Rostad
Ida Emilie Uglem Skoglund

Impact of Shared Battery Energy Storage Systems on Total System Costs and Utilisation of Locally Produced Energy in Commercial Buildings

Master's thesis in Energy and Environmental Engineering

Supervisor: Gro Klæboe

Co-supervisor: Kasper Emil Thorvaldsen

June 2021

Mette Rostad
Ida Emilie Uglem Skoglund

Impact of Shared Battery Energy Storage Systems on Total System Costs and Utilisation of Locally Produced Energy in Commercial Buildings

Master's thesis in Energy and Environmental Engineering
Supervisor: Gro Klæboe
Co-supervisor: Kasper Emil Thorvaldsen
June 2021

Norwegian University of Science and Technology
Faculty of Information Technology and Electrical Engineering
Department of Electric Power Engineering



Abstract

The demand for electrical power and the share of distributed renewable energy production is increasing. These changes are straining the grid by causing a demand for higher grid capacities, which in turn requires costly grid investments. As a response to this issue, the interest in local energy communities with shared battery energy storage systems is increasing. With shared storage, the community power peak can be reduced, relieving the stress on the external grid. However, the realisation of local energy communities is facing a variety of regulatory barriers.

This thesis seeks to investigate the benefit of shared battery energy storage systems for community peak shaving, cost reduction and self-consumption of locally produced energy for commercial buildings. The optimal scheduling of the battery is solved with a two-stage stochastic linear programme implemented with a receding horizon optimisation approach that considers monthly measured peak tariffs. The optimisation model is applied to a Norwegian case study with six different configurations for battery allocation within a local energy community. The case study includes configurations with both joint and individual metering. The model is tested for three different months; January, March and June.

As it is the only configuration with direct incentives for community peak reduction, the shared battery energy storage system with joint metering outperforms all other configurations. The community power peak was reduced by 7-11% and the total system costs by 10-20%, depending on the season. Shared storage within a local energy market where the participants are metered individually is revealed to perform almost equally well. The community power peak was reduced by 2-8%, and total costs were reduced by 6-17%. The self-consumption was increased by an additional 45-46% in June for all configurations that included a shared battery energy storage system.

The main results show that there is a significant community benefit for shared battery energy storage systems considering peak shaving, self-consumption and monetary savings. Although shared storage with joint metering faces regulatory limitations, shared storage within local energy communities with individual metering proves to be a good alternative. It is therefore concluded that adaptation of current regulations to local energy communities with shared battery energy storage systems should be considered.

Sammendrag

Forbruket av elektrisk kraft og mengden distribuert produksjon av fornybar energi øker. Disse endringene fører til et behov for økt overføringskapasitet i kraftnettet, noe som igjen krever kostbare nettinvesteringer. Med bakgrunn i denne problemstillingen øker interessen for lokale energisamfunn med felles batterilagringsystemer. Med felles batterilagringsystemer kan den totale effekttoppen til energisamfunnet reduseres og dermed avlaste det eksterne distribusjonsnettet. Realiseringen av lokale energisamfunn står imidlertid overfor en rekke regulatoriske barrierer.

Denne oppgaven undersøker hvorvidt felles batterilagringsystemer for kommersielle bygninger kan bidra til å redusere effekttopper og totale kostnader, samt øke forbruket av lokalt produsert energi. En stokastisk to-steps modell kombinert med en receding horizon optimeringsmetode har blitt utviklet for å optimalisere driften av batteriet. Modellen har blitt brukt i en case-studie som tar for seg seks ulike konfigurasjoner for plassering av et felles batteri innen et lokalt energisamfunn i Norge. Studien baserer seg på bruk av månedlige effekttariffer og inkluderer konfigurasjoner med både felles og individuell måling av byggene. Modellen ble testet for både januar, mars og juni.

Ettersom det er den eneste konfigurasjonen med direkte insentiver for reduksjon av totale effekttopper, gir felles batterilagringsystemer med felles måling for alle bygg klart best resultater. Den totale effekttoppen ble redusert med 7-11 % og de totale kostnadene ble redusert med 10-20 %, avhengig av sesong. Felles batterilagringsystemer i et lokalt energimarked hvor deltakerne måles individuelt, viser også svært lovende resultater. Den totale effekttoppen ble redusert med 2-8 %, og de totale kostnadene med 6-17 %. Forbruket av lokalt produsert energi ble i juni økt med ytterligere 45-46 % for alle konfigurasjoner som inkluderte et delt batterilagringsystem.

Hovedresultatene viser at felles batterilagringsystemer kan bidra betydelig til kostnadsreduksjoner, reduksjon av effekttopper og økt forbruk av lokalt produsert energi. Til tross for at mulighetene for felles batterilagringsystemer med felles måling begrenses av nåværende reguleringer, viser det seg at tilsvarende systemer med individuell måling er et godt alternativ. Dermed konkluderes det med at tilpasning av nåværende reguleringer til lokale energisamfunn med felles batterilagringsystemer bør tas opp til vurdering.

Preface

This master's thesis marks our final project as part of the Master of Science degree (MSc) in Energy Systems Planning at the Norwegian University of Science and Technology, Department of Electric Power Engineering. This thesis is written in cooperation with TrønderEnergi AS in relation to their ongoing work on the +CityxChange project.

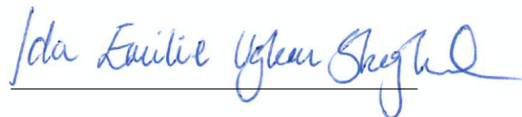
We would like to extend our deepest gratitude towards our supervisor Gro Klæboe for her guidance, support, drive, effort and for always sharing her knowledge. We would also like to give great thanks to our co-supervisor Kasper Emil Thorvaldsen, for his enthusiasm and expertise. Thanks to you did we not only manage to write our master's thesis, but a scientific paper on the same topic as well. The interested reader is referred to Appendix J.

Additionally, we would like to thank our friends for always contributing to a fun and inclusive community, making our 5 years at NTNU unforgettable. Last but not least, we would like to thank each other for a supporting and exceptional partnership.

Trondheim, June 2021



Mette Rostad



Ida Emilie Uglem Skoglund

Abbreviations

BESS	Battery Energy Storage System
BTM	Behind the Meter
DER	Distributed Energy Resources
DSO	Distribution System Operator
LEC	Local Energy Community
LP	Linear Programme
MP	Measured Peak
NVE	The Norwegian Water Resources and Energy Directorate
PV	Photovoltaic
RH	Receding Horizon
RHO	Receding Horizon Optimisation
RMSE	Root Mean Square Error
s-BESS	Shared Battery Energy Storage System
ToU	Time-of-use

Nomenclature

Sets

- S: Set of all possible scenarios
 B: Set of buildings in the community
 H: Set of remaining hours of the month
 H_1 : Subset of H containing all hours in the first stage/prediction horizon of the stochastic problem
 H_2 : Subset of H containing all hours in the second stage stochastic problem

Indices

- s: A scenario s in set S
 h: An hour h in set H
 l: The first hour in set H
 f: The final hour in set H
 b: A building in set B
 k: The building in set B operating an individual battery

Deterministic parameters

- C_h^E : The energy spot price in hour h paid to the power retailer [NOK/kWh]
 C^P : The peak power price paid to the DSO [NOK/kWh/h]
 C^V : The volumetric costs paid to the DSO [NOK/kWh]
 C^F : The fixed cost paid to the DSO [NOK/month]

- E^{max} : Maximum energy storage capacity of the battery
 K^{max} : Maximum charge and discharge capacity of the battery
 η^{cha} : Charging efficiency of the battery
 η^{dch} : Discharging efficiency of the battery
 S_0 : Initial stored energy in the battery before the first hour in the analysis period
 S_f : Stored energy in the battery at the final hour of the analysis period
 π_s : The probability of scenario s
 $R_{h,b}^{prod}$: The real production in hour h by building b revealed in the first stage/prediction horizon
 $R_{h,b}^{cons}$: The real consumption in hour h for building b revealed in the first stage problem/prediction horizon
 P^{sys} : The highest power peak for the total system stored from past iterations of the receding horizon algorithm
 $P_b^{building}$: The highest power peak for building b stored from past iterations of receding horizon algorithm
 $P^{battery}$: The highest power peak for the battery stored from past iterations of the receding horizon algorithm

Stochastic parameters

$D_{h,b,s}^{cons}$: Consumption in hour h at building b in scenario s in the second stage hours

$D_{h,b,s}^{prod}$: Production for hour h at building b in scenario s in the second stage hours

Decision variables

$p_{h,s}^{Gimp}$: Power imported from grid in hour h for scenario s

$p_{h,s}^{Gexp}$: Power exported to grid in hour h for scenario s

$b_{h,b,s}^{Gimp}$: Power imported from grid to building b in hour h for scenario s

$b_{h,b,s}^{Gexp}$: Power exported to grid from building b in hour h for scenario s

$b_{h,b,s}^{Limp}$: Power imported from local energy market to building b in hour h for scenario s

$b_{h,b,s}^{Lexp}$: Power exported to local energy market from building b in hour h for scenario s

Δp_s^{sys} : The additional power for reaching the predicted maximum peak in scenario s for the remaining hours of the analysis period

$\Delta p_{b,s}^{building}$: The additional power for reaching the predicted maximum peak for building b in scenario s

$\Delta p_s^{battery}$: The additional power for reaching the predicted maximum peak for the battery in scenario s

$e_{h,s}$: The energy stored in the battery in hour h for scenario s

$x_{h,s}^{cha}$: Power consumed by the battery at hour h in scenario s

$x_{h,s}^{dch}$: Power delivered by the battery at hour h in scenario s

$x_{h,s}^{Lcha}$: Power consumed from local energy market for charging the battery in hour h for scenario s

$x_{h,s}^{Ldch}$: Power delivered to the local energy market for discharging the battery in hour h for scenario s

Contents

Abstract	i
Preface	v
Abbreviations	vi
Nomenclature	vii
1 Introduction	1
1.1 Motivation	1
1.2 Objective	2
1.2.1 Approach	2
1.2.2 Contributions	3
1.2.3 Limitations	3
1.3 Structure	4
2 Framework	5
2.1 Batteries	5
2.2 Shared Battery Energy Storage Systems for Commercial Buildings . . .	6
2.3 Local Energy Markets	8
2.4 Regulations for the Norwegian Power System	8

2.4.1	The Norwegian Pricing Model	9
2.4.2	Individual and Joint Metering	10
2.4.3	Local Energy Markets	11
3	Optimisation and scenario modelling	12
3.1	Optimisation Models	12
3.1.1	Stochastic Programming	12
3.1.2	Receding Horizon Optimisation	14
3.2	Time Series Analysis and Forecasting	16
3.2.1	Time Series Analysis	16
3.2.2	Autoregressive Models	18
3.2.3	Scenario Generation	19
3.2.4	Scenario Reduction	20
4	Problem Formulation	21
4.1	Shared Battery Energy Storage System Configurations	21
4.1.1	Configuration 1: All Buildings Behind One Meter	21
4.1.2	Configuration 2: Individual Metering for the Buildings and the Battery	22
4.1.3	Configuration 3: Individual Storage for One Building	23
4.1.4	Configuration 4: Community Owned Battery with Individual Metering	23
4.1.5	Configuration 5: Local Energy Market with Individual Metering for the Battery and Buildings	24
4.1.6	Configuration 6: Local Energy Market with Individual Storage	25
4.2	Receding Horizon Optimisation	25
4.3	Mathematical Problem Formulation	27

4.3.1	Assumptions and Simplifications	27
4.3.2	Mathematical Model	28
4.3.3	Adaptations to the optimisation model for other configurations	32
5	Case Study Specifications	33
5.1	Assumptions and Settings for the Case Study	33
5.2	Background	34
5.2.1	Brattøra	34
5.2.2	Buildings	35
5.2.3	The Battery	36
5.2.4	Energy Price and Grid Tariff Pricing Models	37
5.3	Simulated Cases	38
6	Scenario Modelling	40
6.1	Time Series Analysis for Case Study	40
6.1.1	Introduction of Forecast Variables	40
6.1.2	Auto Regressive Model	41
6.2	Scenario Generation and Reduction	49
6.2.1	Scenario Generation	49
6.2.2	Scenario Reduction	50
6.2.3	Optimising the Amount of Scenarios	50
7	Results and Observations	52
7.1	Battery Scheduling	52
7.2	Peak Shaving	53
7.3	Self-Sufficiency and Self-Consumption	57
7.4	Cost Analysis	58

7.4.1	Total Costs and Savings	58
7.4.2	Cost Contributions	59
7.5	Sensitivity Analysis on MP tariff	60
8	Discussion	62
8.1	Battery Scheduling	62
8.2	Peak Shaving	63
8.3	Self-Sufficiency and Self-Consumption	65
8.4	Costs	66
8.5	Configurations and Regulations	67
9	Concluding Remarks	69
9.1	Further Work	70
	References	71
	Appendices	79
A	Optimisation Model: Configuration 1	80
B	Optimisation Model: Configuration 2	81
C	Optimisation Model: Configuration 3	82
D	Optimisation Model: Configuration 4	83
E	Optimisation Model: Configuration 5	84
F	Optimisation Model: Configuration 6	86
G	Predictions by the Autoregressive Models	87
H	Preliminary Results of Scenario Generation	89
I	Cost Contribution Tables	91
J	Scientific Paper: Impact of shared battery energy storage system on total system costs and power peak reduction in commercial buildings	93

List of Figures

3.1	Illustration of the general structure of scenario trees	14
3.2	Illustration of a receding horizon framework.	15
3.3	Typical autocorrelation and partial autocorrelation plot	17
4.1	Illustration of configuration 1 for battery allocation	22
4.2	Illustration of configuration 2 for battery allocation	22
4.3	Illustration of configuration 3 for battery allocation	23
4.4	Illustration of configuration 4 for battery allocation	24
4.5	Illustration of configuration 5 for battery allocation	24
4.6	Illustration of configuration 6 for battery allocation	25
4.7	Algorithm for the receding horizon approach	26
4.8	The receding horizon optimisation framework	26
5.1	Map of the area (Brattøra) applied for the case study	35
5.2	The spot prices for January, March and June 2020	37
6.1	Presentation of the time series of each forecast variable	41
6.2	Correlation between temperature and the forecast variable at each building	42
6.3	Correlation between solar irradiation and production at BK16($y_{3,t}$) . . .	43
6.4	Autocorrelation and partial autocorrelation plots for the consumption at BK15AB($y_{1,t}$).	44

6.5	Autocorrelation and partial autocorrelation plots for consumption at Sjøgangen($y_{4,t}$).	44
6.6	Weekly seasonal plot of the power consumption at BK15AB in 2019 . . .	45
6.7	Daily seasonal plot of the power consumption at BK15AB in 2019 . . .	45
6.8	Distribution of the prediction error for each forecast variable	48
7.1	The battery energy storage pattern for configuration 1 in March	53
7.2	The battery energy storage pattern for configuration 3.2 in June	53
7.3	BK15AB's import and predicted power peak for configuration 1 in January.	54
7.4	BK16's import, export and predicted power peak for configuration 6.2 in March.	57
7.5	Graph showing the increase in peak reduction with increasing power tariff.	61
7.6	Graph showing the increase in cost reduction with increasing power tariff.	61

List of Tables

- 5.1 Battery parameters used for the optimisation model 36
- 5.2 The pricing model used for the case study 38
- 5.3 Overview of case specifications for the case study 39

- 6.1 Results from the Augmented Dickey-Fuller test 42
- 6.2 Presentation of the parameters for the autoregressive models 47
- 6.3 Standard deviation and mean of prediction error for each forecast variable 48
- 6.4 Overview of solution stability with varying number of reduced scenarios 51

- 7.1 Peak values for each configuration in January. 54
- 7.2 Peak values for each configuration in March. 55
- 7.3 Peak values for each configuration in June. 55
- 7.4 Self-sufficiency and self-consumption for each configuration in June . . 57
- 7.5 Costs and savings compared to base case for all configurations in January. 59
- 7.6 Costs and savings compared to base case for all configurations in March. 59
- 7.7 Costs and savings compared to base case for all configurations in June. 59

1 | Introduction

1.1 Motivation

The power system is experiencing an increase in electricity demand and share of distributed renewable and intermittent energy production. These changes are straining the grid by causing large power peaks, potentially leading to a need for large grid investments in expansions and improvements. Batteries are key enablers in tackling this change. Batteries have the potential to reduce power peaks and thereby enable higher consumption than offered by the grid capacity [1]. The ability to store energy also encourages increased energy efficiency by increased self-sufficiency and self-consumption of distributed renewable production. Self-sufficiency is defined as the share of consumption which is covered by local production, and self-consumption is the share of local production which is consumed within the building or system [2]. A report by The Norwegian Water Resources and Energy Directorate (NVE), clearly states that batteries will become a natural part of the grid structure as an important component in the future renewable power system [3].

A report commissioned by NVE on local energy communities (LECs), states that the interest in local energy communities, where a community has a collective ownership of storage units, is increasing [4]. The report presents two key motivations for local energy communities; postponing grid investments and adding value for property owners. Postponement of grid investments typically implies reducing power peaks, while increased self-sufficiency is targeted when aiming for added value for property owners.

The concept of local energy communities is still a novel phenomenon, making it hard to provide an explicit definition of what qualifies as a local energy community. Based on the motivation presented in the two previous paragraphs, this thesis will focus on local energy communities in the form of shared battery energy storage systems (s-BESS). More specifically, shared battery energy storage systems for commercial buildings will be targeted. Commercial buildings in Norway are subject to monthly measured peak (MP) grid tariffs, which provide economical incentives for the end users to reduce their monthly power peaks. Together with large energy consumption and high power peaks,

commercial buildings therefore serve as an interesting use case for shared battery energy storage systems.

It is reasonable to assume that some of the activities normally addressed by the distribution system operator (DSO), would be undertaken by the local energy community in order to enable a practical solution for the operation strategy of the shared battery energy storage systems. However, this creates several potential regulatory barriers for local energy communities. Current regulations do not allow joint metering for buildings that do not belong to the same legal entity [5]. Even so, the project preceding this master's thesis revealed that with joint metering for all members, shared battery energy storage systems for commercial buildings has the potential to reduce both power peaks and total costs for the community [6].

1.2 Objective

Based on the aforementioned report on LECs and current regulatory barriers, the main objective of this thesis is to investigate the potential benefits of shared battery energy storage systems within the Norwegian distribution system, by considering various configurations for battery placement within the local energy community. This thesis will investigate how common cost, and consequently power peaks (due to the MP tariff model), can be reduced. The thesis will also analyse how this contributes to increased utilisation of locally produced energy.

1.2.1 Approach

Based on current regulations, different configurations for battery placement within the local energy community will be developed. The configurations are intended to illustrate what the authors consider plausible strategic solutions for shared battery energy storage systems, based on current regulations and licensing regimes. It is assumed that a local energy market structure must be established to enable efficient management of the shared battery energy storage system. However, the feasibility of these configurations within the current regulatory regime is not thoroughly investigated.

With respect to each configuration, the optimal scheduling of the shared battery energy storage system is formulated as a stochastic linear program (LP) with a receding horizon (RH) approach. The mathematical problem is modelled using the Python-based optimisation modelling language, Pyomo 5.7. Statistical theory of time series analysis and forecasting will be applied to develop autoregressive models to generate scenarios for consumption and local production. The generated scenarios will then be reduced to a reasonable amount using SCENRED and incorporated in the optimisation problem.

The presented strategy will be used to perform a real life Norwegian case study on shared battery energy storage systems and a sensitivity analysis on the impact of the peak tariff on system scheduling.

1.2.2 Contributions

The contributions of this thesis are:

- The development of an RH optimisation model for shared commercial community under the influence of long-term capacity-based grid tariffs.
- Quantified gains of shared battery energy storage solutions for urban area commercial buildings compared to configurations in line with regulatory regimes.
- A socio-economic perspective on the benefits of s-BESS for commercial buildings.

1.2.3 Limitations

The configurations for shared battery energy storage systems presented in this thesis will be inspired by what is considered plausible in terms of adaptability to current regulations, with the intention of illustrating the differences between the configurations. To ensure that this is done efficiently, this thesis will not consider the actual pricing model for local energy markets, but assume that power can flow freely within the local energy market. Hence, neither export or import within the local energy community will be subject to grid costs or energy market prices.

1.3 Structure

The remainder of this thesis is structured as follows

Chapter 2 Framework: Provides insight into relevant subjects within shared battery energy storage systems, local energy markets and regulations for the Norwegian power system. A literature review on previous research of shared battery energy storage systems will be presented.

Chapter 3 Optimisation and Scenario Modelling: Gives a brief introduction to stochastic linear programming and presents the concept of receding horizon optimisation together with a literature review on previous research within relevant application areas. The second part of the chapter presents relevant theory on time series analysis for data forecasting, scenario generation and scenario reduction.

Chapter 4 Problem Formulation: Presents the underlying procedure for the analysis of this thesis. The configurations for shared battery energy storage systems developed for the analysis are presented. Further specifications of the receding horizon optimisation approach applied for these systems are given, and finally the stochastic LP programme is presented.

Chapter 5 Case Study: Presents the area and commercial buildings used for this study together with a description of the battery that has been modelled. An introduction to the grid tariff pricing model and spot prices of the analysis period is given, followed by the framework for the case study with a presentation of the cases, each representing a configuration for shared battery energy storage.

Chapter 6 Scenario Modelling: The methodology for scenario modelling based on the uncertain variables of the case study is presented together with the resulting autoregressive functions for scenario generation. A description of the scenario generation and reduction process is given, together with an analysis of solution stability and optimal amount of generated and reduced scenarios for the case study.

Chapter 7 Results: Presents and analyse the results from the case study.

Chapter 8 Discussion: Presents a discussion on the main findings from the results, with emphasis on battery scheduling, peak shaving, cost reductions and self-sufficiency and self-consumption.

Chapter 9 Concluding Remarks: Concludes and summarises the key findings of this study together with suggestions for further work.

2 | Framework

This Chapter presents the relevant conceptual framework for this thesis regarding storage technologies, local energy communities and associated regulations.

For the content in Section 2.1, 2.2 and 2.4 the identification of the relevant background material were carried out in the project preceding this thesis[6]. The sections have been reviewed and modified in line with the thesis' objective and amended with discussions of a few papers that have been studied after the project.

2.1 Batteries

The increased integration of variable renewable energy sources such as solar and wind power poses a challenge to the balancing of energy production and demand. Battery energy storage technology has emerged as an enabling technology to tackle the intermittency of renewable energy sources [7]. Battery storage, stationary in particular, enables both reduced curtailment of renewable energy and can provide other services to the grid such as frequency regulation. There exists a number of different battery chemistry technologies, but the Li-ion battery has the largest share of market growth [8].

Battery cycle life is a function of discharge rate and depth and is the number of charge/discharge cycles a battery can achieve before failing to meet a certain performance criteria. Cycle life is estimated based on predetermined charge and discharge conditions. In fact, battery degradation is greatly affected by the battery operation and actual operating life is largely dependent on discharge rate and depth. If operated too vigorously the battery lifetime will be reduced [9].

Owing to an increasing industry and demand, Li-ion battery prices have plummeted, experiencing a price drop of 87% from 2010 to 2019 [10]. The Norwegian market for stationary battery storage has not fully matured, but costs in the range of 4000-6000NOK/kWh have been registered [11].

2.2 Shared Battery Energy Storage Systems for Commercial Buildings

Batteries can reduce overall grid costs in different grid tariff regimes. A number of papers have specifically studied the integration of battery energy storage system(BESS) in commercial buildings. Tiemann et al. evaluate the cost efficiency of BESS implementation for grid fee reduction in commercial buildings. One of the grid fees used in this case study correspond to the MP tariff, and with this tariff a maximum grid power reduction of 10% is obtained for most cases [12]. Sepúlveda-Mora et al. mainly focus on the economic value of behind the meter(BTM) photovoltaics(PV) coupled with battery storage (PV-BESS) subject to a time-of-use(ToU) rate as opposed to a standard MP tariff. However, they also state that the battery also provides a significant peak shaving effect with the MP tariff [13]. Similar peak shaving effects are expected with the MP tariff that will be used in this thesis. A ToU rate refers to a grid tariff where charges are higher during peak hours and lower during off-peak hours, whereas MP tariffs charge the highest peak during a selected interval (usually 1 month). Meinrenken et al. also consider a ToU tariff while investigating the value of concurrently optimising thermal and battery storage in an office building [14]. The study finds that concurrent demand side management(DSM) is the most effective approach, but it also obtains an electric cost reduction of 6.5% with battery storage alone. They reason that tariffs with demand charges are effective incentives for smarter grid operation [14]. This conclusion will be continued and is assumed to apply for the case study of this thesis as well.

Berglund et al. present a mixed-integer linear program (MILP) based optimisation model for battery storage implementation into an existing grid-connected PV integrated system. They focus on minimising the cost of both battery degradation and peak power, and they also perform sensitivity analyses over a single month interval on important system parameters [15]. Wang et al. develop a two-stage stochastic program for demand side management for cost optimisation in a commercial building with integrated PV and both stationary and mobile (i.e. electric vehicles) battery storage. The study finds that the stochastic model outperforms the deterministic counterpart [16]. All of the aforementioned papers seek to reduce electricity costs for commercial buildings in their analyses, however, none of them mentions the possibility of shared battery energy storage systems.

Shared battery energy storage systems have the potential of reducing community electricity costs. It can be a reasonable solution for communities where investment in individual storage is considered too expensive. Moreover, shared storage can decrease the peak power of the community as a whole. There exists a considerable volume of literature dedicated to shared battery energy storage systems(s-BESS) in the residential sector. Keck and Lenzen conduct a thorough Australian case study on the benefits of

s-BESS and its main enablers [17]. Some studies, such as those of Oh and Son, Roberts et al. and Syed et al., target the use of s-ESS in apartment buildings, motivated by the potential monetary savings by BESS integration and the typical lack of space for individual storage systems in these complexes [18][19][20]. The two latter studies also consider PV-BESS systems and report increased self-sufficiency by BESS integration. Such an increase is also expected for the results of this thesis, though the magnitudes are unknown.

Several other papers also focus on residential areas for s-BESS integration with single family homes. The following literature consider prosumers with integrated PV systems and generally include some parameters to ensure fair allocation of the profit between the users based on their usage of the s-BESS. However, all of the studies assume possibilities for local production with each building. Zhu and Ouahada propose a centralised and distributed real-time sharing control algorithm, taking into account the stochastic nature of PV production and load demand of the prosumers. Their aim is to minimise the long term time-averaged costs of all households [21][22]. Boulaire et al. compare the benefits of shared versus individual battery storage based on residential dwellings by means of a custom-developed simulation software. They present a customer assessment based on operational costs, and a network assessment considering the power consumption among other variables [23]. With a similar agenda, Walker and Kwon propose optimisation models for optimal daily storage operations of individual and shared energy storage systems. The results are used to compare the two storage strategies economically and operationally [24]. The case study in this thesis will unveil weather similar results for cost reduction as in these papers can be obtained when considering shared storage for buildings with different possibilities for local production.

Taşcıkaraoğlu presents an optimisation algorithm for a s-BESS in a residential area with installed PV, that aims to minimise total neighbourhood energy costs while considering fair distribution of the profit between households [25]. The study conducted by Taşcıkaraoğlu can be considered a continuation of the works of Rahbar et al., however, the case study of Rahbar et al. consider three differently classified users, one an apartment building, the other a medium sized office and the last a restaurant [26]. To the authors' knowledge, this makes Rahbar et al. stand out as one of the few studies including s-BESS for commercial buildings. Although comparing slightly different systems, it will therefore be interesting to use their results for verification of the ones obtained in the case study of this thesis. Oh and Son also investigate the use of s-BESS in commercial buildings and propose a s-BESS service model and strategy for apartment-type factory buildings [27]. They define apartment-type factory buildings as as "[...]a complex of multiple individually owned small factories and/or offices" [27]. Their study includes a considerable number of units which summarises to a large total consumption which provided interesting insight into s-BESS for commercial buildings.

2.3 Local Energy Markets

A local energy market(LEM) is a group of loads, energy storage units and distributed energy generators within a geographically limited area with a provided market platform for trading of locally produced energy and consumer flexibility [28]. The low voltage distribution network is not designed to support the increase of distributed energy resources (DER), like PV panels, and the penetration of electric vehicles (EVs) are posing challenges regarding energy transition and congestion [29][30]. Several studies has shown that local energy markets can improve the capacity of distribution grids to adapt to local power generation, increase energy efficiency, reduce congestion and reduce consumer costs [29][30][31].

Mengelkamp et al. investigated the role of energy storage in local energy markets [28]. The simulation study created an optimisation model for a peer-to-peer energy market with the objective to minimise the overall costs. The model was used for a community microgrid for residential buildings with distributed PV generation. The study compared local energy market with and without energy storage, and showed that self-consumption was increased by 38.7% when energy storage was integrated within the LEM. In addition, simulation results indicated that local energy markets can be economically profitable under the assumption of scalable electricity taxes and fees [28].

Many local energy and flexibility market projects are research projects and pilots as local energy and flexibility markets are all new developments and consequently relatively immature [4]. One example of an international case study is the Cornwall Local Energy Market in the United Kingdom finalised in November 2020 [4][32]. The project successfully managed to accommodate increasing renewable generation, reduce carbon emissions and increase monetary benefit from flexible energy resources [32]. In Norway, the maturity level of Norwegian local energy communities varies greatly [4]. A commenced smart city project in Trondheim called +CityxChange includes local energy and flexibility markets. The project aims to engage citizens and companies within the community to create a sustainable and energy positive city [33].

2.4 Regulations for the Norwegian Power System

The Norwegian Energy Regulatory Authority(NVE-RME) is the national regulator for the power market and grid transmission system in Norway, with their regulatory power delegated by the Norwegian Energy Act [34][35]. In general, RME seeks to promote effective energy production, consumption, transmission and trading [35]. The grid companies' regional monopolies are regulated by not only securing safe and effective operation, but also by limiting their profit by setting and upper limit on annual income

[35]. In addition to regulating the grid companies, RME also regulates the electricity market by ensuring well-functioning and effective trading [35]. The following sections underline RME's regulations regarding the Norwegian pricing model, energy metering and local energy markets which is relevant for this master thesis.

2.4.1 The Norwegian Pricing Model

Norway's retailer market is separated between the competition oriented power producers, which the end users are trading power with, and the monopoly regulated grid companies who are responsible for power transmission [36]. The grid companies, also referred to as distribution system operators (DSOs), are issuing an invoice for transmission called the grid tariff. In order to buy electricity, a customer will make a contract with both a grid operator and a power retailer [37].

2.4.1.1 The Power Retailers' Supply Agreements

The consumers are free to choose its power retailer, which is responsible for buying electricity from the electricity market on the customer's behalf. If the consumer has a contractual agreement based on market price, the hourly consumption will be measured and billed according to the spot price with an additional surcharge and/or monthly fixed cost [37]. The hourly spot price, given in NOK/MWh, is given by Nord Pool [37][38], which is the physical marketplace for power suppliers and retailers [37][39]. With hourly spot price deals the consumer has a great possibility to affect its electricity bill by shifting or reducing its consumption to other times of the day where the spot price is cheaper [37].

2.4.1.2 Grid Tariff

Energy consumers pay a grid tariff to the distribution system operators (DSO) for the transmission of the power bought by the power retailers to their home or business. The grid tariff revenue should cover costs for operation and maintenance, given that the grid is operated efficiently. Each DSO in Norway determines the grid tariff for the customers in their concession area in line with RME's tariff design and total tariff revenue regulations [40].

According to RME, there are a few components to the grid tariff that affect the total electricity costs. The volumetric costs are supposed to reflect the customer's utilisation of the grid, and is therefore based on the customer's total energy consumption for the billing month. Another component is the power tariff, which is often based on the

maximum measured power peak over a defined billing period. The DSOs can choose not to add this cost to the consumers' tariff, or just add it to certain customer groups based on grid utilisation. The maximum peak (MP) tariff is often paid by commercial actors, but they can be implemented for residential buildings as well. The fixed tariff is defined as an annual monetary tariff that customers connected to the grid must pay in order to cover the operational costs of the power transmission system [41].

In addition to the grid companies' tariffs there are governmental fees, consumption tax, Value Added Tax (VAT) and surcharge to Enova's energy fund [41].

2.4.1.3 Prosumers

Prosumers are a special group of the DSO's customers that both consume and produce electricity. The excess power production of a prosumer can not be sold to other end users directly, and participation in the wholesale market is not allowed. Instead, the prosumer must sell the excess power to its power retailer as long as the sold power does not reach above 100kW. Prosumers do not pay the fixed grid tariff for exporting power as power producers do, and the export and import can be measured from the same meter [42].

2.4.1.4 Proposal Regarding New Grid Tariffs

Today, the grid tariff does not reflect the actual costs for operating the power transmission system, as the consumption-based volumetric costs for private households stands for 70% of the grid tariff while only 10-20% are direct costs related to energy consumption. As most of the DSOs costs are related to high power peaks, RME has proposed a new grid tariff pricing model that would give the end-users incentives to reduce their power peaks and their overall power consumption on a long-term basis. This will lead to a more even utilisation of the grid which again provides the DSO with additional capacity to expand the number of customer affiliations without further unnecessary and expensive grid expansions [43].

2.4.2 Individual and Joint Metering

Essentially, each customer's energy and power consumption must be measured and billed individually. This is because customers with joint metering, sharing one electricity bill, do not have to same legal rights considering the quality of supply, metering and cost settlement on the same terms individual metered customers. In addition, joint metering will lead to less customers to distribute the DSO's fixed costs between, which

again causes a higher grid tariff for the other customers within the DSO's concession area. According to RME, individual metering gives an incentive for increasing the energy efficiency as the individual customers have a greater incentive for responding to the energy price variations [5].

However, there is an exemption for this regulation for commercial and private customers where individual metering of consumption will give unreasonable costs [5]. For such cases the buildings can be billed and metered per common intake line [5][44]. To give a relevant example, the renters within an office building can be measured and charged as one, while two neighbouring office buildings with separate intake lines must pay separate electricity bills.

2.4.3 Local Energy Markets

Paragraph 4-5 of the Energy Act regarding organised marketplaces says that without concession from RME, no other than the government can undertake the organisation or operation of a marketplace for electrical energy turnover [34]. There are other regulatory limitations considering the Energy Act and its underlying secondary legislation in addition to general Consumer Protection Legislation [4]. However, they will not be considered in detail for this thesis. A commissioned report from NVE states that in order to secure innovation, a standardised process for granting of temporary dispensations for such regulations should be given to local energy community research projects and pilots [4][45].

3 | Optimisation and scenario modelling

This chapter presents the basic principles of optimisation and stochastic linear programming. An introduction to time series analysis will follow, describing how these methods can be utilised for scenario generation to model the uncertainty associated with stochastic programs.

3.1 Optimisation Models

An optimisation model is a mathematical problem formulation which seeks to minimise or maximise an objective function that is subject to one or more constraints. This thesis will focus on linear programs (LP). Typically, linear programs search for a minimal-cost solution with respect to some demand requirement. Deterministic linear programs can be described, in matrix form, as shown in equation (3.1) [46].

$$\begin{aligned} \min \quad & z = c^T x & (3.1) \\ \text{s.t.} \quad & Ax = b, \\ & x \geq 0 \end{aligned}$$

x is a vector of decision variables, z describes the objective function, whereas c , A and b are known data.

3.1.1 Stochastic Programming

Stochastic linear programs are linear programs where some program data is considered uncertain. This data is represented as random variables and described by corresponding probability measures. The value of the random variables can only be known after

information about them is obtained. Due to the uncertainty of the random variables, the set of decisions is divided into two groups. In the *first-stage* all decisions that must be made prior to receiving new information are made. In the *second-stage*, all decisions that can be taken after receiving new information are made. The second-stage decisions are a function of the first-stage decision and the new information [46].

3.1.1.1 The Two-Stage Stochastic Program

The two-stage stochastic program with fixed recourse is a well known stochastic program. First-stage decisions are made in the first stage, then decisions are updated or corrected in the second stage by second-stage actions, commonly referred to as *recourse* actions. For the formulation of the stochastic two-stage problem the reader is referred to Birge and Louveaux [46]. Assuming there are S outcomes(scenarios) and that p_s is the probability of outcome s , the second-stage problem can be reformulated to build a deterministic equivalent of the stochastic problem as shown in equation (3.2). This enables easier handling of the stochastic problem.

$$\begin{aligned} \min \quad & z = c^T x + \sum_{s=1}^S p_s q(s)^T y_s & (3.2) \\ \text{s.t.} \quad & Ax = b \\ & x \geq 0 \\ & Wy_s = h(s) - T(s)x \quad s = 1, \dots, S \\ & y_s \geq 0 \quad s = 1, \dots, S \end{aligned}$$

x denotes the first-stage decisions and y denotes the second-stage variables, representing the ability to correct the first-stage decisions. $q(s)$, $h(s)$ and $T(s)$ represents second-stage data.

Scenario trees are a common way to describe the information flow in stochastic programs. They also provide a good presentation of the problem structure. The scenario tree branches out for every uncertain parameter to create one branch per possible outcome. There can be several time periods within each stage. Each path through the tree is called a scenario and describes a deterministic sequence of events [47]. The information flow links the scenarios, all decisions that are based on the same information must be equal for all scenarios. These restrictions are referred to as non-anticipativity constraints. A simple illustration of a typical scenario tree is shown in Figure 3.1.

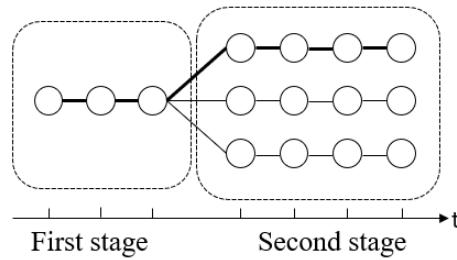


Figure 3.1: Illustration of the general structure of scenario trees. The bold line represents one scenario.

3.1.2 Receding Horizon Optimisation

Rolling horizon algorithms have been applied to many scheduling problems and are often used to solve such problems under uncertainty or large-scale optimisation problems. They have become important in energy system operation because of the uncertainty of demand and intermittent renewable production during optimal scheduling [48]. Rolling horizon models offer a flexible solution strategy for optimisation problems by updating system data and allowing rescheduling within each time step. There exists different methods of rolling horizon optimisation. This thesis will adopt a receding horizon framework, which differs from that of rolling horizon in the sense that the size of the scheduling horizon is reduced by each iteration.

The receding horizon approach is used for optimal scheduling within a specific time horizon and allows for an iterative solution method to handle the nature of uncertainty more delicately. The receding horizon framework used in this thesis is based on the approach presented by Kopanos et al. [49]. The approach considers a scheduling horizon (SH) that is decomposed into equally sized time intervals, and a given control horizon (CH) and prediction horizon (PH). The control horizon defines the time period in which the optimal scheduling is solved and is usually the length of one time step. The prediction horizon contains data of future time steps that can be considered known with some certainty. The length of the prediction horizon depends on the specific problem and to which extent system data of future time steps can be considered reasonably accurate.

The basic concept of receding horizon optimisation is that for each control horizon the system operation is optimised with respect to the data within the prediction horizon. The solution is saved and the value of the decision variables are used as initial conditions for the next time step. The algorithm continues to "roll" onward to the next time step where the prediction horizon is updated with new information. The optimal scheduling is re-solved using data from the last optimisation, and so the algorithm continues throughout the scheduling horizon. Figure 3.2 illustrates the receding horizon approach.

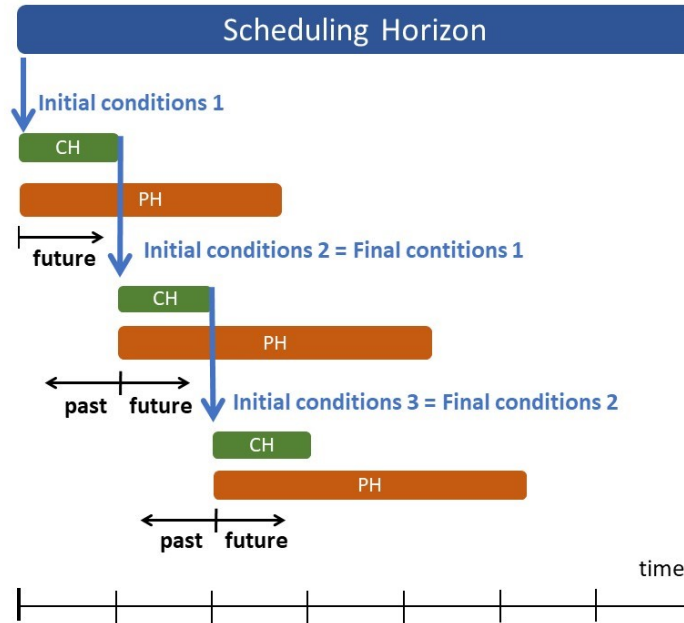


Figure 3.2: Illustration of a receding horizon framework.

A number of works implement a rolling horizon approach for the optimal management of microgrids. Although pursuing a slightly different objective, many of the principles applied in these papers are transferable to the monthly optimal scheduling of a shared battery energy storage system with respect to total costs for the end-users. Silvente et al. apply rolling horizon methodology for the simultaneous management of energy production and demand within a microgrid. They highlight that the solution of the overall problem potentially could be suboptimal as future information outside the prediction horizon is not taken into account. They also consider the data within the prediction horizon deterministic and conclude that longer prediction horizons contribute to significantly reduce the imported power from the external grid and consequently increase profits [50]. However, there is a trade off between the length of the prediction horizon and computational time [51]. The methodology of Silvente et al. is considered to be highly relevant for the receding horizon framework that will be implemented for the optimisation model in this thesis.

Elkazaz et al. applies a two stage rolling horizon technique for optimal operation of a battery energy storage system within a microgrid. Their sole objective is to minimise the daily costs of energy drawn from the grid while also investigating the impact on self-consumption of renewable energy sources. They conclude that the model effectively reduces the daily cost of energy imported from the main grid, and increases self-consumption within the microgrid [52]. Due to their simple objective, the results of Elkazaz et al. can easily be compared with and used as a verification method for some of the cases in this thesis.

Due to their implementation of relevant methods for modelling uncertainty within a receding horizon framework the following papers have also been investigated. Both Gao et al. and Yang et al. consider the information in the prediction horizon uncertain and utilise an autoregressive integrated moving average (ARIMA) model to forecast data [53][54]. The latter also presents a mixed receding horizon control strategy that successfully applies both short-term and long-term forecasting within the prediction horizon [54]. Silvente et al. introduce a two-stage stochastic mixed integer linear programme into a rolling horizon approach for the optimal management of a microgrid. Hence, the model is solved under predicted conditions. They derive that the presence of uncertainty can increase operational costs by 19.6%, and conclude that longer prediction horizons, assuming precise predictions of the uncertain variables, are favourable [55].

3.2 Time Series Analysis and Forecasting

Statistics Norway define time series as a sequence of observations at successive points in time over a period of time [56]. This section will introduce basic concepts of time series analysis and autoregressive processes as a tool for time series forecasting.

A time series can be either additive or multiplicative [57] depending on its properties. The decomposition of a time series based on its type is commonly represented as presented in equations (3.3) and (3.4).

$$y_t = S_t + T_t + R_t \quad (3.3)$$

$$y_t = S_t \cdot T_t \cdot R_t \quad (3.4)$$

At time step t , y_t is the forecasting variable, S_t is the seasonal component, T_t is the trend component and R_t is the residual component consisting of a base level and error term.

3.2.1 Time Series Analysis

The following section will introduce relevant aspects of time series analysis. Time series analysis is a necessary step to enable time series forecasting. The process unveils characteristics of the time series that determine how the data should be handled to ensure accurate forecasting.

3.2.1.1 Autocorrelation

Autocorrelation is the correlation of a variable with a former value of itself, also referred to as lags [57]. It is the similarity between observations as a function of the time lag between them [58]. Autocorrelation plots (correlograms) are therefore a valuable tool for identifying correlation with time lags. Partial autocorrelation plots illustrate the direct correlation between a specific lag, without the influence of previous lags, and the observation [59]. This is useful for time series forecasting when determining if lags are to be used in a regression model. An illustration of a typical autocorrelation plot with the corresponding partial autocorrelation plot is shown in Figure 3.3.

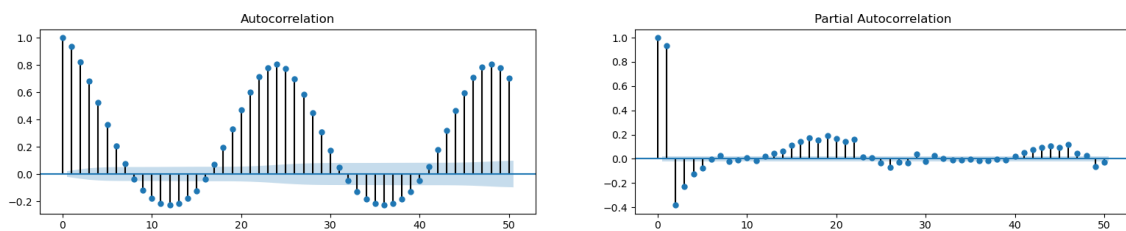


Figure 3.3: Typical autocorrelation and partial autocorrelation plot showing correlation between time lags. The lags are shown on the x-axis, the correlation is shown on the y-axis.

3.2.1.2 Stationarity

Stationarity implies that the statistical properties of the time series do not change over time. Thus, properties such as the mean and variance and autocorrelation of the data remain constant, even while the time series itself does change [58]. This will in turn enable easier prediction of the data as stationarity is a common assumption for many tools in time series analysis [57].

The Augmented Dickey-Fuller Test The Augmented Dickey-Fuller (ADF) test is a statistical procedure commonly used to determine if a time series is stationary or not. The null hypothesis (H_0) propose the presence of a unit root, implying that the time series is not stationary. The alternate hypothesis (H_1) states that the time series does not have a unit root and is thereby stationary [60].

The test statistic, its critical values and the p-value of the Augmented Dickey-Fuller test, provides the necessary information to determine weather or not the null hypothesis can be rejected. The p-value is given a predetermined significance level, usually at 5% [61]. A resulting p-value below the specified threshold suggest that the null hypothesis can be rejected [62].

3.2.1.3 Seasonality

Time series often exhibit seasonal behaviour. Seasonality refers to the presence of a repeating pattern that occurs at a constant frequency[59]. If seasonality is present, it must be accounted for when modelling time series data.

Dummy Variables Dummy variables can be used to capture seasonal effects in time series data [63]. Dummy variables are explanatory variables that take the value $d_{n,t} \in \{0, 1\}$, depending on whether or not the dependent variable falls within a pre-determined category n at the relevant time step. When utilising dummy variables perfect multicollinearity must always be avoided as this will cause failure due to too many dummy variables. The problem occurs when a dummy is assigned to a category that is already defined by the intercept of dummies for existing categories. It is easily avoided by ensuring that there is one fewer dummy variables than categories [57]. The effects of climate on seasonality can also be accounted for by including measures of precipitation and temperature when modelling time series [63]. Such explanatory variables are referred to as predictor variables[57]. Dummy variables can be considered as a specific type of predictor variable. Forecasting of y_t by using a regression model with predictor variables can be modelled as shown in equation (3.5).

$$y_t = \alpha + \beta_1 p_{1,t} + \beta_2 p_{2,t} + \cdots + \beta_n p_{n,t} + \varepsilon_t \quad (3.5)$$

3.2.2 Autoregressive Models

In general, time series regression models assume that the time series of interest has a linear relationship with other time series [57]. The forecast variable y is estimated by its linear relationship to predictor variables x . Autoregressive models incorporate a regression of the forecast variable on past values from the same series[59]. Hence, autoregressive models are useful when forecasting time series that are typically auto-correlated, such as electricity demand. An autoregressive process of order p , commonly referred to as AR(p), is described by equation (3.6).

$$y_t = \alpha + \phi_1 y_{t-1} + \phi_2 y_{t-2} + \cdots + \phi_p y_{t-p} + \varepsilon_t \quad (3.6)$$

α is a constant, ϕ is the autocorrelation of y_t with lag p and ε_t is normally distributed white noise with zero mean and constant variance [57]. ε_t should ideally be a white noise process in order to ensure independent and identically distributed values. The parameters α and ϕ of the autoregressive model can be estimated through vari-

ous methods. This process is commonly referred to as model fitting. Ordinary least squares (OLS) estimation is one such method commonly used for fitting autoregressive models [64]. The principle of the method is to minimise the sum of the squared errors between the observed and predicted values of the dependent variable. Further elaboration on the statistical theory behind these methods is considered out of scope for this thesis.

3.2.2.1 Forecast Accuracy

Forecast accuracy must be evaluated based on new data that was not used when estimating model parameters, only then can true model performance be evaluated. It is common practice to divide the available data set into subsets consisting of a training and test period. This enables model fitting based on the train set, while the actual forecasting and evaluation of model accuracy is based on the test set [57].

Forecast model accuracy is determined by forecast errors, the difference between the observed value and its predicted value [57]. The forecast error should ideally be a white noise process. This serves as evidence that the model successfully incorporates all information of the time series and that the residuals of the model are solely white noise, which cannot be modelled. The root mean square error (RMSE) of the forecast is a common measure for comparing the accuracy of time series.

3.2.3 Scenario Generation

In two-stage stochastic optimisation programs, a set of scenarios that approximates the actual distribution of the uncertain variables is necessary [65]. The aim of the scenario generation process is to attain a representative scenario tree that encourage reasonable decisions [66]. An adequate amount of scenarios should therefore be generated to ensure sufficient representation of the actual distribution of the uncertain variable.

Scenario generation based on various autoregressive models is a common approach [67]–[70]. Assuming the error term $\varepsilon_t \sim N(0, \sigma^2)$ of the model is a white noise process, a scenario can be generated by randomly drawing ε_t from a normal distribution and adding it to the model. This method allows generation of as many scenarios as desired to complete the scenario tree.

3.2.4 Scenario Reduction

Due to the computational complexity of stochastic optimisation programs with large scenario trees, it may be desirable to reduce the number of scenarios to a reasonable figure. The scenario reduction process aims to reduce the number of scenarios while maintaining reasonably good approximations of the stochastic data.

Scenario reduction algorithms determine a scenario subset of the finite amount of scenarios and assign new probabilities to the preserved scenarios by minimising the distance between the original probability distribution P and the reduced probability measure Q [71]. Other papers, such as [72]–[74], have investigated the optimal approach for scenario reduction, but further elaboration on the subject is considered out of scope for this thesis.

4 | Problem Formulation

In order to quantify the possible benefits with s-BESS, 6 configurations regarding different battery allocations within a local energy community is created. Based on these configurations, a receding horizon optimisation algorithm which seeks to minimise total system costs for these configurations is implemented and presented in this chapter. Due to the monthly maximum peak power tariff for commercial buildings, the mathematical problem formulation uses stochastic linear programming with the receding horizon control approach. This will allow for the monthly peak power tariff to be taken into consideration for all iterations within the RHO algorithm.

4.1 Shared Battery Energy Storage System Configurations

The probability of external vendors owning and operating batteries in the future and the regulation against joint metering are key inspirations for the configuration development process[1]. A total of six different configurations will be presented in the following sections. Configurations 2 and 3 do not represent a shared energy storage system, but serve as examples of configurations that are considered to be in line with current regulations due to individual metering and storage. For the remaining configurations, the local energy market is assumed to encounter some regulatory barriers. Many of the presented configurations are quite similar, but they are considered to reflect plausible allocations of a s-BESS and are implemented in order to perform a comprehensive analysis.

4.1.1 Configuration 1: All Buildings Behind One Meter

In the first configuration, all the buildings and the battery operate together behind the meter as shown in Figure 4.1. Other than the battery's capacity limitations, there are no other restrictions on power flow between the buildings or utilisation of the battery to shift the buildings' consumption and production. Due to joint metering, only the

community power peak will be "seen" by the DSO and not the buildings' individual power peaks. The configuration bares similarities to that of a microgrid. This creates an opportunity for the buildings' power peaks to equalise each other. Therefore, this case is assumed to be the case with the maximum monetary savings, peak shaving and self-sufficiency although current Norwegian regulations do not allow joint metering.

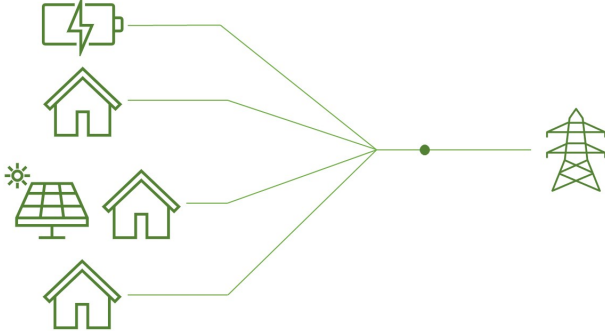


Figure 4.1: Illustration of configuration 1, where all buildings and the battery are placed together BTM.

4.1.2 Configuration 2: Individual Metering for the Buildings and the Battery

For the second configuration, shown in Figure 4.2, all the buildings and the battery are metered individually. The battery is considered to be owned by a third party, not the by the DSO or any of the member buildings of the community, and operates by itself. Such a configuration might be of interest for commercial actors who want to achieve a monetary benefit by delivering services or doing arbitrage operations and adaptations to the energy pricing model. Still, since the battery is metered individually, the revenue gained by arbitrage operations must make up for the grid tariff and energy costs for the battery.

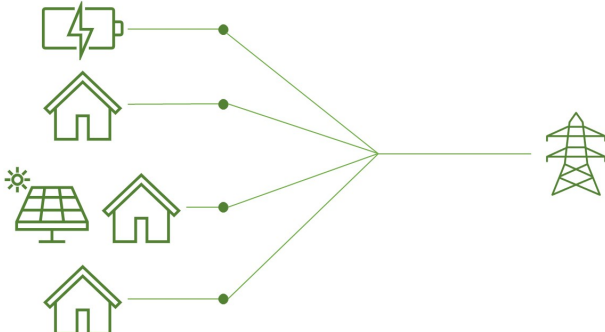


Figure 4.2: Illustration of configuration 2, where all buildings and the battery are metered individually, and the battery is operated independently.

4.1.3 Configuration 3: Individual Storage for One Building

In configuration 3, the battery is owned and operated by one of the buildings in the community, as shown in Figure 4.3. The building which operates the battery will have the opportunity to shave its own power peaks and perform price arbitrage operations to reduce individual costs. The configuration represents an interesting case for analyses of how an individually operated battery can contribute to community benefits.

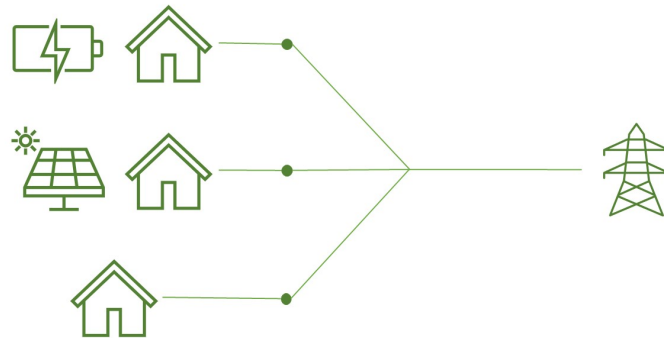


Figure 4.3: Illustration of configuration 3, where the buildings are metered individually and the battery is owned and operated by one of the buildings.

4.1.4 Configuration 4: Community Owned Battery with Individual Metering

In configuration 4 all buildings are metered individually, in addition, a local energy market is included to enable shared battery energy storage. The battery is owned by the community and can only operate within the local energy market. Hence, the battery is not billed separately by the DSO or the power retailer as shown in Figure 4.4. The dashed lines in the figure represents the flow within the local energy market. It is important to note that these lines do not necessarily need to represent a physical grid. They mainly represent the local energy market, separated from the Nordic power trading market.



Figure 4.4: Illustration of configuration 4, where the buildings are metered individually and the battery capacity is shared within a local energy market.

4.1.5 Configuration 5: Local Energy Market with Individual Metering for the Battery and Buildings

Figure 4.5 shows configuration 5 where all buildings and the battery is metered individually by the DSO, as for configuration 2. The battery is also considered to be owned by a third party. However, similar to configuration 4, this configuration includes a local energy market as well. The difference between configuration 4 and 5 is that, here, the battery operates individually. It has the opportunity to import power directly from the power grid, and not only through the local energy market.

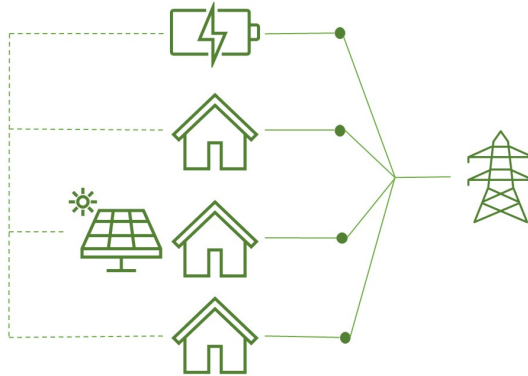


Figure 4.5: Illustration of configuration 5, where all buildings and the battery is metered individually, the battery is operated separately within a local energy market.

4.1.6 Configuration 6: Local Energy Market with Individual Storage

Configuration 6, like the past two configurations, includes a local energy market. However, for this configuration the battery is considered to be owned and operated by one of the buildings, as in configuration 3, but with the possibility to share the capacity with other buildings within the community. The buildings are metered individually as shown in Figure 4.6.

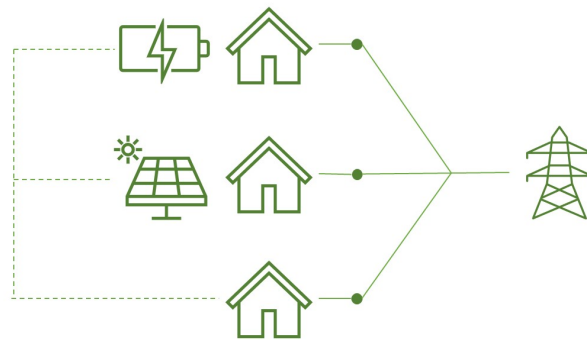


Figure 4.6: Illustration of configuration 6, where all buildings are metered individually, the battery is owned and operated by one of the building and there is a local energy market.

4.2 Receding Horizon Optimisation

Decision making for battery scheduling within a long time horizon can be challenging as accurate forecasting of consumption and production for longer time periods is a difficult task. However, as time moves on, new information and updated consumption and production forecasts will be obtained. It is therefore desirable to use a receding horizon approach to iteratively solve the battery scheduling problem.

The optimisation problem of this study is implemented as a stochastic linear programme with a receding horizon approach. The model will consider a scheduling horizon of one month in order to account for the monthly MP tariff. The data within the prediction horizon will be considered deterministic. However, this model deviates from the traditional receding horizon framework illustrated in Figure 3.2, by also considering the data beyond the prediction horizon in each control horizon. This data will be considered stochastic and will represent the second-stage problem, whereas the deterministic prediction horizon will represent the first-stage problem. Such long-term considerations are implemented into the receding horizon optimisation model in order to solve the scheduling problem within every time step with respect to the monthly

power peak. An illustration of the receding horizon approach of this thesis is shown in Figure 4.8. The figure shows how the control and prediction horizon are shifted within the scheduling horizon for each iteration. The scenario tree showed for the first iteration depicts the different scenarios of the stochastic problem.

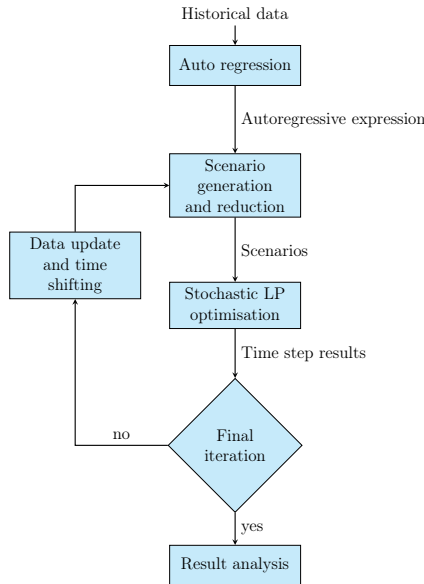


Figure 4.7: Flow chart showing the process of optimising with receding horizon control including scenario generation and data updates.

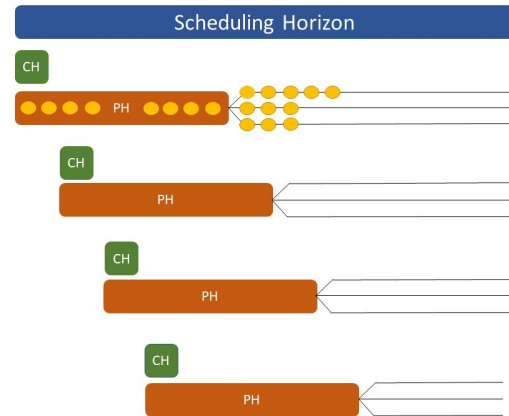


Figure 4.8: The iterative process of the receding horizon approach, showing how the scenario tree, control and prediction horizon is shifted through time.

The algorithm for the receding horizon approach of this study is described in Figure 4.7. First, an autoregressive model for each uncertain parameter is developed. The autoregressive model is then used to create several scenarios for the stochastic variables of the second-stage problem. The scenarios are then reduced to a reasonable amount and implemented in the second stage of the scheduling problem. The stochastic optimisation problem is then solved. The optimal values of the decision variables in the current control horizon will be fixed and stored as initial conditions for the following iteration in the receding horizon algorithm. The two most important variables that follow through the iterations are the energy level stored in the battery and the power peak for imported power from the grid. Following this step, the control and prediction horizon are shifted by one time step. If this step corresponds to the final period of time, the procedure is completed, if not, the process is repeated until the final time step.

A more detailed description of the scenario generation and reduction process will be given in Chapter 6.

4.3 Mathematical Problem Formulation

The stochastic LP optimisation model seeks to minimise total system cost in every iteration of the RH model for a local energy community with an analysis period lasting from the beginning of the prediction horizon and till the end of the scheduling horizon. The stochastic problem is a two-stage problem with the first-stage problem having the same duration as the prediction horizon. It is assumed that the stochastic variables for production and consumption will be known in this period. For the following hours in the second-stage problem, several predicted scenarios regarding production and consumption for each building will be considered, creating the stochasticity of the problem.

The mathematical problem presented in this section is for configuration 1, the Stochastic LP optimisation models for the other configurations are based on this formulation, with a few added adaptations. The adaptations will be further explained in Section 4.3.3. The full representations of all the six configurations are showed in Appendix A-F.

4.3.1 Assumptions and Simplifications

This section explains the limitations and the basis of the assumptions for the mathematical optimisation formulation. A fundamental aspect of the mathematical problem is that the production and consumption of the buildings within the community are stochastic. However, within the first-stage problem it is assumed that the predicted consumption and production will be good enough to be deterministic. However, in the second-stage problem of the model, the consumption and production must be predicted by creating realistic scenarios.

While consumption and production variables are considered to be stochastic, the spot prices are considered to be deterministic. It is assumed because the spot prices are known the day ahead, in addition to relatively easily predictable daily patterns in pricing levels.

The first assumption is that there is negligible losses in transmission between the distribution grid, buildings and the battery. In addition, no transmission line congestion is assumed and power floats freely behind the meter. In addition, the presented model allows for bidirectional power flow within one time step as long as the objective value is not increased. This can be accounted for by adding small penalties for export, such that power is not imported and exported to and from the same receiver at once.

One simplification done for the mathematical model was neglecting the degradation costs, even though this would affect battery operation and and operating life of the

battery[9]. Due to the time limitation for this thesis, degradation costs were not included in the model. Instead, a charging and discharging capacity limit were added for the battery in order to limit the amount of full battery cycles.

Another limitation ignored for this thesis is the export limitation for the prosumers. There is no upper limit for export to the grid, and there is no additional costs for exporting more power than this limit.

Finally, note that the mathematical model for configuration 3 and 6 only considers individual operation of the battery for one of the buildings in the community at a time. In order to consider individual storage for several buildings at once, other features must be implemented in the mathematical model.

4.3.2 Mathematical Model

The principles regarding the objective function and the different constraints in this section is presented for configuration 1. The parameters and variables used are explained and summarised in Nomenclature.

4.3.2.1 Objective Function

The objective function seeks to minimise the total system costs based on the grid tariff and spot price energy costs for a community with joint metering as shown in equation (4.1) . This means that the volumetric and energy costs only depend on the total energy demand of all buildings and the battery in the community together, and that the MP costs only depend on the community power peak. The peak costs are based on the highest imported power level from past iterations P^{sys} and an additional term, Δp_s^{sys} , in case the scenarios predict a higher future power peak.

$$\min \sum_{s \in S} \pi_s \sum_{h \in H} ((p_{h,s}^{Gimp} (C_h^E + C^V) - C_h^E p_{h,s}^{Gexp}) + C^P (P^{sys} + \Delta p_s^{sys})) + C^F \quad (4.1)$$

4.3.2.2 Energy Balance Constraints

The energy balance constraints ensures that power flows between the distribution grid, battery and the buildings in the right way. There are two different balance equations considered: one distribution grid balance constraint and one balance constraint for the different buildings in the system.

Balance Constraint for Distribution Grid The balance constraint for the power flow between the distribution grid and the legal entities in the community ensures that net import from grid equals net import to the buildings and the battery as shown in equation (4.2).

$$p_{h,s}^{Gimp} - p_{h,s}^{Gexp} = \sum_{b \in B} (b_{h,b,s}^{Gimp} - b_{h,b,s}^{Gexp}) + x_{h,s}^{Lcha} - x_{h,s}^{Ldch} \quad \forall h \in H, s \in S \quad (4.2)$$

Balance Constraint for Buildings in the System The balancing constraints for each building in the community system ensures that the consumption and production correspond to the imported and exported power from the distribution grid. There are two different constraints for the buildings' power balance. The first constraint includes balance constraints for the hours within the first stage problem in which the production and consumption of the building is considered to be known. The second balance equation includes balance constraints for the second stage problem in which the consumption and production is uncertain. The building balance constraints are shown in equation (4.3) for the first stage problem and in equation (4.4) for the second stage problem.

$$b_{h,b,s}^{Gimp} - b_{h,b,s}^{Gexp} = R_{h,b}^{cons} - R_{h,b}^{prod} \quad \forall h \in H_1, b \in B, s \in S \quad (4.3)$$

$$b_{h,b,s}^{Gimp} - b_{h,b,s}^{Gexp} = D_{h,b,s}^{cons} - D_{h,b,s}^{prod} \quad \forall h \in H_2, b \in B, s \in S \quad (4.4)$$

4.3.2.3 Battery Constraints

The battery constraints are constraints concerning the operation of the battery alone. First, there are a few capacity constraints that must be complied with. Second, there is a battery efficiency constraint which is set to address both the power losses for the battery and the power balance between charging and discharging operations and the stored energy level. The initial storage capacity is also considered. Lastly, the final condition of the battery's energy storage level is addressed.

Capacity Constraints There are three capacity constraints: One constraint ensures that the stored energy does not exceed the maximum storage capacity of the battery, as shown in equation (4.5). The other two capacity constraints ensure that the battery can not charge or discharge more power than the charging and discharging limit. This is not an absolute physical limit, but rather a restriction set to ensure a lower number of battery cycles in order to prolong the battery lifetime, as explained in Section 2.1. The charging and discharging constraints are shown in equation (4.6) and (4.7) respectively.

$$e_{h,s} \leq E^{max} \quad \forall h \in H, s \in S \quad (4.5)$$

$$x_{h,s}^{Lcha} \leq K^{max} \quad \forall h \in H, s \in S \quad (4.6)$$

$$x_{h,s}^{Ldch} \leq K^{max} \quad \forall h \in H, s \in S \quad (4.7)$$

Battery Efficiency Constraints The battery efficiency constraints address the charging and discharging power losses when operating the battery. In addition, the constraint ensure the power balance between the energy stored in the battery and the power charged or discharged to/from the battery. There are two different constraints concerning the battery efficiency. The first constraint is used for all hours in the analysis period, excluding the first. The second constraint is only applied for the first hour of the analysis period because it need to take the initial condition of the energy storage level into consideration. These battery efficiency constraints are shown in equation (4.8) for normal operating hours and for equation (4.9) for the first operating hour.

$$e_{h,s} - e_{h-1,s} = \eta^{cha} x_{h,s}^{Lcha} - \frac{x_{h,s}^{Ldch}}{\eta^{dch}} \quad \forall h \in H | h \neq l, s \in S \quad (4.8)$$

$$e_{l,s} - S_0 = \eta^{cha} x_{l,s}^{Lcha} - \frac{x_{l,s}^{Ldch}}{\eta^{dch}} \quad \forall s \in S \quad (4.9)$$

Final Condition Storage Constraint The final condition storage constraint ensures that the battery holds a certain energy level at the end of the scheduling period. This is because the optimisation program doesn't take the next scheduling period into consideration and will therefore wish to empty the battery to the fullest at the end. It is often beneficial to set the final condition equal to the initial condition, so that in sum, no energy is gained or lost to the present or next scheduling period. The final condition constraint is shown in equation (4.10).

$$e_{f,s} = S_f \quad \forall s \in S \quad (4.10)$$

4.3.2.4 Power Peak Constraint

One of the main goals for the stochastic program is to able to see the possible future power peak costs, and schedule the battery according to this already at the early stages of the scheduling period. Therefore, the peak power constraint are of great importance. The constraint ensure that the peak power of one scenario must always be greater than or equal to the maximum import of this scenario. The constraint is shown in equation (4.11).

$$P^{sys} + \Delta p_s^{sys} \geq p_{h,s}^{Gimp} \quad \forall h \in H, s \in S \quad (4.11)$$

4.3.2.5 Non-anticipativity Constraints

The non-anticipativity constraints make sure that variables within the first stage problem remain equal for every scenario. This forces the model to take all scenarios into consideration when making decisions for scheduling import, export and battery charging and discharging within the first-stage problem. As Δp_s^{sys} reflects the maximum peak for each scenario, there are no non-anticipativity constraints for this variable, as that would make the model predict equally peaks for every scenario. The non-anticipativity constraints for the relevant variables are shown in equations (4.12) to (4.18).

$$e_{h,s} = e_{h,s-1} \quad \forall h \in H, s \in S | s \neq s_1 \quad (4.12)$$

$$x_{h,s}^{Lcha} = x_{h,s-1}^{Lcha} \quad \forall h \in H, s \in S | s \neq 1 \quad (4.13)$$

$$x_{h,s}^{Ldch} = x_{h,s-1}^{Ldch} \quad \forall h \in H, s \in S | s \neq 1 \quad (4.14)$$

$$p_{h,s}^{Gimp} = p_{h,s-1}^{Gimp} \quad \forall h \in H, s \in S | s \neq 1 \quad (4.15)$$

$$p_{h,s}^{Gexp} = p_{h,s-1}^{Gexp} \quad \forall h \in H, s \in S | s \neq 1 \quad (4.16)$$

$$b_{h,b,s}^{Gimp} = b_{h,b,s-1}^{Gimp} \quad \forall h \in H, b \in B, s \in S | s \neq 1 \quad (4.17)$$

$$b_{h,b,s}^{Gexp} = b_{h,b,s-1}^{Gexp} \quad \forall h \in H, b \in B, s \in S | s \neq 1 \quad (4.18)$$

4.3.2.6 Non-negativity Constraints

Finally, the non-negativity constraints for all the variables in the optimisation problem are presented in equations (4.19) to (4.22). They are very general and simple, but very important for avoiding that variables achieve a negative value. A negative value could result in negative costs, which would give a misleading objective value.

$$e_{h,s}, x_{h,s}^{Lcha}, x_{h,s}^{Ldch} \geq 0 \quad \forall h \in H, s \in S \quad (4.19)$$

$$p_{h,s}^{Gimp}, p_{h,s}^{Gexp} \geq 0 \quad \forall h \in H, s \in S \quad (4.20)$$

$$b_{h,b,s}^{Gimp}, b_{h,b,s}^{Gexp} \geq 0 \quad \forall h \in H, b \in B, s \in S \quad (4.21)$$

$$\Delta p_s^{sys} \geq 0 \quad \forall s \in S \quad (4.22)$$

4.3.3 Adaptations to the optimisation model for other configurations

In order to adapt the optimisation model for configurations 2-6, a few tweaks must be added. As configuration 1 is the only configuration with shared metering, the objective function in equation (4.1) must be adapted for individual metering for the other configurations. This results in a objective function where the imported and exported energy and the maximum power peak for each building is billed separately. In addition, for configuration 2 and 5 the battery is an independent actor and the objective function must include the battery's import and export as well.

The balance constraints are very similar for all the configurations. However, they all depend on whether the BESS is accessible for the distribution grid or the individual building. For configuration 3, 4 and 5 an additional balance constraint must be added in order to ensure power balance within the local energy market. For configuration 4 the battery is shared and is included in the local market balance constraint. For configuration 5 the battery has access to both local energy market and the distribution grid, and for configuration 6 the battery is only accessible for the building operating it. Since, configuration 1 is the only configuration considering joint metering, the balance constraint for the distribution grid is not needed for the other configurations.

Due to the local energy market in configuration 4, 5 and 6, it is important to separate import and export from/to the distribution grid and to/from the local energy market for the separate buildings. Therefore new variables regarding import and export for the buildings are introduced and added to the balancing constraints where relevant. In addition, the efficiency constraint described by equations (4.8) and (4.9) must separate between charging and discharging from the distribution grid and the local energy market. This also affects constraint (4.7) and (4.6), as they must ensure that the sum of charge/discharge to/from the grid and local market does not exceed the capacity limit.

The power peak constraints are adapted in such a way that it calculates peak import for each of the individual buildings and peak import for the battery in configuration 2 and 5, where it operates as an independent customer of the DSO. Finally, the non-anticipativity and non-negativity constraints are added for the new import, export, charging and discharging variables.

The full model formulation for configuration 1, 2, 3, 4, 5 and 6 are compactly formulated in Appendix A, B, C, D, E and F respectively.

5 | Case Study Specifications

This chapter presents the case specific data implemented when using the RHO model and investigating the case specific performance of the different configurations. The case study is set to a commercial area in Trondheim, including three commercial buildings in the local energy community. The assumptions and settings used for conducting this case study with the RHO model will first be presented followed by background information regarding the area and the buildings together with the battery specifications and pricing model. Finally, the specific cases conducted and their physical characteristics are explicitly presented.

For the content in Section 5.2.1 and 5.2.2 the identification of the relevant background material were carried out in the project preceding this thesis [6]. The sections are amended in line with data studied after the project.

5.1 Assumptions and Settings for the Case Study

The case study will be conducted for January, March and June in the year of 2020. January is considered the darkest and often the coldest month of the year which may result in critical high power peaks and minimal PV production. It is therefore crucial to analyse how a BESS manages to reduce these peaks in January. The complete opposite will happen in June as power consumption will be lower and the PV production is at its maximum. It is therefore interesting to see how the BESS manages to exploit this excess power produced in June. March is a month where the weather is relatively cold, but there will still be higher PV production than in January. It is therefore of interest to run the cases in March to see how the different s-BESS configurations handles both high consumption peaks and PV production at the same time.

The scheduling horizon of the RHO model is set to stretch over a full calendar month. This is because the peak power tariff is based on the highest power consumption value over a month. The prediction horizon is set to be 8 hours, as it is assumed that the consumption and production of the buildings can be predicted with sufficient accuracy for the first 8 hours of the stochastic LP model. The control horizon is for 1 hour only, which means that a new iteration of the RHC model will start for every hour within the scheduling horizon.

Finally, it is worth mentioning that 2020 was an abnormal year, not only due to the COVID-19 pandemic, but the power spot prices were also extremely low compared to previous years [39]. Due to the fact that the AR-model is trained based on 2019 historical data, it is expected that the generated scenarios for 2020 will deviate a little more than normal from middle of March and throughout the rest of 2020.

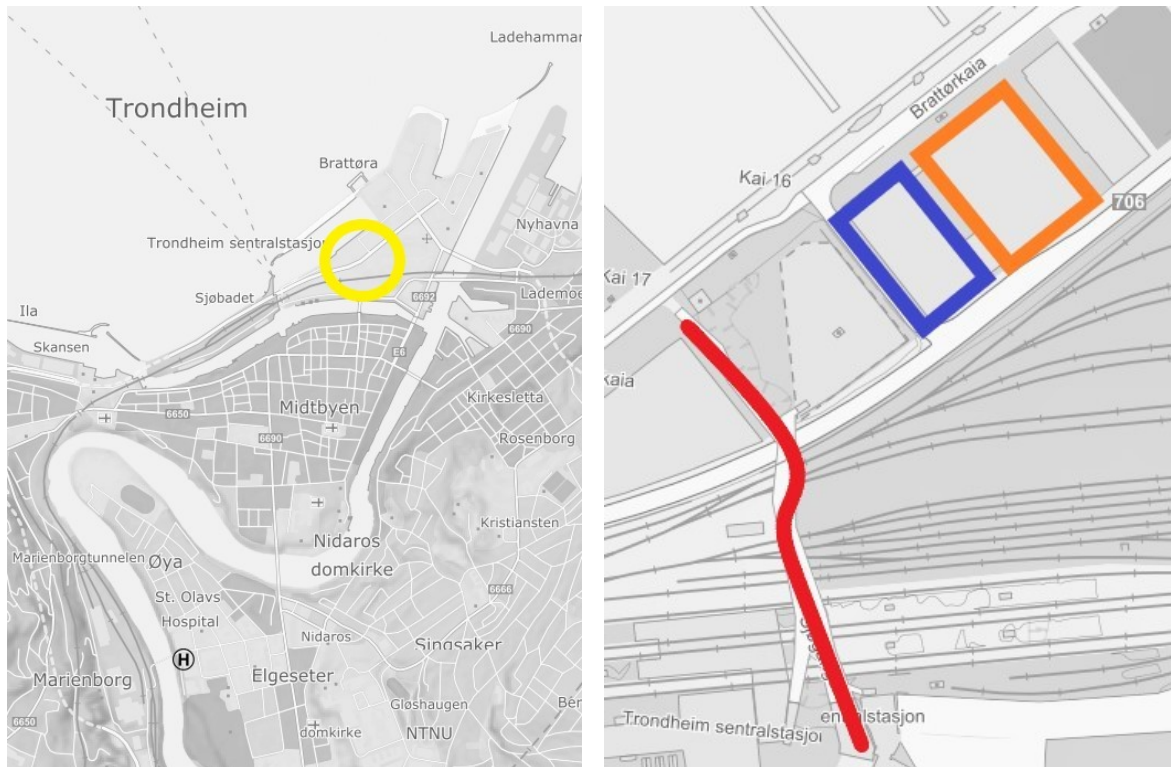
5.2 Background

5.2.1 Brattøra

Brattøra is a city district and harbour area in Trondheim that has been under great urban development the recent years [75][76]. When Brattøra's planned projects are finalised, the district will be an important hub for public transportation and house a great amount of workplaces and businesses, residents, and experience and recreational industries [76][77].

Such fast development of a district will cause an increase in power demand. This comes with a few challenges for the DSO as it potentially leads to congestion and need for grid expansions. With the underlying motivation to increase energy efficiency and postpone possible grid investment costs, the case study is relevant for seeing the effects of using a battery for increasing energy efficiency, peak shaving for the respective buildings and decreasing total system costs for the community.

There are three "buildings" analysed in this case study; two office buildings: Brattørkaia 15A,B and Brattørkaia 16. They will be referred to as BK15AB and BK16 respectively. Lastly, there is a walking bridge called Sjøgangen. The two office buildings and Sjøgangen will be referred to as "buildings", and they are located at Brattøra as marked in Figure 5.1a. The geographical relation of the buildings at Brattøra is shown in Figure 5.1b, where Sjøgangen is shown in red, BK16 is shown in blue, and BK15AB is shown in orange.



(a) Map over Trondheim city showcasing Brattøra and the specific area investigated for the case study

(b) Map showing Sjøgangen(red), BK16(blue) and BK15AB's(orange) geographical relation

Figure 5.1: Maps over Brattøra and Sjøgangen, BK15AB and 16 specifically (The Norwegian Mapping Authority/Kartverket)

5.2.2 Buildings

This section is a closer description of the buildings included in the community system located at Brattøra. The goal is to give an understanding of the consumption and production patterns and the factors in which they depend on.

5.2.2.1 Brattørkaia 15AB

At Brattørkaia 15AB, there are two associated buildings with 5 and 6 stories that are mainly used as office buildings [78]. BK15AB is a passive house built in 2013 [79], and is BREEAM(Building Research Establishment Environment Assessment Method) certified as a "Very Good" building when it comes to energy efficiency and sustainability [78][80].

5.2.2.2 Brattørkaia 16

The building at Brattørkaia 16 was built for BI Norwegian Business School, and was finalised in 2018 [81]. The intention was to build a sustainable and energy efficient building, which is now BREEAM-NOR certified as "Excellent" [82]. The building has PV panels installed on the roof with an expected solar power production of 152MWh per year [82].

5.2.2.3 Sjøgangen

Sjøgangen is a walking bridge that stretches across Trondheim central station and the railroad tracks connecting the Brattøra area to Trondheim city centre [83]. A conversation with a service electrician that has been working with the bridge the recent years, conveyed that there are heating cables in the concrete walkway in order to keep the bridge free from snow and ice during the winter. A control system turns the heating cables on when a weather station placed on the bridge detect any precipitation with temperatures under a specific set-value.

5.2.3 The Battery

According to key sources from Trønderenergi AS, an Alfen battery that is currently used for a microgrid project will be moved to Brattøra to contribute to a local flexibility market project. The case study will be based on utilising this specific battery. It is a battery of the type "TheBattery TB-548-1C" with a usable energy storage capacity of 521kWh [84]. The battery have been operated by Trønderenergi for a while and shows a 92% charging efficiency and 95% discharging efficiency.

The rated power for the battery is 636 kVA at 25°C[84]. However, the active power limit for charging and discharging is set to 200kWh/h for the optimisation programme. This limit is set to restrict the amount of battery cycles. It is assumed that the initial energy stored in the battery is 300kWh, and therefore the final condition of energy stored in the battery at the end of the scheduling horizon should be 300kWh as well. The battery parameters used in the RHC model is summarised in Table 5.1.

Parameter	Value
Energy storage capacity	521kWh
Charge/Discharge limit	200kWh/h
Charging efficiency	92%
Discharging efficiency	95%
Initial battery storage	300kWh
Final battery storage	300kWh

Table 5.1: Battery parameters used for the optimisation model

5.2.4 Energy Price and Grid Tariff Pricing Models

5.2.4.1 Spot Prices

For the case studies it is assumed that all buildings at Brattøra have a market based spot price agreement with their power retailer. Another assumption regarding the spot prices is that they will be known for the full analysis month. The pricing values for 2020 are retrieved from Nord Pool[39], and the obtained prices are concerning the area surrounding Trondheim, called NO3[38]. The spot prices for January, March and June 2020 are plotted in Figure 5.2.

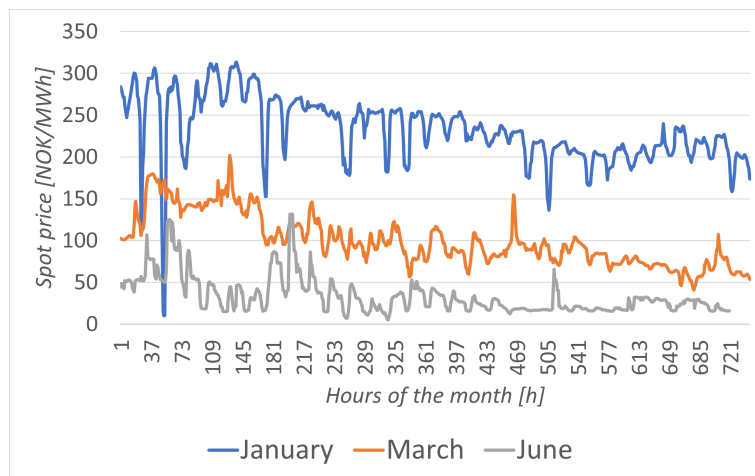


Figure 5.2: The spot prices for January, March and June 2020

5.2.4.2 Pricing Model

Since this study seeks to examine a s-BESS's ability to shave the power peaks, a pricing model which gives a reasonable peak shaving incentives will be applied to the optimisation model. The case study will therefore be based on Elvia's winter pricing model for commercial buildings in 2020[85]. Elvia is the DSO of Oslo/Viken and Innlandet, and since Oslo is a city with assumable similar congestion problems as Trondheim, Elvia's winter pricing model, shown in Table 5.2, will be representative for this case study, which includes consumption tax and the surcharge to Enova's energy fund[85][86]. VAT is excluded[85], and it is assumed that all the buildings in the case study has a main fuse over 125A by 230V or 80A by 400V[85].

The power tariff in winter is usually higher than in summer, this is to reflect that winter season is the most critical season as the power consumption is at its highest. Although the case study is conducted for several seasons, Elvia's winter pricing model is used for all months investigated. This is because these winter dominated power tariffs creates incentives to reduce maximum power consumption[85].

Fixed part	
Fixed price	3280 NOK/yr/meter-ID
Surcharge to Enova's energy fund	800 NOK/yr/meter-ID
Energy based part	
Energy price winter (nov-mar)	0.07 NOK/kWh
Consumption tax	0.1613 NOK/kWh
Power based part	
Power tariff winter 1 (dec-jan)	150 NOK/kW/month

Table 5.2: Elvia's power based grid tariff pricing model for low voltage commercial buildings

5.3 Simulated Cases

The cases investigated for this study are based on the configurations presented in Section 4.1 in order to compare the different approaches to shared storage storage with each other and with individual storage and base case. The base case configuration is a business as usual case with no available BESS or local energy market and with individual metering for the respective buildings in the case study.

For configuration 3 and 6 with individual storage, three cases will be run with individual storage for each of the buildings. Case 3.1, 3.2 and 3.3 are all run with the mathematical model for configuration 3, referring to individual storage for BK15AB, BK16 and Sjøgangen respectively. The same yields for case 6.1, 6.2 and 6.3, where all cases are run with the mathematical model formulation for configuration 6.

There are two cases conducted for configuration 4 as well, one with a shared community BESS and one without access to battery storage at all. This is done in order to quantify the possible benefits of a local energy market alone and the benefits by including a BESS in a local energy market.

The different cases investigated in this case study is summarised in Table 5.3, where the description of their configuration's physical characteristics are showed.

Cases	Base case	Configuration 1	Configuration 2	Configuration 3.1 (BK15AB)	Configuration 3.2 (BK16)	Configuration 3.3 (Sjøgangen)	Configuration 4 with battery	Configuration 4 without battery	Configuration 5	Configuration 6.1 (BK15AB)	Configuration 6.2 (BK16)	Configuration 6.3 (Sjøgangen)
Characteristics												
Joint metering												
Local energy market												
No battery												
Individual battery												
Battery access to grid												
Battery access to local energy market												

Table 5.3: Overview over the different cases investigated in the case study with their physical characteristics

6 | Scenario Modelling

As described in Chapter 4, the production and consumption of the different commercial buildings analysed are seen as stochastic beyond the prediction horizon. This chapter describes the procedure of creating realistic scenarios for these variables, by means of time series forecasting, that will be used for the stochastic optimisation problem.

Historical data of the power production and consumption are analysed, modelled and later used to create forecasts used for scenario generation. The analysis of this chapter will be based on historical data from 2019. The analysis will consider four forecast variables $y_{1,t}$, $y_{2,t}$, $y_{3,t}$ and $y_{4,t}$, referring to the consumption at BK15AB, consumption at BK16, production at BK16 and consumption at Sjøgangen respectively. The regression expressions of the forecast variables will be derived in the following sections.

6.1 Time Series Analysis for Case Study

This section will analyse the $y_{1,t}$, $y_{2,t}$, $y_{3,t}$ and $y_{4,t}$ time series. Autoregressive models of each variable y , will be developed through systematic investigation of appropriate predictor and lag variables.

6.1.1 Introduction of Forecast Variables

In order to visualise patterns and seasonal trends, Figure 6.1 show plots of historical data from 2019 for all forecast variables. Simple analyses of the entire data set of each forecast variable allow easier selection of which factors should be considered for the more detailed analysis.

BK15AB and BK16 are both office buildings, and therefore present similar consumption patterns. There exists an obvious pattern in both Figure 6.1a and 6.1b, that repeats at constant intervals, indicating that the time series has a prominent seasonal component. The plots also show a conspicuous reduction in power consumption during Easter, summer and Christmas holidays.

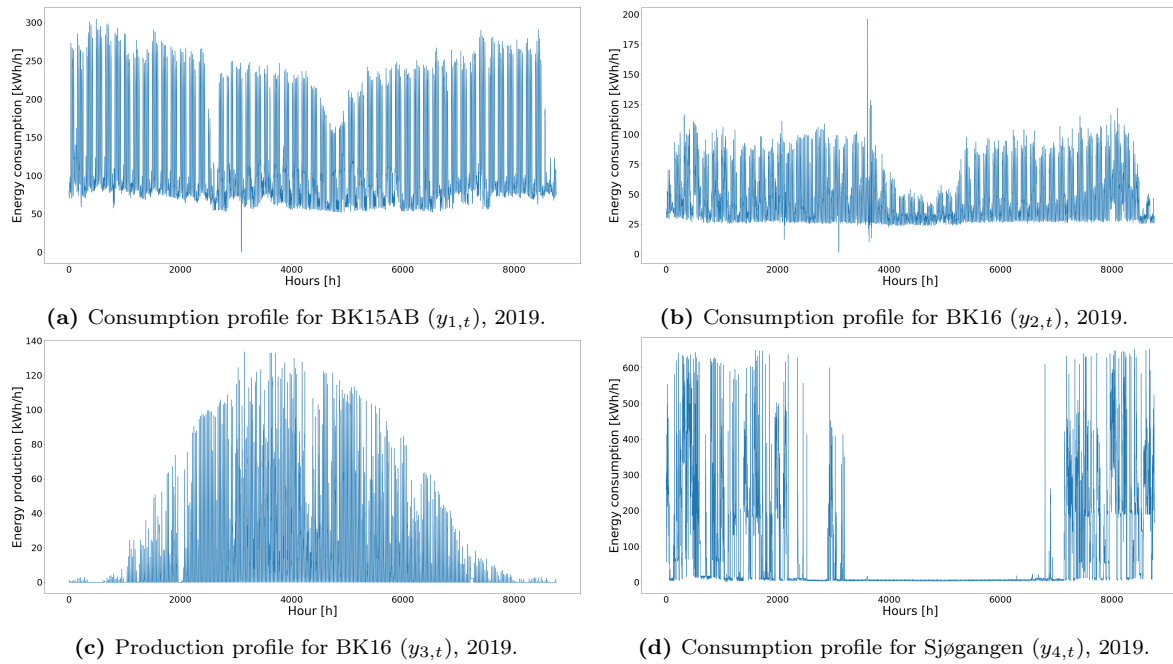


Figure 6.1: Presentation of the time series of each forecast variable

As one would expect, Figure 6.1c reveals increasing power production during summer months when solar irradiation is higher and regular drops representing the no production hours during night time. It is reasonable to assume the irregular drops are caused by random factors such as clouds, which would restrict production.

For simplicity, it is assumed that the consumption at Sjøgangen act as a regular time series. In reality, the irregular consumption at Sjøgangen makes it an intermittent time series, however, such special treatment of time series are considered out of scope. Still, this will affect the results of the scenario modelling at Sjøgangen. As the need for snow melting varies, Figure 6.1d shows fluctuating and seemingly random large power consumption peaks during winter season, whereas the consumption during summer season appears stable and close to zero.

6.1.2 Auto Regressive Model

6.1.2.1 Checking for Stationarity in Forecast Variables

Each forecast variable is checked for stationarity by means of the Augmented Dickey-Fuller test. The test is run on historical data from 2019, which is the data that will be used to derive the regression expression for each forecast variable. The critical limit for the p-value was set to 5%. The results can be found in Table 6.1. All variables are well within the critical limits for both the p-value and test statistic, even with a 1% significance level. Consequently, the null hypothesis can be rejected for all cases, implying that all forecast variables are stationary.

	$y_{1,t}$	$y_{2,t}$	$y_{3,t}$	$y_{4,t}$
ADF test statistic	-13,075	-9,615	-5,808	-6,655
p-value	$1.920 \cdot 10^{-24}$	$1.774 \cdot 10^{-16}$	$4.460 \cdot 10^{-7}$	$5.022 \cdot 10^{-9}$
1%	-3.431	-3.431	-3.431	-3.431
10%	-2.567	-2.567	-2.567	-2.567
5%	-2.862	-2.862	-2.862	-2.862

Table 6.1: Results from the Augmented Dickey-Fuller test for each forecast variable

6.1.2.2 Correlation with Temperature

Building energy consumption in Norway can be assumed to increase during the winter season for heating purposes when outdoor temperatures are low. Consumption at Sjøgangen occurs at low outdoor temperatures, and though not caused by increased temperatures, solar power production increases during summer months when irradiation and, consequently, temperatures are higher. Correlation plots between the consumption of each building and temperature was created and can be seen in Figure 6.2. Although showing weak correlation with temperature, the consumption at each building is negatively correlated to outdoor temperature, while the production is positively correlated, as expected. To simplify the scenario generation process it will therefore be assumed that all forecast variables are correlated to outdoor temperature and therefore dependent on the same predictor variable T_t . This allows for fewer simulations as each realisation of the forecast variables can be assumed to belong to the same scenario when generated in the same simulation.

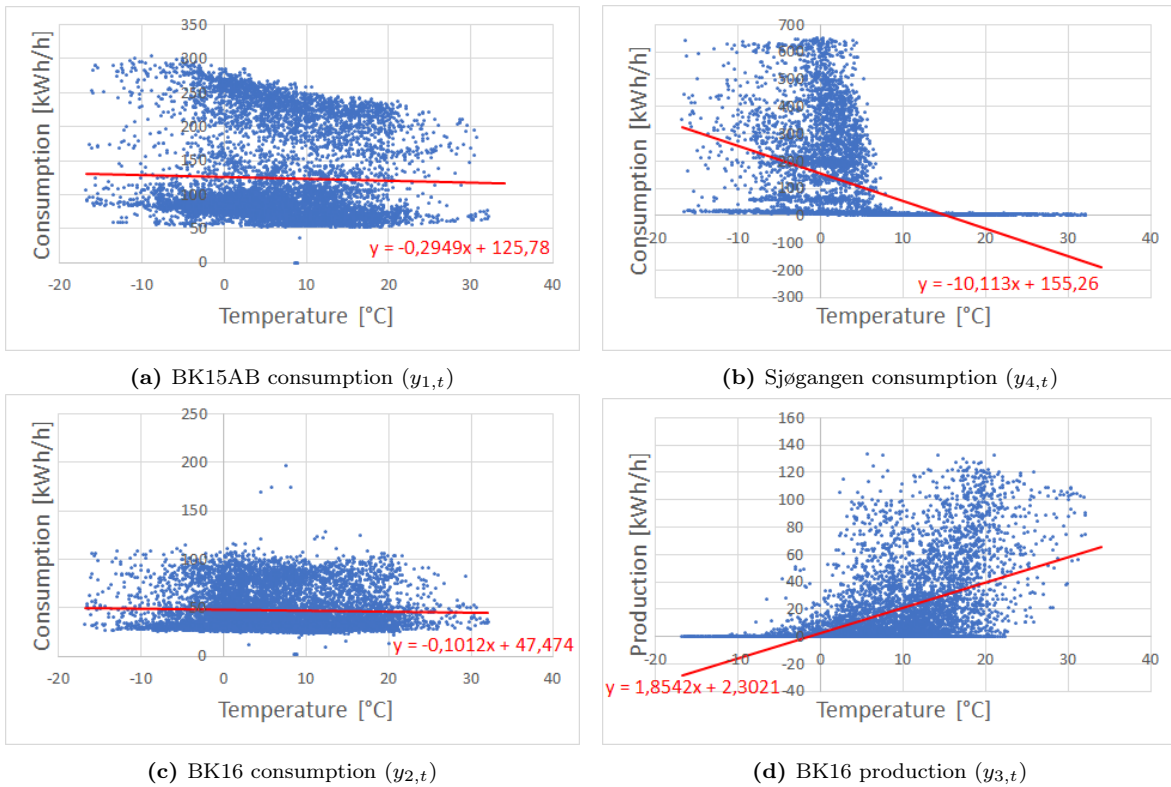


Figure 6.2: Correlation between temperature and the forecast variable at each building

6.1.2.3 Non-seasonal Predictor Variables

As stated in section 6.1.2.2, solar irradiation can be considered closely related to the amount of solar power production. The correlation between solar irradiation and power production at BK16($y_{3,t}$) is shown in Figure 6.3. There exists an obvious positive linear relationship between the two variables. Therefore, solar irradiation, I_t , is added as a predictor variable for the regression expression of $y_{3,t}$.

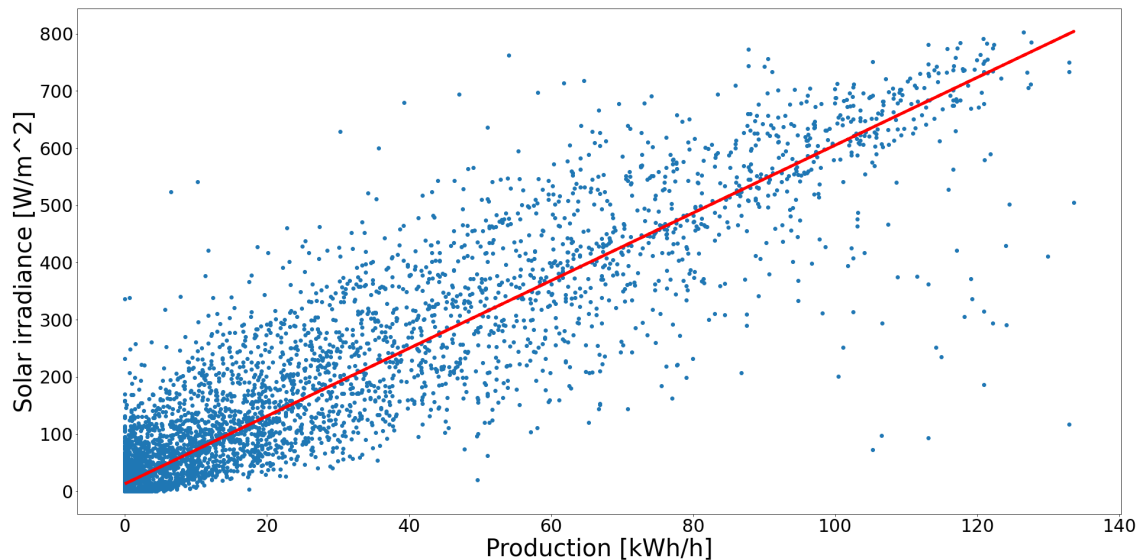


Figure 6.3: Correlation between solar irradiation and production at BK16($y_{3,t}$)

Figure 6.2b depicts an obvious correlation between outdoor temperatures and power consumption at Sjøgangen, however, the relation does not appear to be linear. The control system of the bridge is programmed to turn on whenever temperatures below a critical limit and precipitation occurs simultaneously. In an attempt to imitate this effect, three dummy variables are added to the regression expression for $y_{4,t}$. The dummies $d_{1,t}$, $d_{2,t}$ and $d_{3,t}$ are created to represent the occurrence of cold temperatures, the occurrence of precipitation and the union of the occurrence of both cold temperatures and precipitation. The first two dummies, $d_{1,t}$ and $d_{2,t}$, are mainly added to enhance the effect of the third dummy as the power consumption can be relatively large.

6.1.2.4 Autocorrelation in Forecast Variables

As stated in Section 3.2.2, electricity demand is typically an autocorrelated time series. As the probability of solar irradiation also can be considered conditional given the event that there was irradiation in previous hours, autocorrelation and partial autocorrelation plots are created for all forecast variables. The plots for BK15AB($y_{1,t}$) and Sjøgangen($y_{4,t}$) can be seen in Figure 6.4 and 6.5 respectively. The autocorrelation and partial autocorrelation plots for energy consumption and production at BK16($y_{2,t}$ and $y_{3,t}$) show similar patterns as in Figure 6.4. Figure 6.4b show significant correlation between the forecast variable and its first two time lags, indicating that these should be included in the autoregressive model for $y_{1,t}$, $y_{2,t}$ and $y_{3,t}$. The damped sinusoidal pattern in Figure 6.4a indicates the presence of a seasonal component in the time series data, which repeats every 24 hours. Figure 6.5b shows significant correlation between the forecast variable and the first time lag, this suggests that only the first lag should be included in the autoregressive model for $y_{4,t}$.

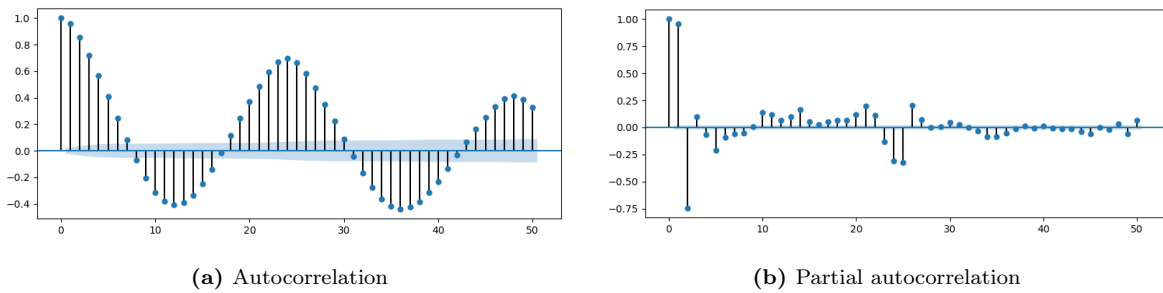


Figure 6.4: Autocorrelation and partial autocorrelation plots for the consumption at BK15AB($y_{1,t}$).

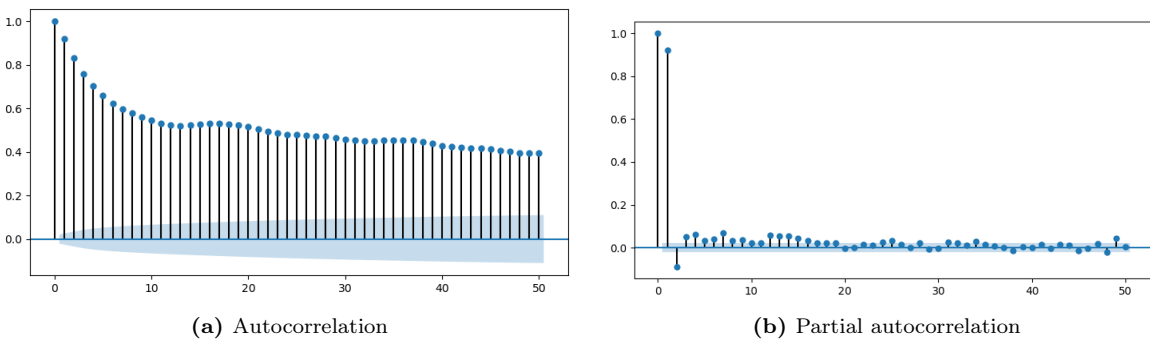


Figure 6.5: Autocorrelation and partial autocorrelation plots for consumption at Sjøgangen($y_{4,t}$).

6.1.2.5 Seasonality in Forecast Variables

The consumption profile for BK15AB and BK16, depicted in Figure 6.1a and 6.1b, both show a distinct and similar weekly pattern. Seasonality curves for the two forecast variables $y_{1,t}$ and $y_{2,t}$ are therefore created, using historical data from 2019, for further insight into the seasonality of the time series. The plots for weekly and daily seasonality for $y_{1,t}$ can be seen in Figure 6.6 and 6.7 respectively. By analysing Figure 6.6 it is evident that the power consumption during weekends is much lower than for the rest of the week. Figure 6.7 provides a more detailed illustration of which hours during the day consumption is high. The plot shows a clear correlation between working hours and peak consumption hours. Similar trends can be seen in the seasonality plots for $y_{2,t}$.

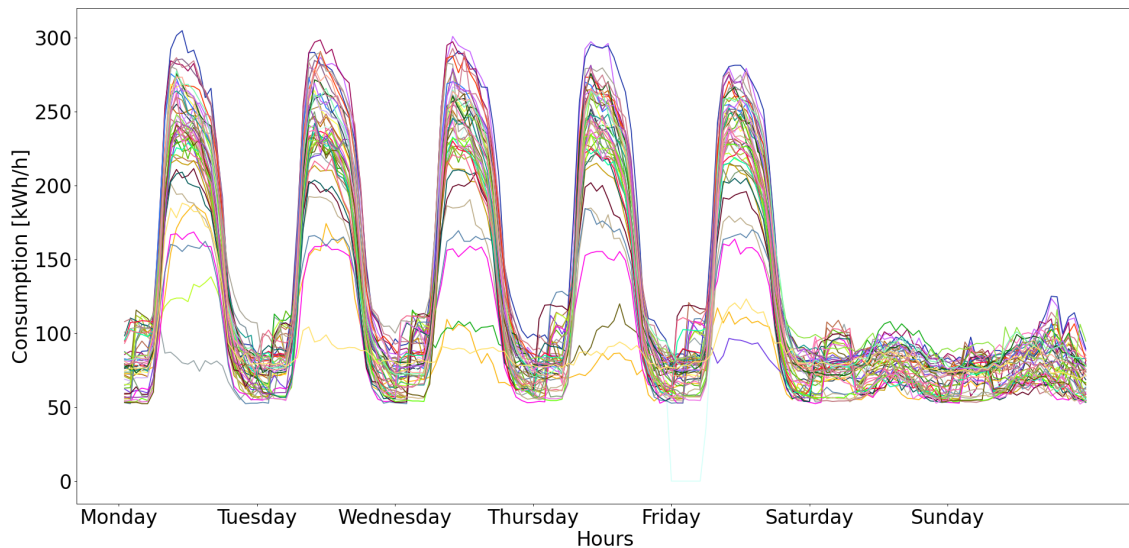


Figure 6.6: Weekly seasonal plot of the power consumption at BK15AB in 2019

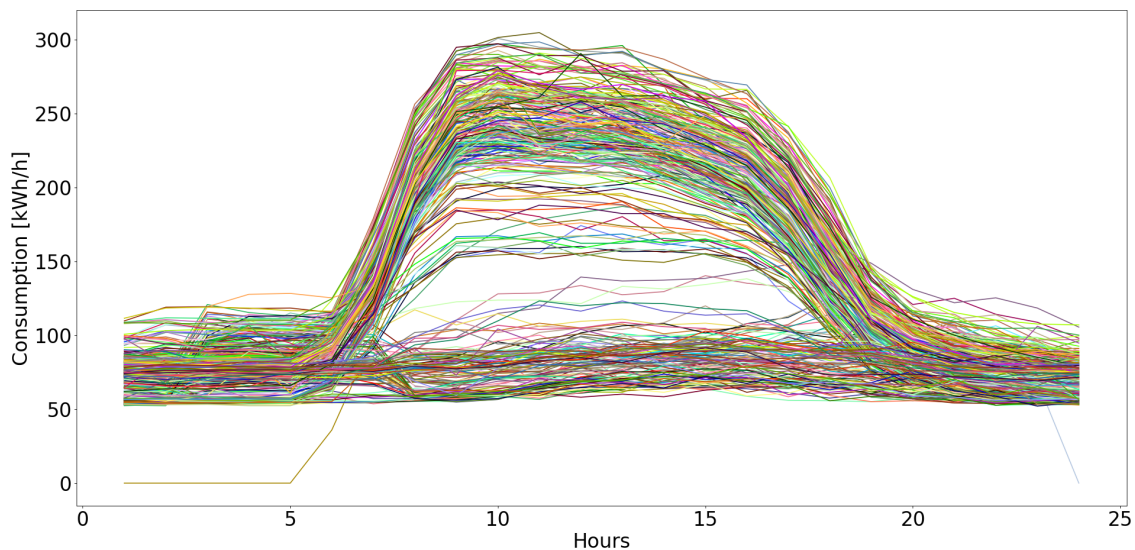


Figure 6.7: Daily seasonal plot of the power consumption at BK15AB in 2019

Based on the seasonality plots the regression expression for $y_{1,t}$ and $y_{2,t}$ is extended by a set of dummy variables to encapsulate the seasonality of the time series. Three dummy variables $d_{1,t}$, $d_{2,t}$ and $d_{3,t}$ are added to represent weekday working hours, weekday peak working hours and weekend working hours respectively. The dummies take the value $d_{w,t} = 1$ if the current time step is classified as a working hour within their respective working hour categories w . For example, if considering $y_{1,t}$, $d_{1,t} = 1$ if t falls within hours 7-18 of the nychthemeron, 0 otherwise. It should be emphasised that the working hour categories overlap so as to enhance each others effects and do not cause perfect multicollinearity, as no dummy is created for the intercept of each category. In other words, the perfect multicollinearity is avoided by ensuring that no category for non-working hours exist. As stated previously in this chapter, consumption for the two office buildings tends to be lower during holidays. Therefore, a fourth dummy variable, $d_{4,t}$, for working hours during a holiday, is also added to account for this effect.

6.1.2.6 Resulting Autoregressive Models of the Time Series

The resulting autoregressive model for each forecast variable is shown in equations (6.1) to (6.4). The parameter values for the predictor variables were estimated based on historical data from the first 4380 hours of 2019, for each forecast variable. The parameters were estimated by means of the AutoReg function, available through the statsmodels module in Python.

$$y_{1,t} = \alpha + \beta_0 T_t + \beta_1 d_{1,t} + \beta_2 d_{2,t} + \beta_3 d_{3,t} + \beta_4 d_{4,t} + \phi_1 y_{1,t-1} + \phi_2 y_{1,t-2} + \varepsilon_t \quad (6.1)$$

$$y_{2,t} = \alpha + \beta_0 T_t + \beta_1 d_{1,t} + \beta_2 d_{2,t} + \beta_3 d_{3,t} + \beta_4 d_{4,t} + \phi_1 y_{2,t-1} + \phi_2 y_{2,t-2} + \varepsilon_t \quad (6.2)$$

$$y_{3,t} = \alpha + \beta_0 T_t + \beta_1 I_t + \phi_1 y_{3,t-1} + \phi_2 y_{3,t-2} + \varepsilon_t \quad (6.3)$$

$$y_{4,t} = \alpha + \beta_0 T_t + \beta_1 d_{1,t} + \beta_2 d_{2,t} + \beta_3 d_{3,t} + \phi_1 y_{4,t-1} + \varepsilon_t \quad (6.4)$$

An overview of the predictor variables and their respective parameters for each forecast variable is shown in Table 6.2. As the intercept α of $y_{3,t}$ was estimated to less than zero, the forecast variable was manually forced to never be negative.

Stochastic Variables	Predictor Variables	Variable	Parameter	p-value P > z	z-value	Standard Error
$y_{1,t}$ (BK15AB Consumption)	Intercept		$\alpha = 35.7653$	0.000	65.638	0.545
	Outdoor temperature	T_t	$\beta_0 = -0.5502$	0.000	-26.214	0.021
	Weekday working hour	$d_{1,t}$	$\beta_1 = 30.2184$	0.000	41.536	0.728
	Weekday peak working hour	$d_{2,t}$	$\beta_2 = 29.4528$	0.000	38.890	0.757
	Weekend working hour	$d_{3,t}$	$\beta_3 = 1.0036$	0.040	2.056	0.488
	Holiday Hours	$d_{4,t}$	$\beta_4 = -14.0224$	0.000	-9.838	1.425
	Time lag 1	$y_{1,t-1}$	$\phi_1 = 1.0243$	0.000	77.197	0.013
	Time lag 2	$y_{1,t-2}$	$\phi_2 = -0.4166$	0.000	-44.350	0.009
$y_{2,t}$ (BK16 Consumption)	Intercept		$\alpha = 8.7955$	0.000	26.252	0.335
	Outdoor temperature	T_t	$\beta_0 = -0.0805$	0.000	-5.269	0.015
	Weekday working hour	$d_{1,t}$	$\beta_1 = 5.8251$	0.000	15.125	0.385
	Weekday peak working hour	$d_{2,t}$	$\beta_2 = 4.6921$	0.000	10.711	0.438
	Weekend working hour	$d_{3,t}$	$\beta_3 = 3.7521$	0.000	9.346	0.401
	Holiday Hours	$d_{4,t}$	$\beta_4 = -1.3215$	0.221	-1.224	1.079
	Time lag 1	$y_{2,t-1}$	$\phi_1 = 1.0747$	0.000	68.077	0.016
	Time lag 2	$y_{2,t-2}$	$\phi_2 = -0.3221$	0.000	-23.429	0.014
$y_{3,t}$ (BK16 Production)	Intercept		$\alpha = -0.6951$	0.000	-5.010	0.139
	Outdoor temperature	T_t	$\beta_0 = 0.0365$	0.045	2.002	0.018
	Solar irradiation	I_t	$\beta_1 = 0.0714$	0.000	59.437	0.001
	Time lag 1	$y_{3,t-1}$	$\phi_1 = 0.6682$	0.000	47.684	0.014
	Time lag 2	$y_{3,t-2}$	$\phi_2 = -0.1271$	0.000	-11.358	0.011
$y_{4,t}$ (Sjøgangen Consumption)	Intercept		$\alpha = 15.4098$	0.009	2.599	5.928
	Outdoor temperature	T_t	$\beta_0 = -1.7726$	0.000	-3.657	0.485
	Cold temperatures	$d_{1,t}$	$\beta_1 = 9.6798$	0.167	1.381	7.007
	Precipitation	$d_{2,t}$	$\beta_2 = 7.3687$	0.406	0.830	8.873
	Cold temp. \cup precipitation	$d_{3,t}$	$\beta_3 = 52.4760$	0.000	5.006	10.482
	Time lag 1	$y_{1,t-1}$	$\phi_1 = 0.8112$	0.000	70.335	0.012

Table 6.2: Table showing the predictor variables used to model the consumption and production for the different buildings and their respective parameters. The less significant parameters are marked in grey.

The p-values above 5% for Cold temperatures and Precipitation ($d_{1,t}$ and $d_{2,t}$ for $t_{4,t}$) and Holiday Hours ($d_{4,t}$ for $y_{2,t}$) indicate that these parameters are unnecessary. Simple tests without the aforementioned parameters were conducted. The results indicated that the model performed worse, and the parameters were therefore kept. The large z-values for the lag variables indicate that the autoregressive models could have been improved. However, due to time restrictions and based on the results from the Dickey-fuller test which proved stationarity, no corrections were made. Generally the standard errors are small, indicating that the confidence interval for the value of most parameters is relatively narrow, which in turn implies rather accurate values.

6.1.2.7 Evaluation of Model Performance

In order to investigate the accuracy of the autoregressive models, the first three models were tested for the last 4380 hours of 2019, while $y_{4,t}$ was tested for the last 2190 hours of 2019 due to inactivity during the summer months when temperatures are high. The lag variables and dummies were assumed to be known and based on historical data from 2019. Figures G.1 to G.4 in Appendix G show a segment of the predictions for forecast variable $y_{1,t}$, $y_{2,t}$, $y_{3,t}$, $y_{4,t}$ respectively.

The error between the actual realisation of each forecast variable and its predicted value was recorded in order to find the mean, μ_n , and standard deviation, σ_n of the sample. The results are presented in Table 6.3 together with the root mean square error. The prediction errors for each forecast variable was deemed qualified to be considered normally distributed. Their distributions can be seen in Figure 6.8.

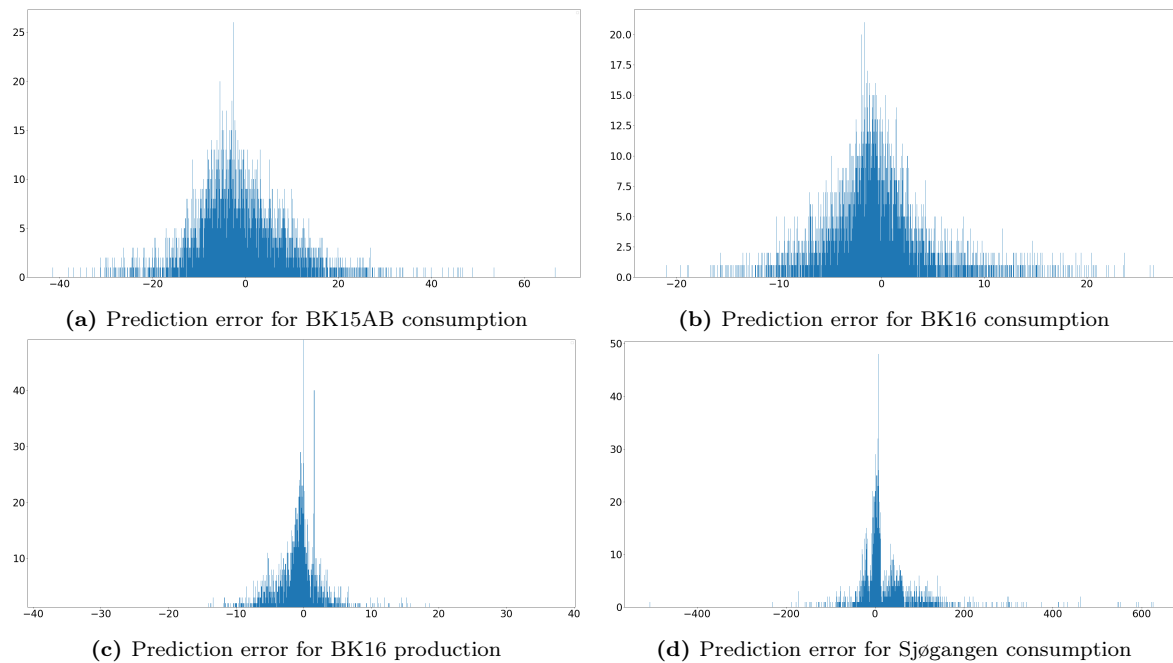


Figure 6.8: Distribution of the prediction error for each forecast variable

	$y_{1,t}$	$y_{2,t}$	$y_{3,t}$	$y_{4,t}$
Standard Deviation σ_n	10.4799	5.4933	4.7517	79.3525
Mean μ_n	-1.0468	-0.3597	-0.2277	28.4954
RMSE	10.532	5.505	4.757	84.314

Table 6.3: Standard deviation and mean of prediction error for each forecast variable

The standard deviation and mean of the prediction error for $y_{4,t}$ is relatively large, indicating that the time series is not modelled well enough. In general it is expected that the mean of the sample should be zero. However, the inaccuracy of the autoregressive model for $y_{4,t}$ is ignored as Sjøgangen in reality should have been modelled as an intermittent time series. Based on the RMSE, all autoregressive models were considered sufficiently accurate. Hence, no corrections were made to the regression expressions before applying them for scenario generation.

6.2 Scenario Generation and Reduction

This section will focus on how the autoregressive models derived in the previous sections are used to generate realistic scenarios through time series forecasting. To ensure scenarios that encapsulate usual trends, the amount of generated scenarios should be high enough to cover the spectrum of plausible outcomes and not just extreme values. The generated scenarios should then be reduced to a reasonable amount of scenarios with respect to computational time limitations. The reduced scenarios should reflect the basic trends of the generated scenarios with a corresponding probability of realisation for each scenario.

6.2.1 Scenario Generation

The scenario generation process for this case study is based on the assumption that forecasting of the predictor variables is possible, available through external vendors, and consequently considered known for the entire scheduling horizon.

The solution strategy for the scenario generation process is shown in Algorithm 1. N_s denotes the number of scenarios, N_y denotes the number of forecast variables, while T denotes the hours in the second stage problem.

```
1 while  $s < N_s$  do
2   for  $n \in N_y$  do
3     for  $t \in T$  do
4       generate random error  $\varepsilon_t \sim N(\mu_n, \sigma_n^2)$ ;
5       generate  $y_{n,t}$  with  $\varepsilon_t$ ;
6       add  $y_{n,t}$  to history;
7     end
8   end
9 end
```

Algorithm 1: Algorithm describing the logic of the scenario generation process

To create forecasts of each forecast variable, an error term with a normal distribution and a corresponding mean and standard deviation, was generated and added to the relevant regression expression. The calculated value of $y_{n,t}$ was then stored and used as a lag variable when calculating $y_{n,t+1}$. This will lead to consequential errors (which is one reason why a good prediction model does not necessarily imply good forecasts), however, this is considered to appropriately model the nature of uncertainty in forecasting. This process was repeated for each time step in the remainder of the second stage problem to form a complete scenario. The probability, π_s , of realisation of scenario s was set to be equal for all scenarios in N_s .

Preliminary results from a test run of the scenario generation model can be found in Appendix H. The plots illustrate and provide useful information on the accuracy of the forecasts. $y_{1,t}$ gives pretty accurate forecasts and is able to follow the general trends of the time series. $y_{2,t}$ underestimates power peaks during working hours and predicted peak values stabilise around a level below what could be expected. $y_{3,t}$ is often estimated to have a value larger than zero during night time due to the error term, as nothing corrects for this. However, this will probably not affect optimal scheduling as consumption is low during these hours and therefore already unlikely to affect Δp_s^{sys} . $y_{4,t}$ is largely affected by the error term, leading to predictions of high power peaks far beyond what could be expected.

6.2.2 Scenario Reduction

SCENRED has been used to conduct the scenario reduction process. SCENRED is a tool provided by GAMS Development Corporation. In line with the theory presented in Section 3.2.4, the scenario reduction algorithms provided by SCENRED determine a subset of the initial set of scenarios and assign new optimal probabilities to the preserved scenarios [87]. The number of reduced scenarios can be specified within the program. The preserved scenarios with their respective probabilities are used to model future uncertainty in the second stage problem of the optimisation model.

6.2.3 Optimising the Amount of Scenarios

Prior to performing the case study, a sensitivity analysis was performed to find the optimal amount of generated and reduced scenarios. Due to the stochasticity of the presented optimisation problem, this sensitivity analysis was performed in order to ensure that the optimal solution of the optimisation problem converges. The variability of the objective value was used as the measure of accuracy and the test period was set to 72 hours.

Table 6.4 gives a summary of the stability of the objective value when increasing the number of reduced scenarios and keeping a constant number of generated scenarios of 1000. The analysis shows that the maximum change in objective value, relative to having 3 reduced scenarios, is 1.2%.

6.2. SCENARIO GENERATION AND REDUCTION

Number of reduced scenarios	3	4	5	6	7	8	9	10	11	12
Objective value [NOK]	51580	51147	51031	51371	51142	51187	51052	50962	51014	51053
% change in objective value	0.0	-0.8	-1.1	-0.4	-0.9	-0.8	-1.0	-1.2	-1.1	-1.0

Table 6.4: Evaluation of solution stability with varying number of reduced scenarios and a constant number of generated scenarios of 1000. The percent change in objective value is calculated relative to having 3 reduced scenarios.

The results show no significant change in the objective value with a number of reduced scenarios larger than 3. In line with previous statements of this section, it was considered necessary to generate a sufficient amount of scenarios to ensure a good representation of all possible outcomes. However, with respect to computational time it was concluded that 500 scenarios should be generated and later reduced to 3 scenarios.

7 | Results and Observations

This chapter shows the results and observations obtained from the case study. In addition, deviating values and trends connected to the design of the mathematical model are explained. The most important findings from the case study are considered to be the results regarding battery scheduling, peak shaving effects, self-sufficiency, self-consumption and the cost contributions and savings. When not specifically stated, referring to configuration 3, 4 or 6 will imply all subcases investigated for the respective configuration. Lastly, the results from a brief sensitivity analysis on the MP tariff pricing model is presented.

7.1 Battery Scheduling

The scheduling of the battery differ for every case conducted. An example is the number of battery cycles which varies between 0 and 25 cycles and with different depth of discharge depending on the case and season. Figure 7.1 show the battery energy storage pattern for configuration 1 in March, which shows a lower number of battery cycles, and a high utilisation of the battery charge and discharge capacity when charging or discharging. Figure 7.2 represents the opposite. It depicts the battery energy storage pattern for configuration 3.2 in June, and shows a higher amount of battery cycles. The charging/discharging operations happens often, but the full charge/discharge capacity is rarely fully exploited.

By observing the battery storage curves for each configuration, it is apparent that there are a few trends regarding the number of battery cycles. First, there seem to be a lower number of battery cycles in March compared to January and June. In addition, case 3.1 and 3.2 seem to have a higher number of battery cycles than other configurations throughout the seasons. For configuration 2, the BESS is not utilised at all for any of the investigated months.

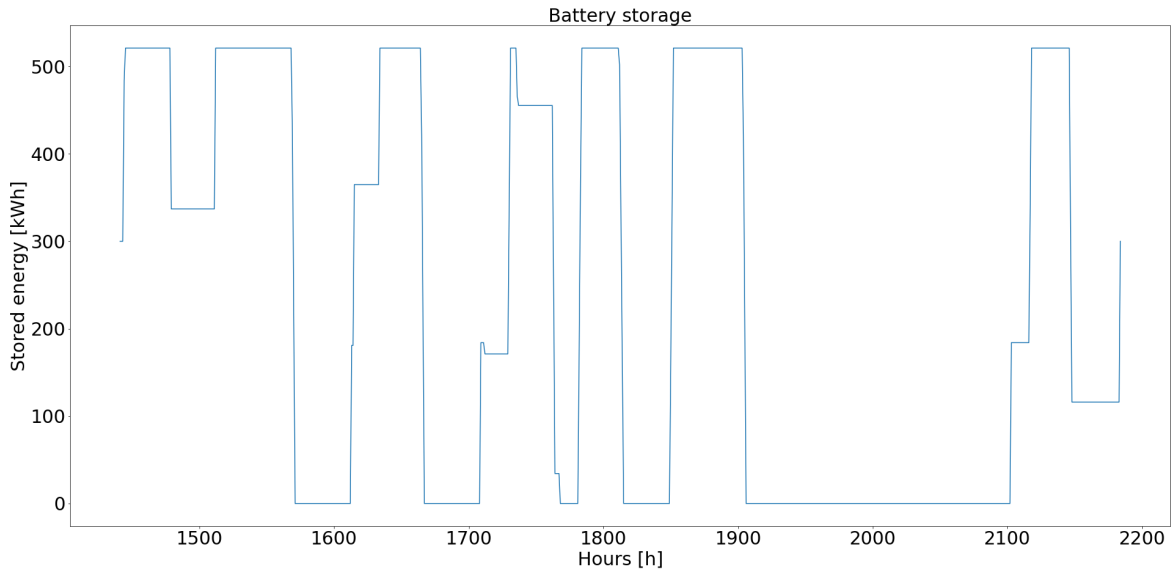


Figure 7.1: The battery energy storage pattern for configuration 1 in March

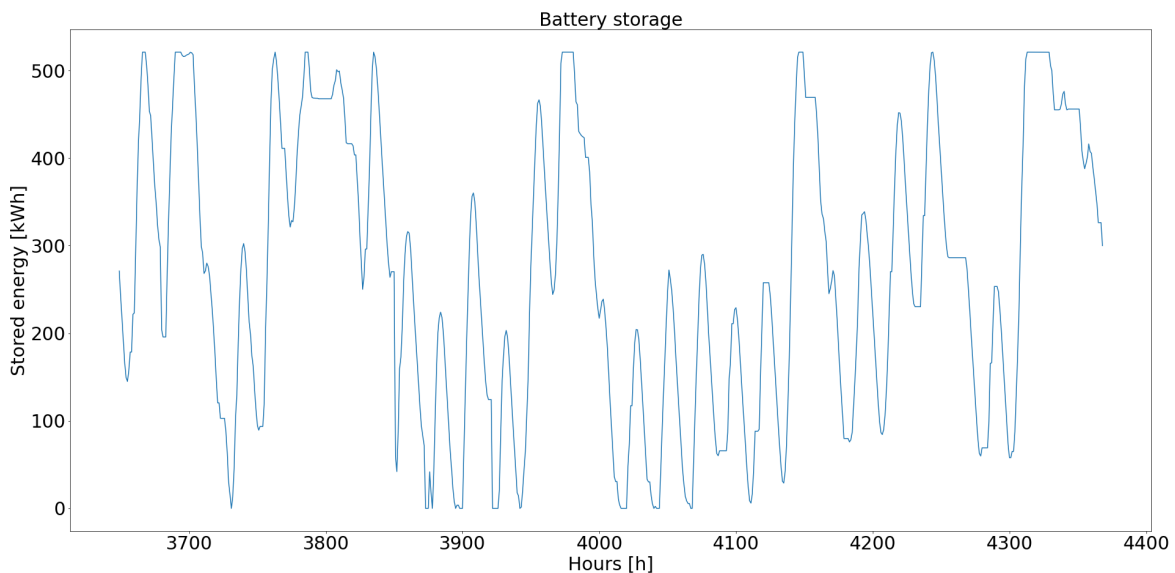


Figure 7.2: The battery energy storage pattern for configuration 3.2 in June

7.2 Peak Shaving

The peak shaving results show to which extent the BESS manages to reduce the community and the buildings' power peaks for the different configurations in different months of the year. In general, the results prove that there is a substantial peak shaving effect when the predicted power peaks of the scenarios correspond well to the actual consumption's peak.

Figure 7.3 show an example of peak shaving after running configuration 3.1 for January. The figure shows the net import for BK15AB in blue in addition to the predicted future power peak for each scenario in each time step. The net import clearly reflects

an increased consumption during working hours. However, the daily import curves are flat for midday hours, indicating a significant peak shaving result. The plotted curves representing the predicted power peak correspond well to actual peaks for all time steps, resulting in a substantial peak shaving result.

There are a few steep power peaks and dips for the net import in Figure 7.3 that deviates from the regular pattern. This is because the building's power import is affected by the decisions regarding charging and discharging of the battery. However, the optimisation model ensures that the net import does not exceed the power peak predictions.

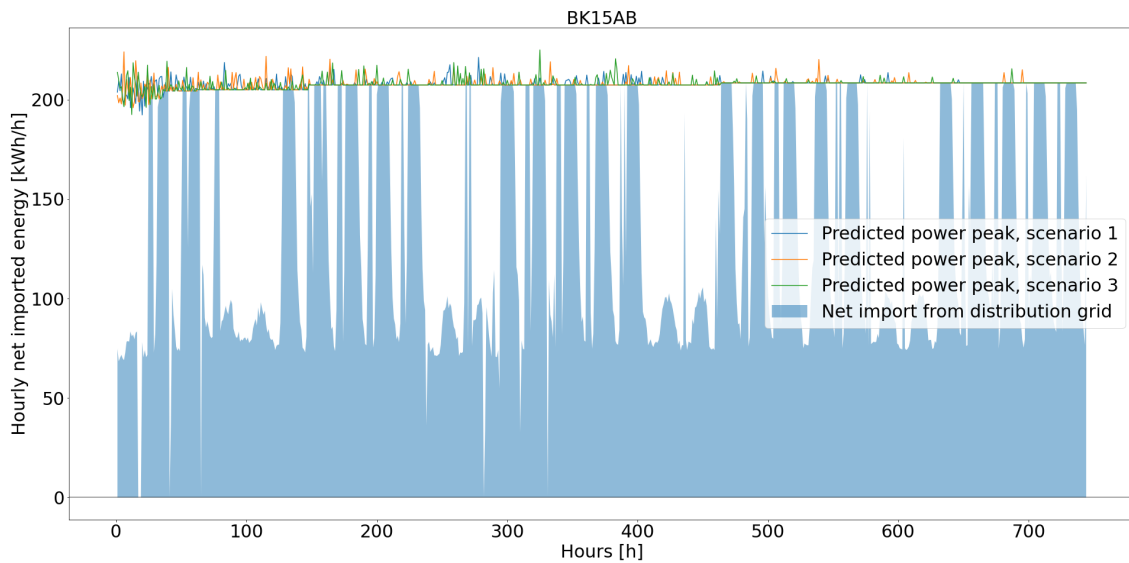


Figure 7.3: BK15AB's import and predicted power peak for configuration 1 in January.

When calculating the power peak reductions, the peaks are compared to base case for the respective month. The different configurations' peak shaving effect for both the community and each individual building are shown for January, March and June in Table 7.1, 7.2 and 7.3 respectively.

Case	January							
	Total system peak		BK15AB		BK16		Sjøgangen	
	Power peak [kWh/h]	Peak reduction [%]	Power peak [kWh/h]	Peak reduction [%]	Power peak [kWh/h]	Peak reduction [%]	Power peak [kWh/h]	Peak reduction [%]
<i>Base case</i>	841	-	270	-	96	-	577	-
1	764	9.2	270	0.0	96	0.0	577	0.0
2	841	0.0	270	0.0	96	0.0	577	0.0
3.1	812	3.5	208	22.8	96	0.0	577	0.0
3.2	830	1.4	270	0.0	70	26.4	577	0.0
3.3	841	0.0	270	0.0	96	0.0	589	-2.2
4 with battery	822	2.3	243	10.2	59	38.1	533	7.6
4 without battery	841	0.0	266	1.4	86	9.9	573	0.6
5	819	2.6	239	11.5	66	31.2	526	8.8
6.1	822	2.3	288	-6.5	62	35.2	493	14.5
6.2	822	2.3	164	39.3	231	-141.1	430	25.5
6.3	822	2.3	242	10.3	60	37.6	527	8.5

Table 7.1: Peak values for each configuration in January.

7.2. PEAK SHAVING

March								
Case	Total system peak		BK15AB		BK16		Sjøgangen	
	Power peak [kWh/h]	Peak reduction [%]	Peak with battery [kWh/h]	Peak reduction [%]	Power peak [kWh/h]	Peak reduction [%]	Power peak [kWh/h]	Peak reduction [%]
<i>Base case</i>	794	-	278	-	98	-	591	-
1	742	6.6	278	0.0	98	0.0	591	0.0
2	794	0.0	278	0.0	98	0.0	591	0.0
3.1	794	0.0	206	25.8	98	0.0	591	0.0
3.2	794	0.0	278	0.0	73	25.3	591	0.0
3.3	794	0.0	278	0.0	98	0.0	536	9.2
4 with battery	758	4.6	255	8.0	66	33.2	437	26.0
4 without battery	794	0.0	274	1.4	76	22.6	535	9.5
5	767	3.4	253	8.7	77	21.6	437	26.0
6.1	747	6.0	248	10.7	59	40.1	440	25.5
6.2	760	4.3	206	25.8	190	-93.4	364	38.3
6.3	754	5.1	234	15.6	59	40.2	461	22

Table 7.2: Peak values for each configuration in March.

June								
Case	Total system peak		BK15AB		BK16		Sjøgangen	
	Power peak [kWh/h]	Peak reduction [%]	Peak with battery [kWh/h]	Peak reduction [%]	Power peak [kWh/h]	Peak reduction [%]	Power peak [kWh/h]	Peak reduction [%]
<i>Base case</i>	246	-	219	-	39	-	8	-
1	218	11.3	219	0.0	39	0.0	8	0.0
2	246	0.0	219	0.0	39	0.0	8	0.0
3.1	223	9.3	182	17.1	39	0.0	8	0.0
3.2	232	5.9	219	0.0	26	33.7	15	-97.4
3.3	245	0.4	219	0.0	39	0.0	9	-16.6
4 with battery	235	4.6	106	51.9	82	-109.0	47	-515.3
4 without battery	247	-0.4	190	13.4	72	-82.5	13	-70.0
5	227	7.6	128	41.5	42	-7.1	57	-647.4
6.1	231	6.1	163	25.6	63	-59.1	5	34.2
6.2	228	7.5	81	63.2	132	-234.6	15	-97.4
6.3	247	-0.4	21	90.6	226	-474.5	0	100.0

Table 7.3: Peak values for each configuration in June.

Based on these results, the most important finding is that configuration 1 considering shared storage with joint metering give the best results for community peak shaving. This configuration is followed by configurations 4 with battery, 5 and 6 considering storage within a local energy market and individual metering. Configuration 4 without battery does not contribute to community peak shaving at all, deviating from the other local energy market cases.

Case 3.1, 3.2 and 3.3 show varying results for each season. However, case 3.1 proves to give a better peak shaving result than the other individual storage configurations. In June, configuration 3.1 manage a 9.3% peak reduction, obtaining the second best results of the month. However, this trend does not apply for the other months investigated. Generally the results for configurations 2, 3 and 4 without battery show lower peak shaving effects compared to the configurations who include shared storage systems. Configuration 2, where the battery operates by itself, tend to not affect the the community peak at all.

An interesting observation from configuration 3.3 in January, shown in Table 7.1, is an increase in individual peak for Sjøgangen instead of a decrease as one would initially expect. Looking further into the data, it is clear that the predicted future peak is generally too high compared to actual consumption. This allows for battery charging during peak hours, increasing the power peak for Sjøgangen. This is caused by the scenarios reflecting an unnecessary high power consumption, due to an inaccurate auto regressive model. The opposite trend is shown in Figure 7.4 where the model underestimates future power peaks.

For each case within a scheduling month, the peak occurs at approximately the same time. This substantiate that the variations in community peak reduction between the cases regarding local markets with individual metering(configurations 4-6) in March and June, are due to stochastic variations. The same is true for January, but stochastic variations are smaller as the predictions are more accurate and are therefore not visible. This is because January is the only simulated month that is not affected by the COVID-19 pandemic in 2020, and consumption and production profiles are therefore better described by the parameters of the autoregressive models.

Due to no market strategy implementation for the optimisation model, there are no major mathematical differences between configuration 4, 5 and 6 that affects the optimal scheduling of the battery. However, it seems rather random which buildings increase or decrease their individual peak. This can be explained by looking at the objective function for these configurations, shown in Appendix D-F. The objective function seeks to minimise total system costs, which includes minimising the sum of each buildings' individual power peak. According to the mathematical model, it does not matter which buildings import excess power in order to reduce total costs. A building can therefore import more than its individual consumption in order to export power to the local energy market, and thereby reducing total system costs.

A clear example of this mathematical occurrence is shown in Figure 7.4 for BK16's power import and export in March for configuration 6.2. The figure shows BK16's net import from the distribution grid in blue and the net import from the local energy market in orange. BK16's power consumption is to some extent reflected by the net import from the grid as a repeated pattern between 0-50kWh/h. However, the power peaks are approximately 4 times as high as the consumption, which is a substantial increase compared to base case. These power peaks for import occurs at the exact same time as the building exports power to the local energy market, which contributes to reducing the other buildings' maximum power peak as shown in Table 7.2.

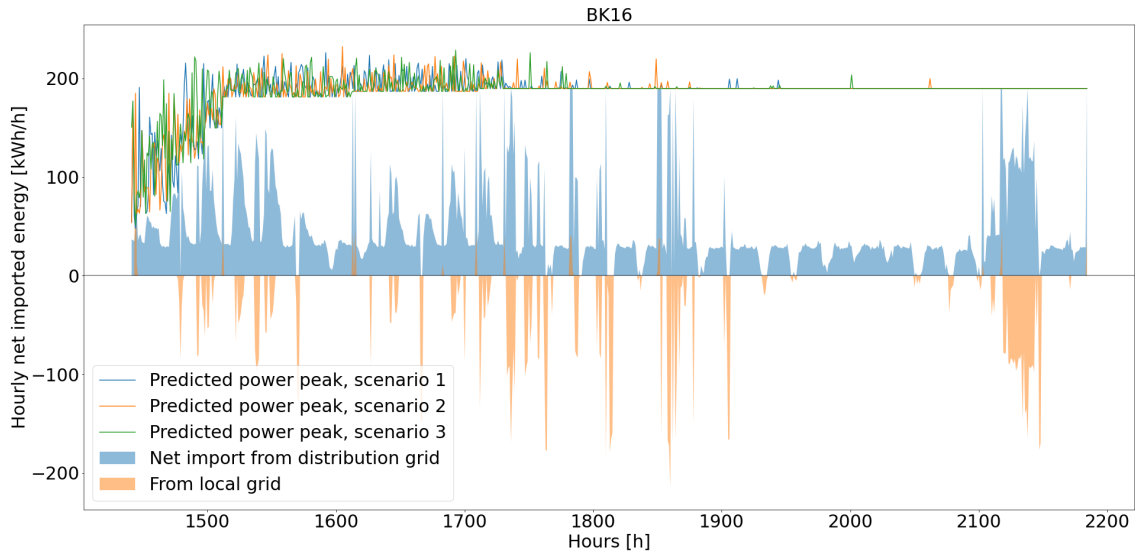


Figure 7.4: BK16's import, export and predicted power peak for configuration 6.2 in March.

7.3 Self-Sufficiency and Self-Consumption

The local consumption and production in terms of self-sufficiency and self-consumption are calculated for each case, including base case. The results for June are displayed in Table 7.4. Naturally, due to low PV production during winter season, self-sufficiency decreases and self-consumption increases. In January and March, the differences in these measures between the configurations will therefore be indistinguishable, which is why the only results displayed are for a high production month.

Case	June			
	Self-sufficiency [%]		Self-consumption [%]	
	Community	BK16	Community	BK16
Base case	13.4	61.9	54.3	54.3
1	24.7	61.9	100.0	54.3
2	13.4	61.9	54.3	54.3
3.1	13.4	61.9	54.3	54.3
3.2	20.3	93.9	82.3	82.3
3.3	13.4	61.9	54.3	54.3
4 with battery	24.7	61.9	100.0	54.3
4 without battery	24.6	61.9	99.2	54.3
5	24.7	61.9	100.0	54.3
6.1	24.7	61.9	100.0	54.3
6.2	24.7	47.0	100.0	41.2
6.3	24.7	61.9	100.0	54.3

Table 7.4: Calculated self-sufficiency and self-consumption for each case in the case run in June.

From Table 7.4, it is clear to see that there are variations for self-sufficiency and self-consumption depending on the configuration, especially for the community. The self-sufficiency and self-consumption for the community is at its greatest for configuration 1, 4 with battery, 5 and 6. Configuration 4 without battery have high energy efficiency values as well, although it is not quite as good as the previously mentioned configurations.

The energy efficiency values for BK16 in general is very similar for most cases, with two exceptions. The first exception is for Case 3.2, with individual storage for BK16, where self-sufficiency and self-consumption is much higher than for other configurations. The second exception is for Case 6.2. In this case BK16 also operates its own battery. However, self-sufficiency and self-consumption has decreased compared to the other cases.

7.4 Cost Analysis

The calculations for the cost analysis section is conducted to clarify the possible monetary savings achieved by BESS within the local energy community. The first section display calculations that are computed for total costs and savings for each case and season, compared to base case. The second section refers to results regarding cost contributions of the different elements of the grid tariff and energy costs.

7.4.1 Total Costs and Savings

The results show a significant cost reduction in many of the cases, but they vary depending on season. The total costs, total savings and reduction of total costs compared to base case for each configuration are calculated for January, March and June showed in Table 7.5, 7.6 and 7.7 respectively.

Through all seasons, configuration 1 manages to reduce the costs the most, followed by configuration 1, 4 with battery and 5, 6. For the configurations with individual operation of the battery, configuration 3.1 tends to give the overall best cost reduction results. However, configurations 2, 3 and 4 without battery, generally present lower cost reductions than the remaining configurations. Due to an additional electricity meter for the battery and its fixed costs, the total costs are actually increased in January and March for configuration 2. Another trend worth mentioning are generally greater cost reductions in March and June compared to January.

January			
Cases	Total costs [kNOK]	Total savings [kNOK]	% of total costs
<i>Base case</i>	273.1	-	-
1	245.4	27.7	10.2
2	273.4	-0.3	-0.1
3.1	263.8	9.3	3.4
3.2	269.4	3.7	1.4
3.3	274.8	-1.7	-0.6
4 with battery	256.7	16.4	6.0
4 without battery	270.6	2.5	0.9
5	256.4	16.7	6.1
6.1	257.9	15.2	5.6
6.2	255.2	18.0	6.6
6.3	255.9	17.2	6.3

Table 7.5: Costs and savings compared to base case for all configurations in January.

March			
Cases	Total costs [kNOK]	Total savings [kNOK]	% of total costs
<i>Base case</i>	209.2	-	-
1	174.7	34.5	16.5
2	209.6	-0.5	-0.2
3.1	198.6	10.6	5.1
3.2	205.5	3.7	1.8
3.3	201.0	8.1	3.9
4 with battery	177.8	31.4	15.0
4 without battery	196.9	12.3	5.9
5	179.6	29.6	14.2
6.1	176.1	33.0	15.8
6.2	178.1	31.0	14.8
6.3	177.2	31.9	15.3

Table 7.6: Costs and savings compared to base case for all configurations in March.

June			
Cases	Total costs [kNOK]	Total savings [kNOK]	% of total costs
<i>Base case</i>	67.8	-	-
1	53.9	13.9	20.5
2	65.4	2.4	3.6
3.1	59.4	8.4	12.4
3.2	62.5	5.3	7.8
3.3	65.3	2.6	3.8
4 with battery	57.1	10.8	15.9
4 without battery	63.2	4.6	6.8
5	56.3	11.5	17.0
6.1	56.5	11.3	16.7
6.2	56.0	11.8	17.4
6.3	58.9	8.9	13.2

Table 7.7: Costs and savings compared to base case for all configurations in June.

7.4.2 Cost Contributions

In order to better understand how the elements of the energy bill affect the total costs and the total savings, the cost contribution from each element in the energy bill is calculated. The cost contributions for January, March and June are shown in Appendix I.

The general trends for the cost contribution is that the peak costs make up most of the total costs covering 50-60% depending on season and configuration. The contribution of the peak costs for the configurations tend to decrease compared to base case.

The volumetric costs make up around 30 % of total costs. An interesting aspect concerning the fixed costs is an increase in contributions for the configurations compared to base case in January and March. In contrast, there is a decrease in cost contributions for the fixed in June.

It is obvious that the fixed costs do not affect the scheduling of the battery at all, and the results proved it is of little significance for the total costs. The small changes in fixed costs are only depended on the number of meters used for each configuration.

The energy costs have varying contribution depending on season. In January the energy costs make up approximately 25% in January, 10% in March and 5% in June.

7.5 Sensitivity Analysis on MP tariff

The purpose of the sensitivity analysis is to analyse to which extent the grid tariff pricing model affects the peak shaving. Since a reduction of the maximum peak is desired by the regulatory authorities and grid companies [43][85], it is important to realise what incentives will trigger customers into reducing their power consumption. For this sensitivity analysis the optimisation model from Chapter 4 is used for investigating the effect of the power tariff term of the MP grid tariff. The analysis is based on configuration 1 for January operation. The different power tariffs tested are for 0, 50, 100, 150 and 250 NOK/kW/month with other components of the energy bill being held equal to the pricing model presented in Table 5.2.

The results from the sensitivity analysis show that the maximum peak reduction clearly increases with increasing power tariff. This is shown in Figure 7.5. There seem to be a relatively abrupt transition between not peak shaving at all and shaving the peak substantially as the power tariff increases. Somewhere between 50 and 100 NOK/kW/month the optimisation model considers peak shaving to be more economically beneficial than spot price arbitrage. The small decrease in power peak reduction from 150 to 250NOK/kW/month is assumed to be caused by the stochasticity of the problem, as there is no mathematical reason to why the peak is slightly increasing when the power tariff is increasing.

When increasing the power tariff and holding all other parameters constant, it is obvious that the total consumer costs will increase. However, this increases the possibility for cost reductions, as shown in Figure 7.6. By increasing power tariff the incentives for the end users to shave the power peaks and save costs are increasing.

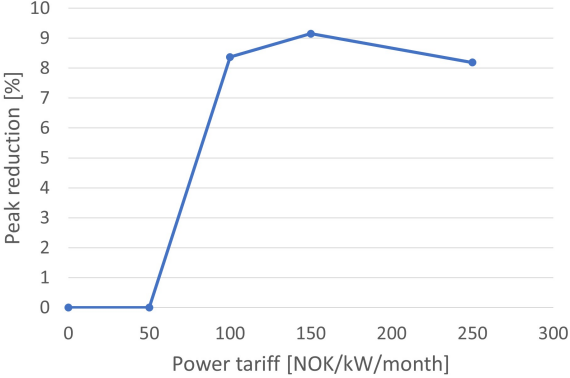


Figure 7.5: Graph showing the increase in peak reduction with increasing power tariff.

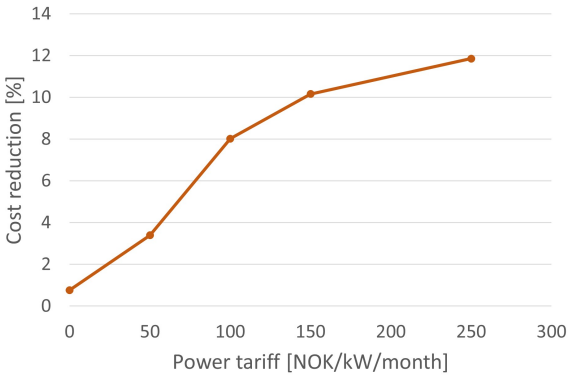


Figure 7.6: Graph showing the increase in cost reduction with increasing power tariff.

8 | Discussion

This Chapter discusses the benefits and the challenges with s-BESS based on the case study results from Chapter 7. First, the peak shaving and energy efficiency effect for the different configurations are discussed. Then, the battery performance will be evaluated in regards to battery costs, and later there will be a summarising comparison of the different configurations. Finally, the regulations for s-BESS are taken into consideration by discussing possible changes that will affect a s-BESS implementation.

8.1 Battery Scheduling

In general, there is not an excessive number of battery cycles in any of the configurations for the case study. This is not only due to the charge and discharge limit implemented in the model formulation, but also because there are energy losses when utilising the battery. Considering the consumption tax and the DSO's volumetric costs, these losses are expensive, and the benefits by utilising the battery must outweigh the costs for these losses.

Although the general number of battery cycles is relatively low, the results show some variations. One example is a lower number of battery cycles in March compared to January and June. This may be caused by a less varying spot price for short time intervals in March, as shown in Figure 5.2. Additionally, there is a smaller number of high power peaks that must be shaved in March than the other months investigated. With high PV production in June, the battery works harder in order to balance consumption and PV production surplus compared to March. This results in an increasing number of cycles for configurations 1, 3.2, 4, 5 and 6.

In addition, there is a generally a higher number of battery cycles for configuration 3.1 and 3.2. This is caused by the many even power consumption peaks for the respective buildings. As long as the power peaks are predicted with some degree of accuracy, successive and even peaks throughout the scheduling horizon lead to a higher utilisation of the battery for peak shaving. Another explanation is a greater battery size relative to the building's shiftable consumption as this configuration only considers individual

storage. For the other configurations the relative battery size is much smaller as the battery is shared between all the buildings.

The reason why there is no utilisation of the battery in configuration 2 is because the objective function does not provide any incentives for utilising locally stored energy. For the buildings, utilising the battery would be just as costly as importing from the grid.

It is known that the battery lifetime depends on the number of battery cycles [9]. Battery degradation costs and life time are not considered when implementing the RHO model. Figure 7.4 show a higher number of battery cycles, and this could have been reduced by including degradation costs as Berglund et. al. states [15]. However, the methodology implemented for this study was simplified to limit the battery cycles by implementing a charge and discharge power as explained in Section 5.2.3. This limitation does not directly reflect the costs of battery degradation, but it limits the battery's cycles which may prolong the battery lifetime.

By observing the charge and discharge occurrences for the case study results, like shown in Figure 7.1 and 7.2, and comparing them to the spot prices shown in Figure 5.2. It is apparent that the battery tend to charge when the spot prices are low compared to hours in the closest time intervals. The battery discharges either when the spot prices are high or during high power peaks. For configurations in June, the battery tend to charge when there is excess power produced at BK16 in order to utilise this energy later for reducing import costs.

8.2 Peak Shaving

One of the main goals for this thesis is to see how a BESS best possibly can contribute to reduce the monthly power peaks and thereby also reducing the total electricity costs. The results from Tables 7.1-7.3 clarified that several of the BESS configurations contributed to community peak shaving. However, the most promising configurations for peak shaving was for the local energy community configurations with either joint or individual metering as they both provide sufficient flexibility to the community.

Still, configuration 1 showed the overall best peak shaving effect. This is because configuration 1 is the only configuration where reducing the community system peak is targeted directly in the objective function. The power peak is reduced by 7-11% depending on the season. This corresponds well with the results presented by Elkazaz et. al who pursue a similar objective [52]. For the local market configurations with individual metering the peak costs are minimised as long as the sum of each individual building's peak is minimised. However, if these peaks are coinciding, the monthly

community peak will get a higher value than for joint metering as there is no direct incentive to avoid coinciding peaks. For the local market configurations 4-6 with battery, the peak is reduced by 2-8%.

One important result to discuss is that a local energy market or joint metering itself does not contribute much for peak shaving alone, this is because a flexible asset within the system, like an integrated BESS, is needed in order to shift the peak consumption. This is clearly shown by comparing the peak reduction for configuration 4 with battery against configuration 4 without battery. Both configurations include local energy markets, but configuration 4 without battery has no flexible assets and does not manage to shave its community peak at all.

The results for the local market cases 4, 5 and 6 indicate that it is economically beneficial for one building to import a larger amount of power in order to export to other buildings or the battery locally, as shown in Figure 7.4. However, it is important to note that the market strategy for the local market was not implemented in the model. Implementing a market strategy that considers fair allocation of profit and where each building seeks to increase its own individual benefit, such as in the works of Taşçıkaraoğlu et. al. and Ouahada and Zhu [25][22], might not give these extreme results. It is also not unlikely that the DSO would want to introduce a small transmission cost for the local energy market, reducing transmission between the buildings directly.

Considering the objective function in the model used for the case study, there are two substantial ways each configuration can reduce the total system costs: The first way is by shaving the greatest power peaks within a month and thereby reduce the MP grid costs, and the second way by doing spot price arbitrage and reducing the energy costs. Sometimes, reducing the power peak might affect the spot price arbitrage operations as the battery capacity might be exhausted for peak shaving. Other times, doing spot price arbitrage might increase the power peaks and thereby the power costs. The results show that there is an economical trade off between doing spot price arbitrage and peak shaving.

Figure 7.4 shows an underestimation of the future power peak. This can lead to unused potential for spot price arbitrage. An overestimation of future power peak causes an unnecessary peak cost, as configuration 3.3 in Table 7.1. These results substantiate the importance of accurate prediction of production and consumption profiles.

As emphasised by Meinrenken et. al., grid tariffs with demand charges are effective incentives for smarter grid operations [14]. Additionally, the studies of Tiemann et. al. and Sepúlveda-Mora et. al. show that the MP pariff effectively contribute to peak shaving for commercial building [12][13]. The sensitivity analysis in Section 7.5 substantiate that the MP pricing level affect the peak shaving for shared storage com-

munities. Increasing the MP tariff makes the peak shaving benefit outweigh the spot price arbitrage benefit, creating a direct incentive for end-user to reduce their maximum power consumption. However, increasing MP costs increases the DSOs revenue, which might be problematic due to RME's regulations of monopoly practices [40]. The DSO's should therefore consider decreasing other elements for the grid tariff, like the volumetric costs, as RME suggests [43].

8.3 Self-Sufficiency and Self-Consumption

Similar to the peak shaving effects, configurations 1, 4, 5 and 6 have the overall best results for self-sufficiency and self-consumption. These cases increase the self-consumption by an additional 45-46%. This is due to the flexibility opportunities these configurations offer as they allow for trading of local production and shifting of power peaks without extra tariff costs.

Configuration 4 without battery however, showed an interesting result as it was almost as good as the other local energy market configurations, but not quite. It is clear that a local energy market will help increasing the community's energy efficiency by distributing local production between the neighbouring buildings. However, energy storage is needed in order store excess production for later consumption and thereby increase self-consumption further. This agrees with Mengelkamp et. al., who conclude that energy storage increases self-consumption within local energy markets [28].

For the self-sufficiency and self-consumption for BK16 alone case 3.2 and 6.2 deviated from the other cases. These are both cases where BK16 operates the battery independently and therefore has the opportunity to control its import and export to some extent. In configuration 3.2 the self-consumption and self-consumption were increased because BK16 had the opportunity to store excess production for later consumption. However, for configuration 6.2 the self-sufficiency and self-consumption decreased. This is because configuration 6.2 includes a local energy market. Therefore, production at BK16 can be sold to the market in order to reduce other buildings' power peak and thereby reducing the total community costs which is the main objective.

8.4 Costs

A few apparent connections between the results are revealed by comparing the cost reductions and contributions against the peak shaving and utilisation of locally produced energy. First, there is a clear link between the cases where the maximum power peak is considerably reduced and the cases with the greatest cost reductions. Due to the high power tariff of 150 NOK/kW, the community receives a high monetary benefit from shaving the peaks. Configuration 1 with s-BESS and joint metering shaves the power peaks the most, leading to a cost reduction of 10-20% depending on season. The second best results in terms of cost reductions are given by configuration 4 with battery, 5 and 6, with cost reductions of 6-17% compared to base case. In line with the results presented by Rahbar et. al, these results show that shared battery energy storage systems for commercial buildings provide a substantial cost saving potential[26].

There is also a link between reduced costs and spot price arbitrage. Although the sensitivity analysis indicate that such a high peak tariff makes the model prefer peak shaving operations over spot price arbitrage, there is a small energy cost reduction for some of the configurations. This is because the battery can still exploit the spot price variations as long as the import does not exceed the predicted future power peaks.

The last link worth mentioning is the connection between self-consumption/ self-sufficiency and savings. It is clear that a higher share of self-sufficiency reduces the need for importing energy. Therefore the energy costs and volumetric costs are clearly reduced in June for configurations where self-sufficiency and self-consumption are increased, like configurations 1, 4, 5 and 6.

The cost contribution results show that the peak costs make up the greatest savings for the different configurations, substantiating that the MP tariff give reasonable incentives for peak shaving. The volumetric costs make up a significant share of the total costs as well. However, they do not affect the battery scheduling to a high extent, but may affect the cost of energy loss within the battery and thereby the battery utilisation as discussed in Section 8.1. This is reflected in the increased volumetric cost in some of the configurations in January and March, indicating that the battery has been utilised. However, the decrease in volumetric costs for some of the configurations in June indicate that the community has decreased its import from the distribution grid by increasing the self-sufficiency.

The seasonal variations for the energy costs are due to the seasonal variations for the spot price as shown in Figure 5.2. With high spot price costs, these costs make up a greater share of the total costs, and thereby increasing the energy costs contribution. Unlike the volumetric costs, the spot price is varying and therefore affect scheduling of the battery. This is reflected in a decreased spot price contribution for some of the configurations when compared to base case.

As mentioned, the case study is based on operation with an already existing battery at Brattøra, neglecting the investment costs and lifetime of the battery. However, if the optimisation model were to be implemented for a new s-BESS community, these factors should be taken into consideration. For a new system, it is not only important that there are sufficient incentives for peak shaving, but there should be sufficient incentives for investing in a BESS as well. As mentioned in Section 2.1, investing in storage technologies are still very expensive [11]. However, as the future BESS pricing levels are expected to decrease the coming years [11][10], and the studies of Keck and Lenzen reveal that s-BESS can be net present value positive by 2023 in Australia [17]. This indicates that shared energy storage within local energy communities in Norway can be beneficial in the near future as well.

8.5 Configurations and Regulations

From the case study it was clear that s-BESS with joint metering was the system configuration which gave the overall best results for peak shaving, self-consumption, self-sufficiency and costs. However, RME argues that joint metering does not provide sufficient rights for consumers and imposes increasing costs for the other users in the concession area [5]. Still, joint metering clearly gives a strong incentive to reduce power peaks, which again might lead to postponement of expensive grid investment. One can argue that these future savings should be considered when processing applications for joint metering dispensation.

As joint metering seem hard to implement due to the regulations, the second best alternative are local energy markets with individual metering as implemented in configuration 4 with battery, 5 and 6. Local energy markets are a great way of utilising a BESS for flexibility purposes. All results presented proves that the aforementioned configurations have close to the same benefits as joint metering results, although with slightly smaller peak and cost reductions. While there is no specific standardise process for granting temporary dispensation for local energy market regulations, dispensation have been given in Norway. There exists projects on flexibility markets that are currently being implemented [33][45][4].

As mentioned, the market strategy for the local energy market in configurations 1, 4, 5 and 6 are not included in the mathematical model, but rather assumes free power flow within the market with no cost limitations. With this in mind, the community benefits for these configurations do not depend on who owns and operates the battery. The monetary savings, energy efficiency and peak shaving effects show similar results for all the local energy market configurations independent of battery allocation. If the local market strategy were to be implemented in the model, there might be apparent differences between the case results for configurations 4, 5 and 6.

In configurations 2 and 3, the BESS's flexibility can not be shared within the local energy community in any way and the results are not very promising in comparison to the other configurations. For configuration 3 with individual storage, the building operating the battery is the only building benefiting from it. However, if joint metering or local energy markets are out of the question, it seems like the best allocation of the battery is with buildings with high and predictable peaks, such as BK15AB in case 3.1. This configuration seem to have a small affect on reducing the community power peak.

A configuration where an external actor operates the battery alone with individual metering, as for configuration 2, seem to provide no benefits for the community at all. There are no incentives for utilising the battery, as stated in Section 8.1. An external actor operating the battery individually is more valuable if there exists a local energy market for the community, as for configuration 5. However, in neither of these cases the external operators will utilise the distribution grid for charging and discharging the battery due to the peak costs.

9 | Concluding Remarks

Based on the recent development of the power system regarding increasing power demand and renewable production, this thesis have investigated how a s-BESS can reduce power peaks and increase energy efficiency for commercial buildings in order to adapt to these changes. This was done by creating a receding horizon optimisation model where a stochastic linear program was solved iteratively in order to operate the BESS in the most cost efficient way for the community as a whole. As shared storage with joint metering is not in line with the Norwegian regulations, the optimisation model was used for different s-BESS configurations that take different stances to these regulations. This is done with the intention to find alternative approaches to s-BESS with joint metering, which would provide the community with approximately the same benefits.

The configurations where the battery's flexibility services can either be shared BTM or sold on a local energy market give the greatest results regarding peak shaving, energy efficiency and electricity cost reductions compared to the configurations with individual storage. Shared storage with joint metering reduced the community power peak by 7-11% and thereby reduced its costs by 10-20% depending on season. With individual metering the system managed to reduce its peak by 2-8% and the costs by 6-7%. For all these configurations self-consumption was increased by an additional 45-46% in June by more efficient utilisation of locally produced energy.

When assuming that a local energy market is a perfect market, it does not matter for the community benefits which actors in the community owns and operates the battery. The individual benefits may differ depending on whether the battery is operated by individual buildings, whether it is shared or operated by external actors. However, fair allocation of monetary benefits between the buildings and implementation of the local energy market strategy was considered to be out of scope for this theses.

A configuration which enables all buildings of the community to utilise the flexibility of the battery is not the only factor which community peak shaving is dependent on. The DSO's pricing model have a huge impact on the consumer's decision making and battery scheduling. When operating a BESS there is often a trade-off between spot price and peak shaving benefits. This study shows that increasing the MP tariff above

a certain level creates higher incentives for peak shaving, and thereby outweighing the spot price arbitrage benefit. The results emphasise the significance of a pricing model that reflects the actual costs of the DSO in order to give reasonable incentives for the community to respond to transmission congestion.

Finally, it should be pointed out that the s-BESS configuration with joint metering is the only configuration which directly seek to minimise the community power peak and not each individual building's peak. Therefore, this configuration gives the overall best results for both peak shaving and cost reductions, challenging the regulations regarding joint metering. Since s-BESS with joint metering have greater incentives for peak reductions and thereby may be able to postpone expensive grid investments due to congestion, these possible benefits versus the disadvantages of joint metering should be discussed further.

Although s-BESS with joint metering proves to give the overall best community benefits, a local energy market with individual metering turns out to be a good alternative as long as dispensation is granted. Anyhow, shared storage behind the meter or within a local energy market has proven to benefit consumers and assist the DSOs with adapting to increasing demand and renewable production, and therefore it should be considered when developing the future power system.

9.1 Further Work

There are several aspects of this study that could be investigated further. The first aspect worth mentioning is the implementation of a market strategy for the local energy market configurations. As each individual building would seek to maximise their own individual benefit, it is assumed that a market strategy implementation would affect the total system costs and optimal scheduling.

Another continuation of the work conducted in this thesis could be to include flexible loads within the commercial buildings in the local market, where the loads' consumption can be shifted in order to reduce total system peak.

As this theses only optimised operation of s-BESS, an investment analysis and calculation on optimal battery size for the community system was considered to be out of scope. However, as s-BESS communities tend to have greater monetary benefits for the community than when a BESS is operated individually, the investment analysis of the s-BESS might have better chances for profitability than individual BESS. The optimal size for the battery in such a community is also of interest.

References

- [1] DNV GL, *Batterier i distribusjonsnettet*, Accessed on 18.02.2021, 2018. [Online]. Available: https://publikasjoner.nve.no/rapport/2018/rapport2018_02.pdf.
- [2] D. Gudmunds, E. Nyholm, M. Taljegard and M. Odenberger, ‘Self-consumption and self-sufficiency for household solar producers when introducing an electric vehicle,’ *Renewable Energy*, vol. 148, pp. 1200–1215, 2020, ISSN: 0960-1481. DOI: <https://doi.org/10.1016/j.renene.2019.10.030>. [Online]. Available: <https://www.sciencedirect.com/science/article/pii/S0960148119315216>.
- [3] J. Hole and H. Horne, *Batterier vil bli en del av kraftsystemet*, Accessed on 18.02.2020, 2019. [Online]. Available: http://publikasjoner.nve.no/faktaark/2019/faktaark2019_14.pdf.
- [4] THEMA Consulting Group and Multiconsult Norge AS, *Descriptive study of local energy communities*, Accessed on 18.02.2020, 2019. [Online]. Available: https://publikasjoner.nve.no/eksternrapport/2019/eksternrapport2019_01.pdf.
- [5] RME, *Individuell måling*, NVE.no, Ed., Mar. 2020. [Online]. Available: <https://www.nve.no/reguleringsmyndigheten/nettjenester/nettleie/individuell-maling/>.
- [6] M. Rostad and I. E. U. Skoglund, ‘Optimal storage operation for commercial buildings,’ Department of Electrical Power Engineering, NTNU - Norwegian University of Science and Technology, Project report in TET4520, Dec. 2020.
- [7] D. M.Hill, *Choosing the right battery storage solution*, Accessed on 25.11.2020, 2020. [Online]. Available: <https://www.dnvgl.com/article/choosing-the-right-battery-storage-solution-140628>.
- [8] IRENA, ‘Innovation landscape brief: Utility-scale batteries,’ International Renewable Energy Agency, Abu Dhabi, 2019.
- [9] M. E. V. Team, ‘A guide to understanding battery specifications,’ Dec. 2008, Accessed on 25.11.2020. [Online]. Available: http://web.mit.edu/evt/summary_battery_specifications.pdf.

- [10] V. Henze, *Battery pack prices fall as market ramps up with market average at \$156/kwh in 2019*, Accessed on 25.11.2020, 2019. [Online]. Available: <https://about.bnef.com/blog/battery-pack-prices-fall-as-market-ramps-up-with-market-average-at-156-kwh-in-2019/?sf113554299=1>.
- [11] J. Hole and H. Horne, *Batterier vil bli en del av kraftsystemet*, Accessed on 25.11.2020, 2019. [Online]. Available: http://publikasjoner.nve.no/faktaark/2019/faktaark2019_14.pdf.
- [12] P. H. Tiemann, A. Bensmann, V. Stuke and R. Hanke-Rauschenbach, 'Electrical energy storage for industrial grid fee reduction – a large scale analysis,' *Energy Conversion and Management*, vol. 208, p. 112539, Mar. 2020, ISSN: 01968904. DOI: 10.1016/j.enconman.2020.112539.
- [13] S. B. Sepúlveda-Mora and S. Hegedus, 'Making the case for time-of-use electric rates to boost the value of battery storage in commercial buildings with grid connected pv systems,' *Energy*, vol. 218, p. 119447, Dec. 2020, ISSN: 03605442. DOI: 10.1016/j.energy.2020.119447.
- [14] C. J. Meinrenken and A. Mehmani, 'Concurrent optimization of thermal and electric storage in commercial buildings to reduce operating cost and demand peaks under time-of-use tariffs,' *Applied Energy*, vol. 254, Nov. 2019, ISSN: 03062619. DOI: 10.1016/j.apenergy.2019.113630. [Online]. Available: <https://doi.org/10.1016/j.apenergy.2019.113630>.
- [15] F. Berglund, S. Zaferanlouei, M. Korpås and K. Uhlen, 'Optimal operation of battery storage for a subscribed capacity-based power tariff prosumer-a norwegian case study,' 2019. DOI: 10.3390/en12234450. [Online]. Available: www.mdpi.com/journal/energies.
- [16] Y. Wang, B. Wang, C. C. Chu, H. Pota and R. Gadh, 'Energy management for a commercial building microgrid with stationary and mobile battery storage,' *Energy and Buildings*, vol. 116, pp. 141–150, Mar. 2016, ISSN: 03787788. DOI: 10.1016/j.enbuild.2015.12.055. [Online]. Available: <http://dx.doi.org/10.1016/j.enbuild.2015.12.055>.
- [17] F. Keck and M. Lenzen, 'Drivers and benefits of shared demand-side battery storage – an australian case study,' *Energy Policy*, p. 112005, Nov. 2020, ISSN: 03014215. DOI: 10.1016/j.enpol.2020.112005.
- [18] E. Oh and S.-Y. Son, 'Optimal energy management scheme for multi-dwelling units with clustered energy storage systems,' Jan. 2017, pp. 314–315. DOI: 10.1109/ICCE.2017.7889334.
- [19] M. B. Roberts, A. Bruce and I. MacGill, 'Impact of shared battery energy storage systems on photovoltaic self-consumption and electricity bills in apartment buildings,' *Applied Energy*, vol. 245, pp. 78–95, Jul. 2019, ISSN: 03062619. DOI: 10.1016/j.apenergy.2019.04.001.

- [20] M. M. Syed, G. M. Morrison and J. Darbyshire, ‘Shared solar and battery storage configuration effectiveness for reducing the grid reliance of apartment complexes,’ *Energies*, vol. 13, p. 4820, 18 Sep. 2020, ISSN: 1996-1073. DOI: 10.3390/en13184820. [Online]. Available: <https://www.mdpi.com/1996-1073/13/18/4820>.
- [21] H. Zhu and K. Ouahada, ‘Cost minimization energy storage sharing management,’ in *2019 IEEE International Conference on Communications, Control, and Computing Technologies for Smart Grids (SmartGridComm)*, 2019, pp. 1–6. DOI: 10.1109/SmartGridComm.2019.8909720.
- [22] K. Ouahada and H. Zhu, ‘Credit-based distributed real-time energy storage sharing management,’ *IEEE Access*, vol. 7, pp. 185 821–185 838, 2019. DOI: 10.1109/ACCESS.2019.2961389.
- [23] F. Boulaire, A. Narimani, J. Bell, R. Drogemuller, D. Vine, L. Buys and G. Walker, ‘Benefit assessment of battery plus solar for customers and the grid,’ *Energy Strategy Reviews*, vol. 26, p. 100 372, Nov. 2019, ISSN: 2211467X. DOI: 10.1016/j.esr.2019.100372.
- [24] A. Walker and S. Kwon, ‘Analysis on impact of shared energy storage in residential community: Individual versus shared energy storage,’ *Applied Energy*, vol. 282, p. 116 172, Jan. 2021, ISSN: 03062619. DOI: 10.1016/j.apenergy.2020.116172.
- [25] A. Taşçikaraoğlu, ‘Economic and operational benefits of energy storage sharing for a neighborhood of prosumers in a dynamic pricing environment,’ *Sustainable Cities and Society*, vol. 38, pp. 219–229, Apr. 2018, ISSN: 22106707. DOI: 10.1016/j.scs.2018.01.002. [Online]. Available: <https://doi.org/10.1016/j.scs.2018.01.002>.
- [26] K. Rahbar, M. R. Vedady Moghadam, S. K. Panda and T. Reindl, ‘Shared energy storage management for renewable energy integration in smart grid,’ in *2016 IEEE Power Energy Society Innovative Smart Grid Technologies Conference (ISGT)*, 2016, pp. 1–5. DOI: 10.1109/ISGT.2016.7781230.
- [27] E. Oh and S. Son, ‘Shared electrical energy storage service model and strategy for apartment-type factory buildings,’ *IEEE Access*, vol. 7, pp. 130 340–130 351, 2019. DOI: 10.1109/ACCESS.2019.2939406.
- [28] E. Mengelkamp, J. Garttner and C. Weinhardt, ‘The role of energy storage in local energy markets,’ in *2017 14th International Conference on the European Energy Market (EEM)*, 2017, pp. 1–6. DOI: 10.1109/EEM.2017.7981906.
- [29] C. Eid, L. A. Bollinger, B. Koirala, D. Scholten, E. Facchinetti, J. Lilliestam and R. Hakvoort, ‘Market integration of local energy systems: Is local energy management compatible with european regulation for retail competition?’ *Energy*, vol. 114, pp. 913–922, 2016, ISSN: 0360-5442. DOI: <https://doi.org/10.1016/>

- j.energy.2016.08.072. [Online]. Available: <https://www.sciencedirect.com/science/article/pii/S0360544216311859>.
- [30] D. Kiedanski, D. Kofman, J. Horta and D. Menga, ‘Strategy-proof local energy market with sequential stochastic decision process for battery control,’ in *2019 IEEE Power Energy Society Innovative Smart Grid Technologies Conference (ISGT)*, 2019, pp. 1–5. DOI: 10.1109/ISGT.2019.8791585.
- [31] F. Teotia and R. Bhakar, ‘Local energy markets: Concept, design and operation,’ in *2016 National Power Systems Conference (NPSC)*, 2016, pp. 1–6. DOI: 10.1109/NPSC.2016.7858975.
- [32] Centrica, *The future of flexibility*, centrica.com, Ed., Accessed on 14.06.2021, Nov. 2020. [Online]. Available: <https://www.centrica.com/media/4609/the-future-of-flexibility-centrica-cornwall-lem-report.pdf>.
- [33] +CityxChange, *Welcome to our project +cityxchange*, cityxchange.eu, Ed., Accessed on 14.06.2021, 2019. [Online]. Available: <https://cityxchange.eu/>.
- [34] Energiloven, *Lov om produksjon, omforming, overføring, omsetning, fordeling og bruk av energi m.m. (energiloven)*, NVE.no, Ed., Jan. 2021. [Online]. Available: <https://lovdata.no/dokument/NL/lov/1990-06-29-50?q=energilov>.
- [35] RME, *Reguleringsmyndigheten for energi (rme)*, NVE.no, Ed. [Online]. Available: <https://www.nve.no/reguleringsmyndigheten/>.
- [36] —, *Sluttbrukermarkedet*, NVE.no, Ed., Feb. 2021. [Online]. Available: <https://www.nve.no/reguleringsmyndigheten/sluttbrukermarkedet/?ref=mainmenu>.
- [37] —, *Strømvtaler, strømpriser og faktura*, NVE.no, Ed., Oct. 2020. [Online]. Available: <https://www.nve.no/reguleringsmyndigheten/stromkunde/stromavtaler-strompriser-og-faktura/?ref=mainmenu>.
- [38] N. Pool, *Historical market data*, Accessed on 19.05.2021. [Online]. Available: <https://www.nordpoolgroup.com/historical-market-data/>.
- [39] —, *Nord pool*, Accessed on 19.05.2021. [Online]. Available: <https://www.nordpoolgroup.com/>.
- [40] RME, *Nettleie*, NVE.no, Ed., Oct. 2019. [Online]. Available: <https://www.nve.no/reguleringsmyndigheten/stromkunde/nettleie/?ref=mainmenu>.
- [41] —, *Nettleie for forbruk*, NVE.no, Ed., Feb. 2019. [Online]. Available: <https://www.nve.no/reguleringsmyndigheten/nettjenester/nettleie/nettleie-for-forbruk/>.
- [42] —, *Plusskunder*, NVE.no, Ed., Feb. 2021. [Online]. Available: <https://www.nve.no/reguleringsmyndigheten/nettjenester/nettleie/tariffer-for-produksjon/plusskunder/>.

- [43] ———, *Høring - forslag til endringer i utformingen av nettleien*, NVE.no, Ed., Oct. 2020. [Online]. Available: <https://www.nve.no/reguleringsmyndigheten/nytt-fra-rme/saker-pa-horing-reguleringsmyndigheten-for-energi-rme/horing-forslag-til-endringer-i-utformingen-av-nettleien/>.
- [44] Lovdata, *Forskrift om økonomisk og teknisk rapportering, inntektsramme for nettvirksomheten og tariffen*, Lovdata.no, Ed. [Online]. Available: https://lovdata.no/dokument/SF/forskrift/1999-03-11-302?q=fellesm%5C%C3%5C%A5ling#KAPITTEL_5.
- [45] S. Bertelsen, K. Livik and M. Myrstad, ‘D2.1 report on enabling regulatory mechanisms to trial innovations in cities,’ +CityxChange, Trondheim, Norway, Tech. Rep. v.2.0, Jul. 2019.
- [46] J. Birge and F. Louveaux, *Introduction to Stochastic Programming*, 2nd ed. Springer, New York, NY, 2007, ISBN: 978-1-4614-0236-7, 978-1-4939-3703-5. DOI: 10.1007/978-1-4614-0237-4.
- [47] H. Andersson, *Lecture notes in Optimization Methods with Applications*, NTNU – Norwegian University of Science and Technology, 2019.
- [48] A. Bischi, L. Taccari, E. Martelli, E. Amaldi, G. Manzolini, P. Silva, S. Campanari and E. Macchi, ‘A rolling-horizon optimization algorithm for the long term operational scheduling of cogeneration systems,’ *Energy*, vol. 184, pp. 73–90, Oct. 2019, ISSN: 03605442. DOI: 10.1016/j.energy.2017.12.022.
- [49] G. M. Kopanos and E. N. Pistikopoulos, ‘Reactive scheduling by a multiparametric programming rolling horizon framework: A case of a network of combined heat and power units,’ 2014. DOI: 10.1021/ie402393s.
- [50] J. Silvente, G. M. Kopanos, E. N. Pistikopoulos and A. Espuña, ‘A rolling horizon optimization framework for the simultaneous energy supply and demand planning in microgrids,’ *Applied Energy*, vol. 155, pp. 485–501, Oct. 2015, ISSN: 03062619. DOI: 10.1016/j.apenergy.2015.05.090.
- [51] A. B. Forough and R. Roshandel, ‘Multi objective receding horizon optimization for optimal scheduling of hybrid renewable energy system,’ *Energy and Buildings*, vol. 150, pp. 583–597, Sep. 2017, ISSN: 03787788. DOI: 10.1016/j.enbuild.2017.06.031. [Online]. Available: <https://www.sciencedirect.com/science/article/pii/S0378778816317406>.
- [52] M. Elkazaz, M. Sumner, S. Pholboon and D. Thomas, ‘Microgrid energy management using a two stage rolling horizon technique for controlling an energy storage system,’ Institute of Electrical and Electronics Engineers Inc., Dec. 2018, pp. 324–329, ISBN: 9781538659823. DOI: 10.1109/ICRERA.2018.8566761.
- [53] H. C. Gao, J. H. Choi, S. Y. Yun, H. J. Lee and S. J. Ahn, ‘Optimal scheduling and real-time control schemes of battery energy storage system for microgrids considering contract demand and forecast uncertainty,’ *Energies*, vol. 11, 6 Jun. 2018, ISSN: 19961073. DOI: 10.3390/en11061371.

- [54] Y. Yang, S. Bremner, C. Menictas and M. Kay, ‘A mixed receding horizon control strategy for battery energy storage system scheduling in a hybrid pv and wind power plant with different forecast techniques,’ *Energies*, vol. 12, 12 2019, ISSN: 19961073. DOI: 10.3390/en12122326.
- [55] J. Silvente, G. M. Kopanos, V. Dua and L. G. Papageorgiou, ‘A rolling horizon approach for optimal management of microgrids under stochastic uncertainty,’ *Chemical Engineering Research and Design*, vol. 131, pp. 293–317, Mar. 2018, ISSN: 02638762. DOI: 10.1016/j.cherd.2017.09.013.
- [56] D. Q. Pham, *Innføring i tidsserier - sesongjustering og x-12-arima*, Accessed on 20.05.2021, 2001. [Online]. Available: https://www.ssb.no/a/publikasjoner/pdf/notat_200102/notat_200102.pdf.
- [57] R. Hyndman and G. Athanasopoulos, *Forecasting: principles and practice*, 2nd ed. OTexts: Melbourne, Australia, 2018, OTexts.com/fpp2. Accessed on 20.05.2021.
- [58] M. Molinas, *Lecture notes in Adaptive Data Analysis - Theory and Application*, NTNU – Norwegian University of Science and Technology, 2020.
- [59] P. Cowpertwait and A. Metcalfe, ‘Introductory time series with r,’ in. Jan. 2009, ISBN: 0387886974, 9780387886978. DOI: 10.1007/978-0-387-88698-5.
- [60] J. G. MacKinnon, ‘Approximate asymptotic distribution functions for unit-root and cointegration tests,’ *Journal of Business & Economic Statistics*, vol. 12, pp. 167–176, 1994.
- [61] W. Kenton, *Statistical significance*, Accessed on 20.05.2021, 2021. [Online]. Available: https://www.investopedia.com/terms/s/statistically_significant.asp.
- [62] B. Beers, *P-value*, Accessed on 20.05.2021, 2021. [Online]. Available: <https://www.investopedia.com/terms/p/p-value.asp>.
- [63] M. C. Lovell, ‘Seasonal adjustment of economic time series and multiple regression analysis,’ *Journal of the American Statistical Association*, vol. 58, no. 304, pp. 993–1010, 1963, ISSN: 01621459. [Online]. Available: <http://www.jstor.org/stable/2283327>.
- [64] J. Hamilton, *Time Series Analysis*. Princeton University Press, 1994.
- [65] M. Kaut, *Scenario generation by selection from historical data*, Accessed on 22.05.2021, 2021. [Online]. Available: http://work.michalkaut.net/papers_etc/scen-gen_hist-data.pdf.
- [66] J. Dupačová, G. Consigli and S. W. Wallace, *Scenarios for multistage stochastic programs*, Accessed on 22.05.2021, 2000. [Online]. Available: http://work.michalkaut.net/papers_etc/scen-gen_hist-data.pdf.
- [67] Q. Zhou, L. Tesfatsion and C.-C. Liu, ‘Scenario generation for price forecasting in restructured wholesale power markets,’ Apr. 2009, pp. 1–8. DOI: 10.1109/PSCE.2009.4840062.

- [68] P. Schütz, A. Tomasgard and S. Ahmed, ‘Supply chain design under uncertainty using sample average approximation and dual decomposition,’ *European Journal of Operational Research*, vol. 199, no. 2, pp. 409–419, 2009, ISSN: 0377-2217. DOI: <https://doi.org/10.1016/j.ejor.2008.11.040>. [Online]. Available: <https://www.sciencedirect.com/science/article/pii/S037722170801031X>.
- [69] K. C. Sharma, R. Bhakar, H. P. Tiwari and S. Chawda, ‘Scenario based uncertainty modeling of electricity market prices,’ in *2017 6th International Conference on Computer Applications In Electrical Engineering-Recent Advances (CERA)*, 2017, pp. 164–168. DOI: 10.1109/CERA.2017.8343320.
- [70] N. Di Domenica, C. Lucas, G. Mitra and P. Valente, ‘Scenario generation for stochastic programming and simulation: a modelling perspective,’ *IMA Journal of Management Mathematics*, vol. 20, no. 1, pp. 1–38, Aug. 2007, ISSN: 1471-678X. DOI: 10.1093/imaman/dpm027. eprint: <https://academic.oup.com/imaman/article-pdf/20/1/1/2045739/dpm027.pdf>. [Online]. Available: <https://doi.org/10.1093/imaman/dpm027>.
- [71] N. Grove-Kuska, H. Heitsch and W. Romisch, ‘Scenario reduction and scenario tree construction for power management problems,’ in *2003 IEEE Bologna Power Tech Conference Proceedings*, vol. 3, 2003. DOI: 10.1109/PTC.2003.1304379.
- [72] J. Dupačová, N. Groewe-Kuska and W. Roemisch, ‘Scenario reduction in stochastic programming: An approach using probability metrics,’ *Mathematical Programming*, vol. 95, pp. 493–, Jan. 2003.
- [73] H. Heitsch and W. Römisch, ‘A note on scenario reduction for two-stage stochastic programs,’ *Operations Research Letters*, vol. 35, no. 6, pp. 731–738, 2007, ISSN: 0167-6377. DOI: <https://doi.org/10.1016/j.orl.2006.12.008>. [Online]. Available: <https://www.sciencedirect.com/science/article/pii/S0167637707000089>.
- [74] R. Henrion and W. Roemisch, ‘Optimal scenario generation and reduction in stochastic programming,’ *Stochastic Programming E-Print Series*, Feb. 2017. DOI: 10.1007/s10107-018-1337-6.
- [75] K. A. Rosvold, *Brattøra*, Accessed on 09.12.2020. [Online]. Available: <https://snl.no/Bratt%C3%B8ra>.
- [76] FramtidsTrondheim, *Strategier for de fem sentrumsområdene*, Accessed on 16.12.2020. [Online]. Available: <https://sites.google.com/trondheim.kommune.no/framtidstrondheim/plan-for-sentrumsutvikling/framtidsbilder-trondheim-sentrum-2050-med-sentrumsstrategi/strategier-for-de-fem-sentrumsomr%C3%A5dene#h.jluy831f986i>.
- [77] PirII, *Brattøra*, Accessed on 09.12.2020. [Online]. Available: <https://www.pir2.no/projects/brattora>.

- [78] Entra, *Info om bk15*, entra.no, Ed., Accessed on 02.06.2021, Sep. 2017. [Online]. Available: https://entra.no/storage/uploads/article-documents/1_info-om-bk15.pdf.
- [79] —, *Brattørkaia 15a,b*, entra.no, Ed., Accessed on 02.06.2021. [Online]. Available: <https://entra.no/properties/brattorkaia-15-a-b/96>.
- [80] N. G. B. Council, *Breeam*, Accessed on 25.11.2020. [Online]. Available: <https://byggalliansen.no/sertifisering/breeam/>.
- [81] T. Kothe-Næss. (2018). ‘Ikke bare bi-studentene som setter pris på bygget,’ [Online]. Available: <https://www.adressa.no/nyheter/okonomi/2018/11/07/Ikke-bare-BI-studentene-som-setter-pris-p%5C%C3%5C%A5-bygget-17835081.ece> (visited on 25/11/2018).
- [82] Entra, *Portefølje*, Accessed on 21.11.2020. [Online]. Available: <https://entra.no/properties>.
- [83] B. N. Eiendom, *Sjøgangen i trondheim*, Accessed on 25.11.2020. [Online]. Available: <https://banenoreiendom.no/sjogangen-i-trondheim>.
- [84] Alfen, *Thebattery specification*, Accessed on 11.05.2021. [Online]. Available: <https://alfen.com/en/energy-storage/thebattery-specifications>.
- [85] Elvia, *Nettleiepriser og effekttariff for bedrifter i oslo og viken*, Accessed on 19.05.2021. [Online]. Available: https://assets.ctfassets.net/jbub5thfds15/2Mjf7J9Iuat11ICKBC0gUo/3f0b60d6752623c1c5c045317271c52f/Nettleiepriser_og_effekttariff_bedrift___Oslo_Viken_2020.pdf.
- [86] Skatteetaten, *Elektrisk kraft*, Accessed on 21.05.2021. [Online]. Available: <https://www.skatteetaten.no/satser/elektrisk-kraft/?year=2020#rateShowYear>.
- [87] G. D. Corporation, *Scenred*, Accessed on 07.04.2021, 2021. [Online]. Available: https://www.gams.com/latest/docs/T_SCENRED.html.

Appendices

A Optimisation Model: Configuration 1

$$\begin{aligned} \min \quad & \sum_{s \in S} \pi_s \sum_{h \in H} ((p_{h,s}^{Gimp} (C_h^E + C^V) - C_{h,s}^E p_{h,s}^{Gexp}) \\ & + C^P (P^{sys} + \Delta p_s^{sys})) + C^F \end{aligned} \quad (\text{A.1a})$$

$$\text{s.t.} \quad \sum_{b \in B} (b_{h,b,s}^{Gimp} - b_{h,b,s}^{Gexp}) = p_{h,s}^{Gimp} - p_{h,s}^{Gexp} \quad \forall h \in H, s \in S \quad (\text{A.1b})$$

$$b_{h,b,s}^{Gimp} - b_{h,b,s}^{Gexp} = R_{h,b}^{cons} - R_{h,b}^{prod} \quad \forall h \in H_1, b \in B, s \in S \quad (\text{A.1c})$$

$$b_{h,b,s}^{Gimp} - b_{h,b,s}^{Gexp} = D_{h,b,s}^{cons} - D_{h,b,s}^{prod} \quad \forall h \in H_2, b \in B, s \in S \quad (\text{A.1d})$$

$$e_{h,s} \leq E^{max} \quad \forall h \in H, s \in S \quad (\text{A.1e})$$

$$x_{h,s}^{Lcha} \leq K^{max} \quad \forall h \in H, s \in S \quad (\text{A.1f})$$

$$x_{h,s}^{Ldch} \leq K^{max} \quad \forall h \in H, s \in S \quad (\text{A.1g})$$

$$\eta^{cha} x_{h,s}^{Lcha} - \frac{x_{h,s}^{Ldch}}{\eta^{dch}} = e_{h,s} - e_{h-1,s} \quad \forall h \in H|_{h \neq 1}, s \in S \quad (\text{A.1h})$$

$$\eta^{cha} x_{l,s}^{Lcha} - \frac{x_{l,s}^{Ldch}}{\eta^{dch}} = e_{l,s} - S_0 \quad \forall s \in S \quad (\text{A.1i})$$

$$e_{f,s} = S_f \quad \forall s \in S \quad (\text{A.1j})$$

$$P^{sys} + \Delta p_s^{sys} \geq p_{h,s}^{Gimp} \quad \forall h \in H, s \in S \quad (\text{A.1k})$$

$$e_{h,s} = e_{h,s-1} \quad \forall h \in H, s \in S|_{s \neq 1} \quad (\text{A.1l})$$

$$x_{h,s}^{Lcha} = x_{h,s-1}^{Lcha} \quad \forall h \in H, s \in S|_{s \neq 1} \quad (\text{A.1m})$$

$$x_{h,s}^{Ldch} = x_{h,s-1}^{Ldch} \quad \forall h \in H, s \in S|_{s \neq 1} \quad (\text{A.1n})$$

$$p_{h,s}^{Gimp} = p_{h,s-1}^{Gimp} \quad \forall h \in H, s \in S|_{s \neq 1} \quad (\text{A.1o})$$

$$p_{h,s}^{Gexp} = p_{h,s-1}^{Gexp} \quad \forall h \in H, s \in S|_{s \neq 1} \quad (\text{A.1p})$$

$$b_{h,b,s}^{Gimp} = b_{h,b,s-1}^{Gimp} \quad \forall h \in H, b \in B, s \in S|_{s \neq 1} \quad (\text{A.1q})$$

$$b_{h,b,s}^{Gexp} = b_{h,b,s-1}^{Gexp} \quad \forall h \in H, b \in B, s \in S|_{s \neq 1} \quad (\text{A.1r})$$

$$e_{h,s}, x_{h,s}^{Lcha}, x_{h,s}^{Ldch} \geq 0 \quad \forall h \in H, s \in S \quad (\text{A.1s})$$

$$p_{h,s}^{Gimp}, p_{h,s}^{Gexp} \geq 0 \quad \forall h \in H, s \in S \quad (\text{A.1t})$$

$$b_{h,b,s}^{Gimp}, b_{h,b,s}^{Gexp} \geq 0 \quad \forall h \in H, b \in B, s \in S \quad (\text{A.1u})$$

$$\Delta p_s^{sys} \geq 0 \quad \forall s \in S \quad (\text{A.1v})$$

B Optimisation Model: Configuration 2

$$\begin{aligned}
\min \quad & \sum_{s \in S} \pi_s \left(\sum_{b \in B} \left(\sum_{h \in H} (b_{h,b,s}^{Gimp} (C_h^E + C^V) - C_h^E b_{h,b,s}^{Gexp}) \right. \right. \\
& + C^P (P_b^{building} + \Delta p_{b,s}^{building}) + C^F) + \sum_{h \in H} (x_{h,s}^{Gcha} (C_h^E \\
& + C^V) - C_h^E x_{h,s}^{Gdch}) + C^P (P_s^{battery} + \Delta p_s^{battery}) + C^F) \quad (B.2a)
\end{aligned}$$

$$\text{s.t.} \quad b_{h,b,s}^{Gimp} - b_{h,b,s}^{Gexp} = R_{h,b}^{cons} - R_{h,b}^{prod} \quad \forall h \in H_1, b \in B, s \in S \quad (B.2b)$$

$$b_{h,b,s}^{Gimp} - b_{h,b,s}^{Gexp} = D_{h,b,s}^{cons} - D_{h,b,s}^{prod} \quad \forall h \in H_2, b \in B, s \in S \quad (B.2c)$$

$$e_{h,s} \leq E^{max} \quad \forall h \in H, s \in S \quad (B.2d)$$

$$x_{h,s}^{Gcha} \leq K^{max} \quad \forall h \in H, s \in S \quad (B.2e)$$

$$x_{h,s}^{Gdch} \leq K^{max} \quad \forall h \in H, s \in S \quad (B.2f)$$

$$\eta^{cha} x_{h,s}^{Gcha} - \frac{x_{h,s}^{Gdch}}{\eta^{dch}} = e_{h,s} - e_{h-1,s} \quad \forall h \in H |_{h \neq 1}, s \in S \quad (B.2g)$$

$$\eta^{cha} x_{l,s}^{Gcha} - \frac{x_{l,s}^{Gdch}}{\eta^{dch}} = e_{l,s} - S_0 \quad \forall s \in S \quad (B.2h)$$

$$e_{f,s} = S_f \quad \forall s \in S \quad (B.2i)$$

$$P_b^{building} + \Delta p_{b,s}^{building} \geq b_{h,b,s}^{building} \quad \forall h \in H, b \in B, s \in S \quad (B.2j)$$

$$P_s^{battery} + \Delta p_s^{battery} \geq x_{h,s}^{Gcha} \quad \forall h \in H, s \in S \quad (B.2k)$$

$$e_{h,s} = e_{h,s-1} \quad \forall h \in H, s \in S |_{s \neq 1} \quad (B.2l)$$

$$x_{h,s}^{Gcha} = x_{h,s-1}^{Gcha} \quad \forall h \in H, s \in S |_{s \neq 1} \quad (B.2m)$$

$$x_{h,s}^{Gdch} = x_{h,s-1}^{Gdch} \quad \forall h \in H, s \in S |_{s \neq 1} \quad (B.2n)$$

$$b_{h,b,s}^{Gimp} = b_{h,b,s-1}^{Gimp} \quad \forall h \in H, b \in B, s \in S |_{s \neq 1} \quad (B.2o)$$

$$b_{h,b,s}^{Gexp} = b_{h,b,s-1}^{Gexp} \quad \forall h \in H, b \in B, s \in S |_{s \neq 1} \quad (B.2p)$$

$$e_{h,s}, x_{h,s}^{Gcha}, x_{h,s}^{Gdch} \geq 0 \quad \forall h \in H, s \in S \quad (B.2q)$$

$$b_{h,b,s}^{Gimp}, b_{h,b,s}^{Gexp} \geq 0 \quad \forall h \in H, b \in B, s \in S \quad (B.2r)$$

$$\Delta p_s^{battery} \geq 0 \quad \forall s \in S \quad (B.2s)$$

$$\Delta p_{b,s}^{building} \geq 0 \quad \forall b \in B, s \in S \quad (B.2t)$$

C Optimisation Model: Configuration 3

$$\min \sum_{s \in S} \pi_s \sum_{b \in B} \left(\sum_{h \in H} (b_{h,b,s}^{Gimp} (C_h^E + C^V) - C_{h,s}^E b_{h,b,s}^{Gexp}) + C^P (P_b^{building} + \Delta p_{b,s}^{building}) + C^F \right) \quad (C.3a)$$

$$(C.3b)$$

$$\text{s.t.} \quad R_{h,k}^{cons} - R_{h,k}^{prod} + x_{h,k,s}^{Gcha} - x_{h,k,s}^{Gdch} = b_{h,b,s}^{Gimp} - b_{h,b,s}^{Gexp} \quad \forall h \in H_1, s \in S \quad (C.3c)$$

$$D_{h,k,s}^{cons} - D_{h,k,s}^{prod} + x_{h,k,s}^{Gcha} - x_{h,k,s}^{Gdch} = b_{h,k,s}^{Gimp} - b_{h,k,s}^{Gexp} \quad \forall h \in H_2, s \in S \quad (C.3d)$$

$$R_{h,b}^{cons} - R_{h,b}^{prod} = b_{h,b,s}^{Gimp} - b_{h,b,s}^{Gexp} \quad \forall h \in H_1, b \in B|_{n \neq k}, s \in S \quad (C.3e)$$

$$D_{h,b,s}^{cons} - D_{h,b,s}^{prod} = b_{h,b,s}^{Gimp} - b_{h,b,s}^{Gexp} \quad \forall h \in H_2, b \in B|_{b \neq k}, s \in S \quad (C.3f)$$

$$e_{h,s} \leq E^{max} \quad \forall h \in H, s \in S \quad (C.3g)$$

$$x_{h,s}^{Gcha} \leq K^{max} \quad \forall h \in H, s \in S \quad (C.3h)$$

$$x_{h,s}^{Gdch} \leq K^{max} \quad \forall h \in H, s \in S \quad (C.3i)$$

$$\eta^{cha} x_{h,s}^{Gcha} - \frac{x_{h,s}^{Gdch}}{\eta^{dch}} = e_{h,s} - e_{h-1,s} \quad \forall h \in H|_{h \neq 1}, s \in S \quad (C.3j)$$

$$\eta^{cha} x_{l,s}^{Gcha} - \frac{x_{l,s}^{Gdch}}{\eta^{dch}} = e_{l,s} - S_0 \quad \forall s \in S \quad (C.3k)$$

$$e_{f,s} = S_f \quad \forall s \in S \quad (C.3l)$$

$$P_b^{building} + \Delta p_{b,s}^{building} \geq b_{h,b,s}^{building} \quad \forall h \in H, b \in B, s \in S \quad (C.3m)$$

$$e_{h,s} = e_{h,s-1} \quad \forall h \in H, s \in S|_{s \neq 1} \quad (C.3n)$$

$$x_{h,s}^{Gcha} = x_{h,s-1}^{Gcha} \quad \forall h \in H, s \in S|_{s \neq 1} \quad (C.3o)$$

$$x_{h,s}^{Gdch} = x_{h,s-1}^{Gdch} \quad \forall h \in H, s \in S|_{s \neq 1} \quad (C.3p)$$

$$b_{h,b,s}^{Gimp} = b_{h,b,s-1}^{Gimp} \quad \forall h \in H, b \in B, s \in S|_{s \neq 1} \quad (C.3q)$$

$$b_{h,b,s}^{Gexp} = b_{h,b,s-1}^{Gexp} \quad \forall h \in H, b \in B, s \in S|_{s \neq 1} \quad (C.3r)$$

$$e_{h,s}, x_{h,s}^{Gcha}, x_{h,s}^{Gdch} \geq 0 \quad \forall h \in H, s \in S \quad (C.3s)$$

$$b_{h,b,s}^{Gimp}, b_{h,b,s}^{Gexp} \geq 0 \quad \forall h \in H, b \in B, s \in S \quad (C.3t)$$

$$\Delta p_s^{battery} \geq 0 \quad \forall s \in S \quad (C.3u)$$

$$\Delta p_{b,s}^{building} \geq 0 \quad \forall b \in B, s \in S \quad (C.3v)$$

D Optimisation Model: Configuration 4

$$\min \sum_{s \in S} \pi_s \sum_{b \in B} \left(\sum_{h \in H} (b_{h,b,s}^{Gimp} (C_h^E + C^V) - C_{h,s}^E b_{h,b,s}^{Gexp}) \right. \\ \left. + C^P (P_b^{building} + \Delta p_{b,s}^{building}) + C^F \right) \quad (\text{D.4a})$$

$$(\text{D.4b})$$

$$\text{s.t.} \quad b_{h,b,s}^{Gimp} - b_{h,b,s}^{Gexp} + b_{h,b,s}^{Limp} - b_{h,b,s}^{Lexp} = R_{h,b}^{cons} - R_{h,b}^{prod} \quad \forall h \in H_1, b \in B, s \in S \quad (\text{D.4c})$$

$$b_{h,b,s}^{Gimp} - b_{h,b,s}^{Gexp} + b_{h,b,s}^{Limp} - b_{h,b,s}^{Lexp} = D_{h,b,s}^{cons} - D_{h,b,s}^{prod} \quad \forall h \in H_2, b \in B, s \in S \quad (\text{D.4d})$$

$$\sum_{b \in B} (b_{h,b,s}^{Limp} - b_{h,b,s}^{Lexp}) = x_{h,s}^{Lcha} - x_{h,s}^{Ldch} \quad \forall h \in H, s \in S \quad (\text{D.4e})$$

$$e_{h,s} \leq E^{max} \quad \forall h \in H, s \in S \quad (\text{D.4f})$$

$$x_{h,s}^{Lcha} \leq K^{max} \quad \forall h \in H, s \in S \quad (\text{D.4g})$$

$$x_{h,s}^{Ldch} \leq K^{max} \quad \forall h \in H, s \in S \quad (\text{D.4h})$$

$$\eta^{cha} x_{l,s}^{Lcha} - \frac{x_{l,s}^{Ldch}}{\eta^{dch}} = e_{h,s} - e_{h-1,s} \quad \forall h \in H |_{h \neq l}, s \in S \quad (\text{D.4i})$$

$$\eta^{cha} x_{l,s}^{Lcha} - \frac{x_{l,s}^{Ldch}}{\eta^{dch}} = e_{l,s} - S_0 \quad \forall s \in S \quad (\text{D.4j})$$

$$e_{f,s} = S_f \quad \forall s \in S \quad (\text{D.4k})$$

$$P_b^{building} + \Delta p_{b,s}^{building} \geq b_{h,b,s}^{building} \quad \forall h \in H, b \in B, s \in S \quad (\text{D.4l})$$

$$e_{h,s} = e_{h,s-1} \quad \forall h \in H, s \in S |_{s \neq 1} \quad (\text{D.4m})$$

$$x_{h,s}^{Lcha} = x_{h,s-1}^{Lcha} \quad \forall h \in H, s \in S |_{s \neq 1}$$

$$x_{h,s}^{Ldch} = x_{h,s-1}^{Ldch} \quad \forall h \in H, s \in S |_{s \neq 1} \quad (\text{D.4n})$$

$$b_{h,b,s}^{Gimp} = b_{h,b,s-1}^{Gimp} \quad \forall h \in H, b \in B, s \in S |_{s \neq 1}$$

$$b_{h,b,s}^{Gexp} = b_{h,b,s-1}^{Gexp} \quad \forall h \in H, b \in B, s \in S |_{s \neq 1} \quad (\text{D.4o})$$

$$b_{h,b,s}^{Limp} = b_{h,b,s-1}^{Limp} \quad \forall h \in H, b \in B, s \in S |_{s \neq 1}$$

$$b_{h,b,s}^{Lexp} = b_{h,b,s-1}^{Lexp} \quad \forall h \in H, b \in B, s \in S |_{s \neq 1} \quad (\text{D.4p})$$

$$e_{h,s}, x_{h,s}^{Lcha}, x_{h,s}^{Ldch} \geq 0 \quad \forall h \in H, s \in S \quad (\text{D.4q})$$

$$b_{h,b,s}^{Gimp}, b_{h,b,s}^{Gexp}, b_{h,b,s}^{Limp}, b_{h,b,s}^{Lexp} \geq 0 \quad \forall h \in H, b \in B, s \in S \quad (\text{D.4r})$$

$$\Delta p_{b,s}^{building} \geq 0 \quad \forall b \in B, s \in S \quad (\text{D.4s})$$

E Optimisation Model: Configuration 5

$$\begin{aligned}
\min \quad & \sum_{s \in S} \pi_s \left(\sum_{b \in B} \left(\sum_{h \in H} (b_{h,b,s}^{Gimp} (C_h^E + C^V) - C_h^E b_{h,b,s}^{Gexp}) \right. \right. \\
& + C^P (P_b^{building} + \Delta p_{b,s}^{building}) + C^F) + \sum_{h \in H} (x_{h,s}^{Gcha} (C_h^E \\
& \left. \left. + C^V) - C^E x_{h,s}^{Gdch}) + C^P (P^{battery} + \Delta p_s^{battery}) + C^F \right) \quad (E.5a)
\end{aligned}$$

$$\text{s.t.} \quad b_{h,b,s}^{Gimp} - b_{h,b,s}^{Gexp} + b_{h,b,s}^{Limp} - b_{h,b,s}^{Lexp} = R_{h,b}^{cons} - R_{h,b}^{prod} \quad \forall h \in H_1, b \in B, s \in S \quad (E.5b)$$

$$b_{h,b,s}^{Gimp} - b_{h,b,s}^{Gexp} + b_{h,b,s}^{Limp} - b_{h,b,s}^{Lexp} = D_{h,b,s}^{cons} - D_{h,b,s}^{prod} \quad \forall h \in H_2, b \in B, s \in S \quad (E.5c)$$

$$\sum_{b \in B} (b_{h,b,s}^{Limp} - b_{h,b,s}^{Lexp}) = x_{h,s}^{Lcha} - x_{h,s}^{Ldch} \quad \forall h \in H, s \in S \quad (E.5d)$$

$$e_{h,s} \leq E^{max} \quad \forall h \in H, s \in S \quad (E.5e)$$

$$x_{h,s}^{Gcha} + x_{h,s}^{Lcha} \leq K^{max} \quad \forall h \in H, s \in S \quad (E.5f)$$

$$x_{h,s}^{Gdch} + x_{h,s}^{Ldch} \leq K^{max} \quad \forall h \in H, s \in S \quad (E.5g)$$

$$\eta^{cha} (x_{l,s}^{Gcha} + x_{l,s}^{Lcha}) - \frac{(x_{l,s}^{Gdch} + x_{l,s}^{Ldch})}{\eta^{dch}} = e_{h,s} - e_{h-1,s} \quad \forall h \in H |_{h \neq l}, s \in S \quad (E.5h)$$

$$\eta^{cha} (x_{l,s}^{Gcha} + x_{l,s}^{Lcha}) - \frac{(x_{l,s}^{Gdch} + x_{l,s}^{Ldch})}{\eta^{dch}} = e_{l,s} - S_0 \quad \forall s \in S \quad (E.5i)$$

$$e_{f,s} = S_f \quad \forall s \in S \quad (E.5j)$$

$$P_b^{building} + \Delta p_{b,s}^{building} \geq b_{h,b,s}^{building} \quad \forall h \in H, b \in B, s \in S \quad (E.5k)$$

$$P^{battery} + \Delta p_s^{battery} \geq x_{h,s}^{Gcha} \quad \forall h \in H, s \in S \quad (E.5l)$$

$$e_{h,s} = e_{h,s-1} \quad \forall h \in H, s \in S |_{s \neq 1} \quad (E.5m)$$

$$x_{h,s}^{cha} = x_{h,s-1}^{cha} \quad \forall h \in H, s \in S|_{s \neq 1} \quad (\text{E.5n})$$

$$x_{h,s}^{dch} = x_{h,s-1}^{dch} \quad \forall h \in H, s \in S|_{s \neq 1} \quad (\text{E.5o})$$

$$x_{h,s}^{Lcha} = x_{h,s-1}^{Lcha} \quad \forall h \in H, s \in S|_{s \neq 1} \quad (\text{E.5p})$$

$$x_{h,s}^{Ldch} = x_{h,s-1}^{Ldch} \quad \forall h \in H, s \in S|_{s \neq 1} \quad (\text{E.5q})$$

$$b_{h,b,s}^{Gimp} = b_{h,b,s-1}^{Gimp} \quad \forall h \in H, b \in B, s \in S|_{s \neq 1} \quad (\text{E.5r})$$

$$b_{h,b,s}^{Gexp} = b_{h,b,s-1}^{Gexp} \quad \forall h \in H, b \in B, s \in S|_{s \neq 1} \quad (\text{E.5s})$$

$$b_{h,b,s}^{Limp} = b_{h,b,s-1}^{Limp} \quad \forall h \in H, b \in B, s \in S|_{s \neq 1} \quad (\text{E.5t})$$

$$b_{h,b,s}^{Lexp} = b_{h,b,s-1}^{Lexp} \quad \forall h \in H, b \in B, s \in S|_{s \neq 1} \quad (\text{E.5u})$$

$$e_{h,s}, x_{h,s}^{Gcha}, x_{h,s}^{Gdch}, x_{h,s}^{Lcha}, x_{h,s}^{Ldch} \geq 0 \quad \forall h \in H, s \in S \quad (\text{E.5v})$$

$$b_{h,b,s}^{Gimp}, b_{h,b,s}^{Gexp}, b_{h,b,s}^{Limp}, b_{h,b,s}^{Lexp} \geq 0 \quad \forall h \in H, b \in B, s \in S \quad (\text{E.5w})$$

$$\Delta p_s^{battery} \geq 0 \quad \forall s \in S \quad (\text{E.5x})$$

$$\Delta p_{b,s}^{building} \geq 0 \quad \forall b \in B, s \in S \quad (\text{E.5y})$$

F Optimisation Model: Configuration 6

$$\min \sum_{s \in S} \pi_s \sum_{b \in B} \left(\sum_{h \in H} (b_{h,b,s}^{Gimp} (C_h^E + C^V) - C_{h,s}^E b_{h,b,s}^{Gexp}) \right. \\ \left. + C^P (P_b^{building} + \Delta p_{b,s}^{building}) + C^F \right) \quad (\text{F.6a})$$

$$(\text{F.6b})$$

$$\text{s.t.} \quad b_{h,k,s}^{Gimp} - b_{h,k,s}^{Gexp} + b_{h,k,s}^{Limp} - b_{h,k,s}^{Lexp} = R_{h,k}^{cons} - R_{h,k}^{prod} \\ + x_{h,k,s}^{Lcha} - x_{h,k,s}^{Ldch} \quad \forall h \in H_1, s \in S \quad (\text{F.6c})$$

$$b_{h,k,s}^{Gimp} - b_{h,k,s}^{Gexp} + b_{h,k,s}^{Limp} - b_{h,k,s}^{Lexp} = D_{h,k,s}^{cons} - D_{h,k,s}^{prod} \\ + x_{h,k,s}^{Lcha} - x_{h,k,s}^{Ldch} \quad \forall h \in H_2, s \in S \quad (\text{F.6d})$$

$$b_{h,b,s}^{Gimp} - b_{h,b,s}^{Gexp} + b_{h,b,s}^{Limp} - b_{h,b,s}^{Lexp} = R_{h,b}^{cons} - R_{h,b}^{prod} \quad \forall h \in H_1, b \in B|_{b \neq k}, s \in S \quad (\text{F.6e})$$

$$b_{h,b,s}^{Gimp} - b_{h,b,s}^{Gexp} + b_{h,b,s}^{Limp} - b_{h,b,s}^{Lexp} = D_{h,b,s}^{cons} - D_{h,b,s}^{prod} \quad \forall h \in H_2, b \in B|_{b \neq k}, s \in S \quad (\text{F.6f})$$

$$\sum_{b \in B} (b_{h,b,s}^{Limp} - b_{h,b,s}^{Lexp}) = x_{h,s}^{Lcha} - x_{h,s}^{Ldch} \quad \forall h \in H, s \in S \quad (\text{F.6g})$$

$$e_{h,s} \leq E^{max} \quad \forall h \in H, s \in S \quad (\text{F.6h})$$

$$x_{h,s}^{Lcha} \leq K^{max} \quad \forall h \in H, s \in S \quad (\text{F.6i})$$

$$x_{h,s}^{Ldch} \leq K^{max} \quad \forall h \in H, s \in S \quad (\text{F.6j})$$

$$\eta^{cha} x_{l,s}^{Lcha} - \frac{x_{l,s}^{Ldch}}{\eta^{dch}} = e_{h,s} - e_{h-1,s} \quad \forall h \in H|_{h \neq l}, s \in S \quad (\text{F.6k})$$

$$\eta^{cha} x_{l,s}^{Lcha} - \frac{x_{l,s}^{Ldch}}{\eta^{dch}} = e_{l,s} - S_0 \quad \forall s \in S \quad (\text{F.6l})$$

$$e_{f,s} = S_f \quad \forall s \in S \quad (\text{F.6m})$$

$$P_b^{building} + \Delta p_{b,s}^{building} \geq b_{h,b,s}^{building} \quad \forall h \in H, b \in B, s \in S \quad (\text{F.6n})$$

$$e_{h,s} = e_{h,s-1} \quad \forall h \in H, s \in S|_{s \neq 1} \quad (\text{F.6o})$$

$$x_{h,s}^{Lcha} = x_{h,s-1}^{Lcha} \quad \forall h \in H, s \in S|_{s \neq 1} \quad (\text{F.6p})$$

$$x_{h,s}^{Ldch} = x_{h,s-1}^{Ldch} \quad \forall h \in H, s \in S|_{s \neq 1} \quad (\text{F.6q})$$

$$b_{h,b,s}^{Gimp} = b_{h,b,s-1}^{Gimp} \quad \forall h \in H, b \in B, s \in S|_{s \neq 1} \quad (\text{F.6r})$$

$$b_{h,b,s}^{Gexp} = b_{h,b,s-1}^{Gexp} \quad \forall h \in H, b \in B, s \in S|_{s \neq 1} \quad (\text{F.6s})$$

$$b_{h,b,s}^{Limp} = b_{h,b,s-1}^{Limp} \quad \forall h \in H, b \in B, s \in S|_{s \neq 1} \quad (\text{F.6t})$$

$$b_{h,b,s}^{Lexp} = b_{h,b,s-1}^{Lexp} \quad \forall h \in H, b \in B, s \in S|_{s \neq 1} \quad (\text{F.6u})$$

$$e_{h,s}, x_{h,s}^{Lcha}, x_{h,s}^{Ldch} \geq 0 \quad \forall h \in H, s \in S \quad (\text{F.6v})$$

$$b_{h,b,s}^{Gimp}, b_{h,b,s}^{Gexp}, b_{h,b,s}^{Limp}, b_{h,b,s}^{Lexp} \geq 0 \quad \forall h \in H, b \in B, s \in S \quad (\text{F.6w})$$

$$\Delta p_{b,s}^{building} \geq 0 \quad \forall b \in B, s \in S \quad (\text{F.6x})$$

G Predictions by the Autoregressive Models

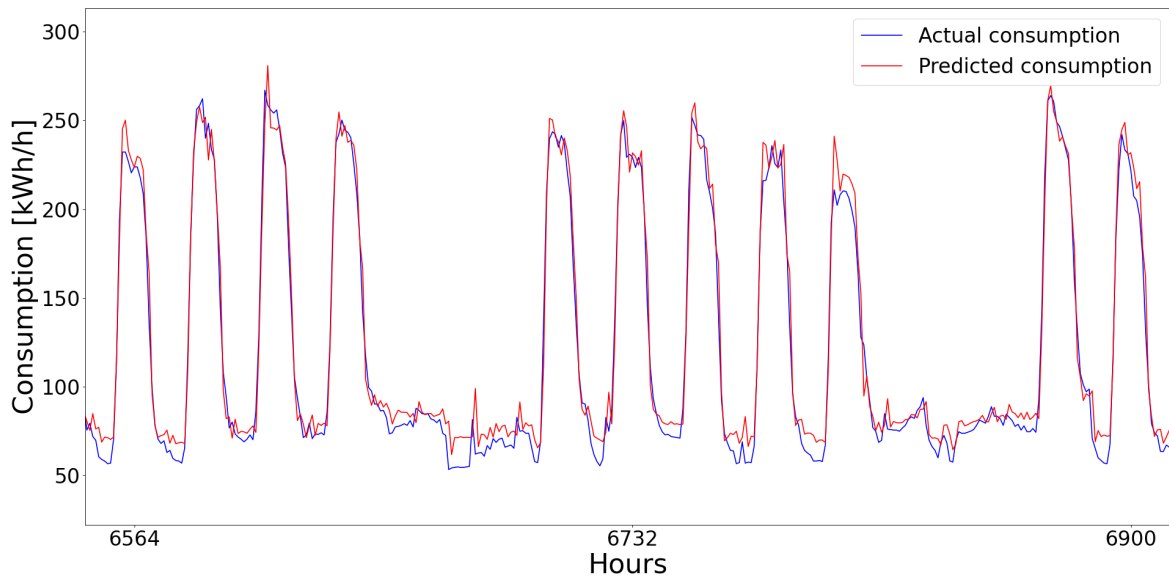


Figure G.1: Prediction of consumption at $BK15AB(y_{1,t})$

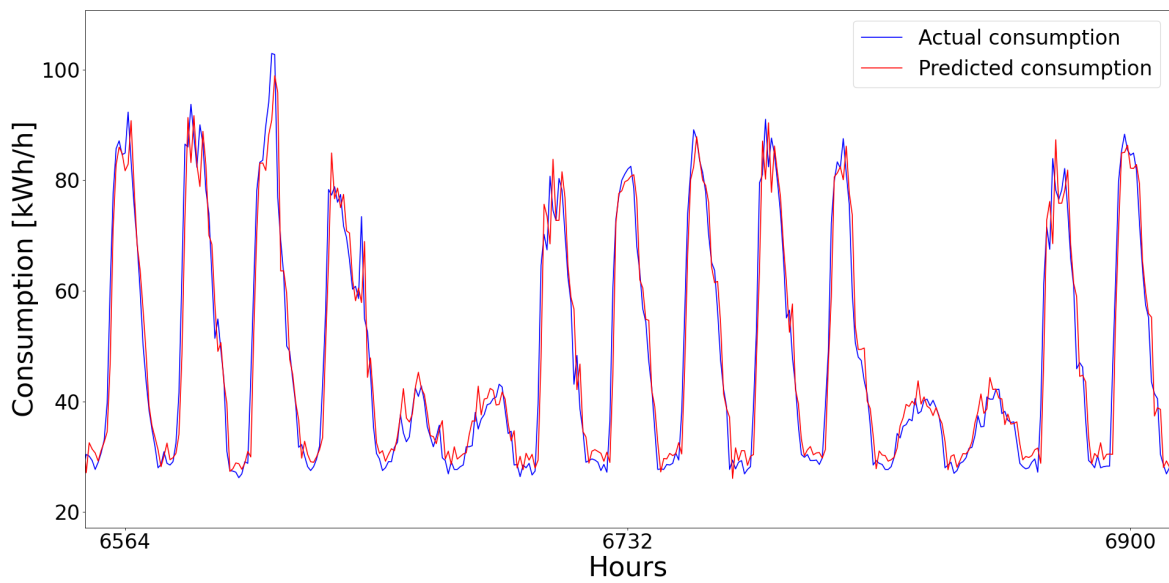


Figure G.2: Prediction of consumption at $BK16(y_{2,t})$

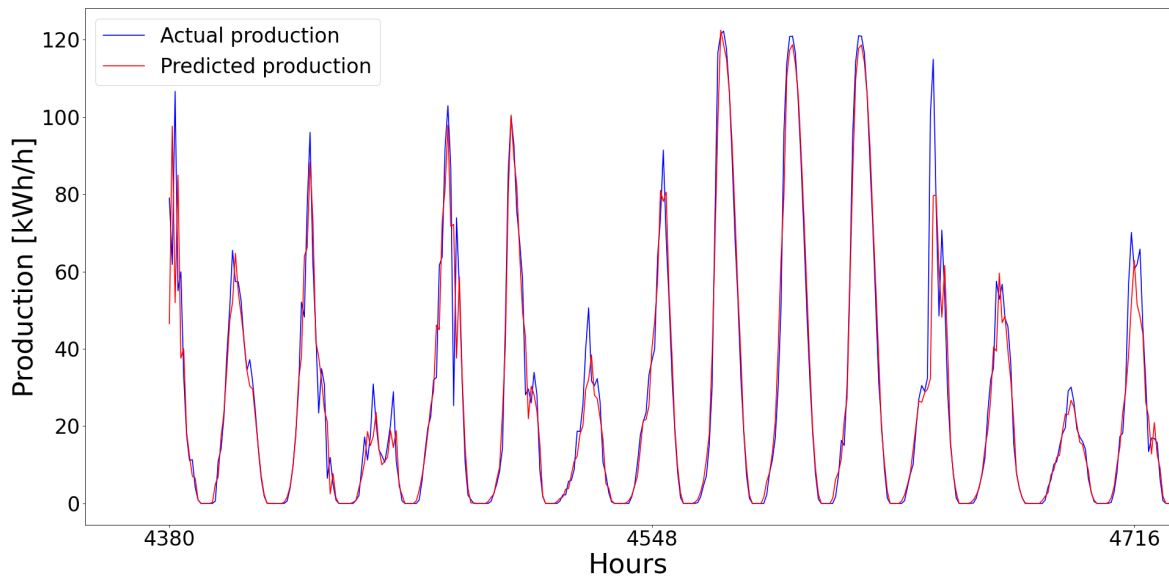


Figure G.3: Prediction of production at $BK16(y_{3,t})$

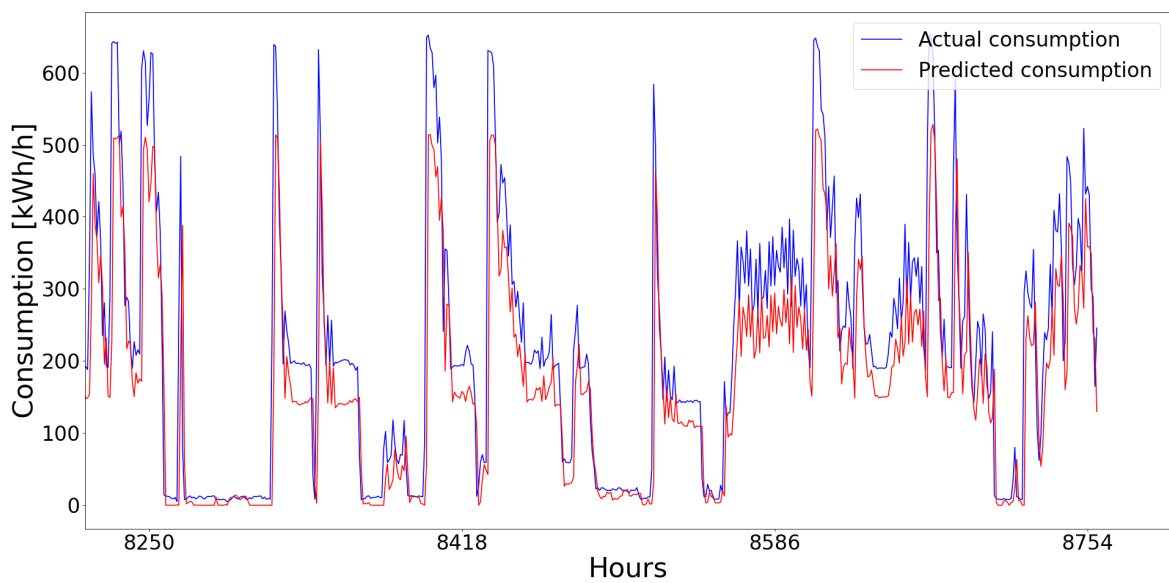


Figure G.4: Prediction of consumption at $Sjogangen(y_{4,t})$

H Preliminary Results of Scenario Generation

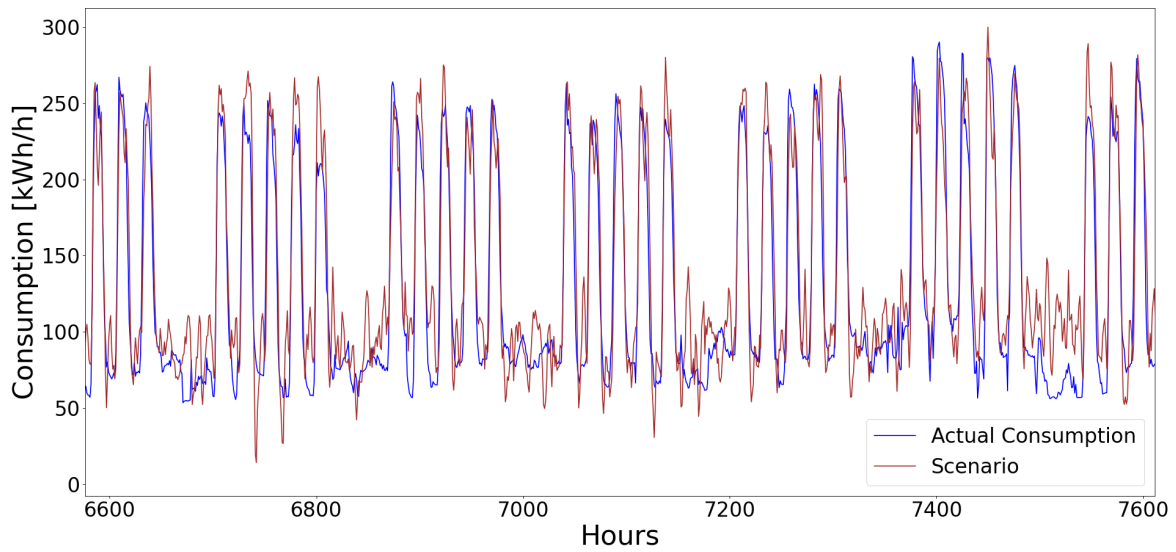


Figure H.1: Preliminary results showing the forecasting accuracy of $y_{1,t}$

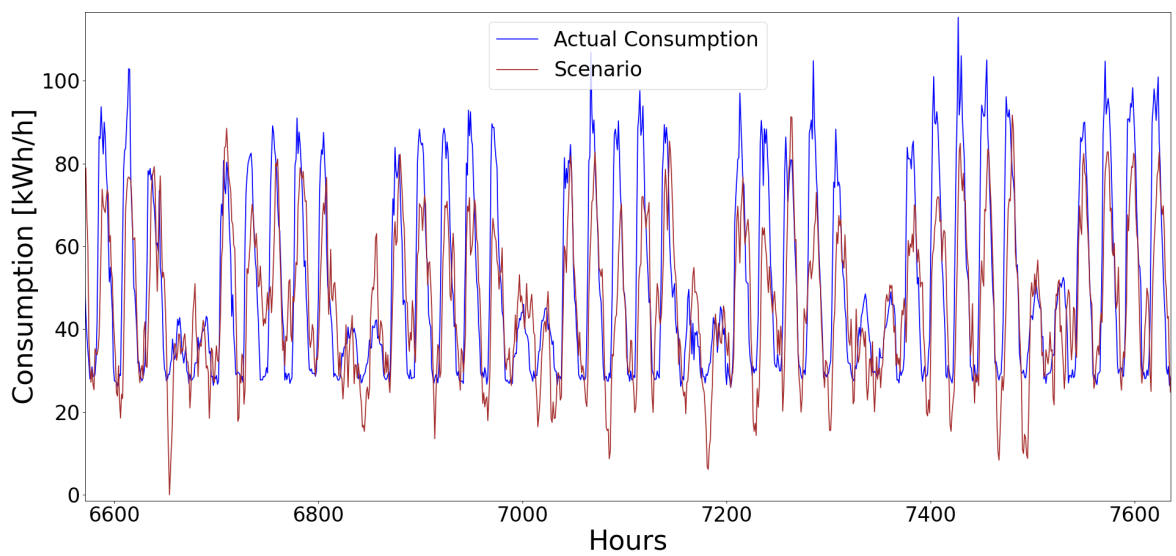


Figure H.2: Preliminary results showing the forecasting accuracy of $y_{3,t}$

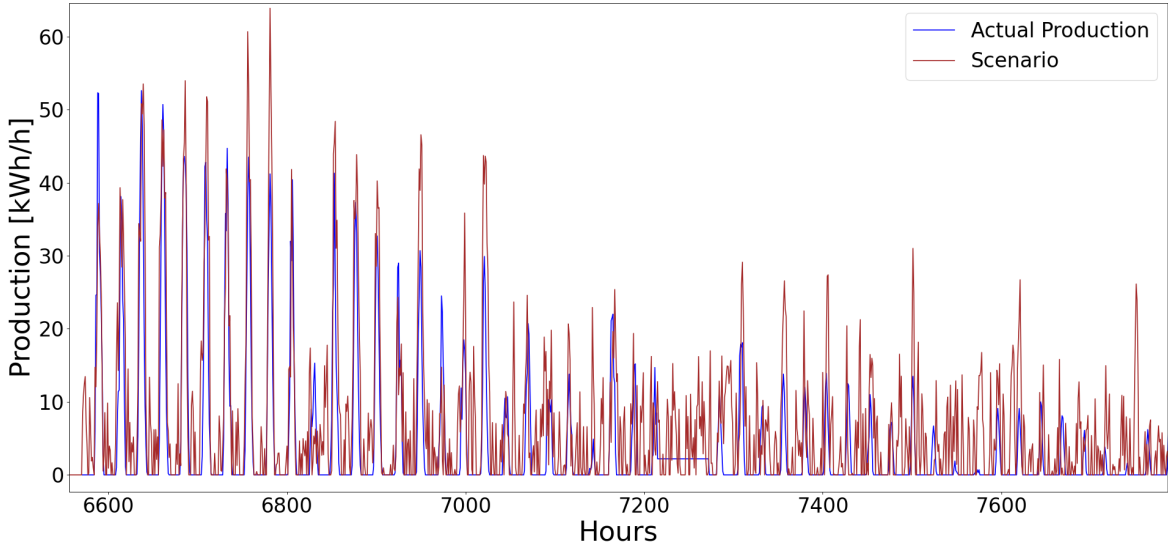


Figure H.3: Preliminary results showing the forecasting accuracy of $y_{3,t}$

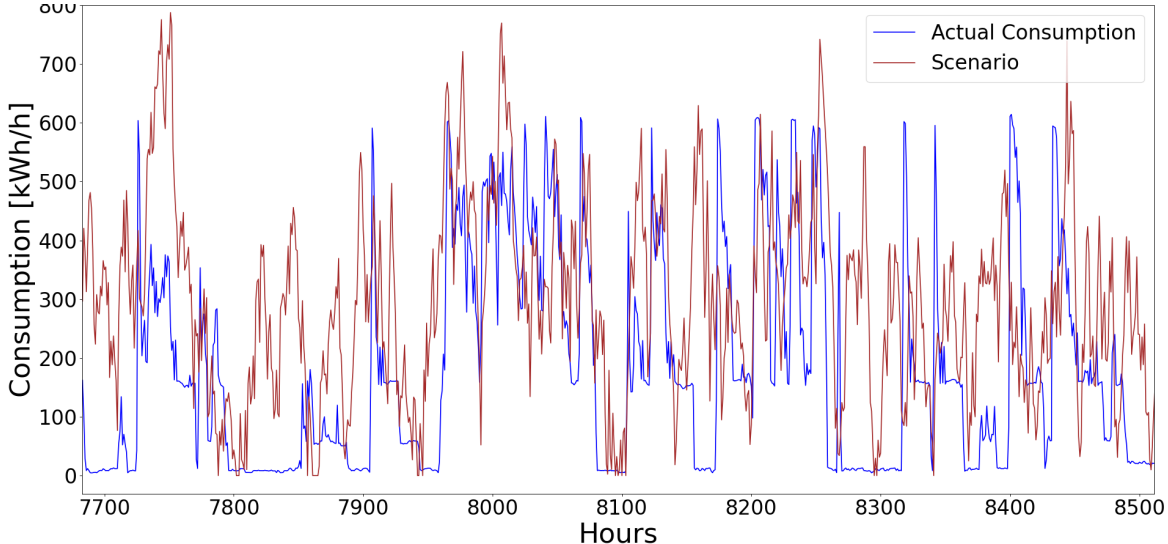


Figure H.4: Preliminary results showing the forecasting accuracy of $y_{4,t}$

I Cost Contribution Tables

Cases		January			Energy costs
		Peak costs	Grid tariff Volumetric costs	Fixed costs	Spot price
<i>Base case</i>	<i>Costs [kNOK]</i>	<i>141.4</i>	<i>65.0</i>	<i>1.0</i>	<i>65.7</i>
	<i>% of total costs</i>	<i>51.8</i>	<i>23.8</i>	<i>0.4</i>	<i>24.1</i>
1	Costs [kNOK]	114.6	65.2	0.3	65.3
	% of total costs	46.7	26.6	0.1	26.6
2	Costs [kNOK]	141.4	65.0	1.4	65.7
	% of total costs	51.7	23.8	0.5	24.0
3.1	Costs [kNOK]	132.1	65.3	1.0	65.4
	% of total costs	50.1	24.8	0.4	24.8
3.2	Costs [kNOK]	137.6	65.1	1.0	65.6
	% of total costs	51.1	24.2	0.4	24.4
3.3	Costs [kNOK]	143.3	65.2	1.0	65.3
	% of total costs	52.1	23.7	0.4	23.8
4 with battery	Costs [kNOK]	125.2	65.2	1.0	65.3
	% of total costs	48.8	25.4	0.4	25.4
4 without battery	Costs [kNOK]	138.8	65.0	1.0	65.7
	% of total costs	51.3	24.0	0.4	24.3
5	Costs [kNOK]	124.6	65.2	1.4	65.3
	% of total costs	48.6	25.4	0.5	25.5
6.1	Costs [kNOK]	126.4	65.2	1.0	65.3
	% of total costs	49.0	25.3	0.4	25.3
6.2	Costs [kNOK]	123.6	65.2	1.0	65.3
	% of total costs	48.5	25.6	0.4	25.6
6.3	Costs [kNOK]	124.4	65.2	1.0	65.3
	% of total costs	48.6	25.5	0.4	25.5

Table I.1: Cost contributions for the energy bill in January

		March			Energy costs
Cases		Peak costs	Volumetric costs	Fixed costs	Spot price
<i>Base case</i>	<i>Costs [kNOK]</i>	<i>145.0</i>	<i>43.7</i>	<i>1.0</i>	<i>19.5</i>
	<i>% of total costs</i>	<i>69.3</i>	<i>20.9</i>	<i>0.5</i>	<i>9.3</i>
1	Costs [kNOK]	111.3	43.8	0.3	19.3
	% of total costs	63.7	25.1	0.2	11.1
2	Costs [kNOK]	145.0	43.8	1.4	19.6
	% of total costs	69.1	20.9	0.6	9.3
3.1	Costs [kNOK]	134.2	43.9	1.0	19.4
	% of total costs	67.6	22.1	0.5	9.8
3.2	Costs [kNOK]	141.2	43.7	1.0	19.5
	% of total costs	68.7	21.3	0.5	9.5
3.3	Costs [kNOK]	136.8	43.8	1.0	19.4
	% of total costs	68.0	21.8	0.5	9.6
4 with battery	Costs [kNOK]	113.7	43.8	1.0	19.4
	% of total costs	63.9	24.6	0.6	10.9
4 without battery	Costs [kNOK]	132.6	43.7	1.0	19.5
	% of total costs	67.4	22.2	0.5	9.9
5	Costs [kNOK]	115.1	43.8	1.4	19.4
	% of total costs	64.1	24.4	0.8	10.8
6.1	Costs [kNOK]	112.0	43.8	1.0	19.4
	% of total costs	63.6	24.9	0.6	11.0
6.2	Costs [kNOK]	114.0	43.8	1.0	19.3
	% of total costs	64.0	24.6	0.6	10.9
6.3	Costs [kNOK]	113.1	43.8	1.0	19.4
	% of total costs	63.8	24.7	0.6	10.9

Table I.2: Cost contributions for the energy bill in March

		June			Energy costs
Cases		Peak costs	Volumetric costs	Fixed costs	Spot price
<i>Base case</i>	<i>Costs [kNOK]</i>	<i>39.9</i>	<i>20.8</i>	<i>1.0</i>	<i>6.1</i>
	<i>% of total costs</i>	<i>58.9</i>	<i>30.7</i>	<i>1.5</i>	<i>8.9</i>
1	Costs [kNOK]	32.7	18.2	0.3	2.6
	% of total costs	60.7	33.8	0.6	4.8
2	Costs [kNOK]	39.9	20.8	1.4	3.3
	% of total costs	61.1	31.8	2.1	5.0
3.1	Costs [kNOK]	34.3	21.0	1.0	3.1
	% of total costs	57.8	35.3	1.7	5.1
3.2	Costs [kNOK]	39.1	19.4	1.0	3.1
	% of total costs	62.5	31.0	1.6	4.9
3.3	Costs [kNOK]	40.1	20.8	1.0	3.3
	% of total costs	61.5	31.9	1.6	5.0
4 with battery	Costs [kNOK]	35.2	18.2	1.0	2.6
	% of total costs	61.7	32.0	1.8	4.6
4 without battery	Costs [kNOK]	41.2	18.2	1.0	2.8
	% of total costs	65.2	28.7	1.6	4.5
5	Costs [kNOK]	34.1	18.2	1.4	2.6
	% of total costs	60.6	32.4	2.4	4.6
6.1	Costs [kNOK]	34.6	18.2	1.0	2.6
	% of total costs	61.3	32.3	1.8	4.6
6.2	Costs [kNOK]	34.1	18.2	1.0	2.6
	% of total costs	60.9	32.6	1.8	4.7
6.3	Costs [kNOK]	37.0	18.2	1.0	2.6
	% of total costs	62.9	31.0	1.7	4.4

Table I.3: Cost contributions for the energy bill in June

J Scientific Paper

Impact of shared battery energy storage system on total system costs and power peak reduction in commercial buildings

Ida E. U. Skoglund*, Mette Rostad, Kasper E. Thorvaldsen

Department of Electric Power Engineering, NTNU - Trondheim, Norway

E-mail: ugleskog@gmail.com

Abstract. The power system is experiencing an increasing share of renewable and intermittent energy production and increasing electrification. However, these changes are creating high power peaks, are straining the grid and call for expensive investments in expansions and improvements. This paper examines how the operational strategy of shared battery energy storage systems (s-BESS) can address these issues for commercial buildings with relatively high power peaks. Due to the uncertainty in long-term costs when subject to a measured peak (MP) grid tariff, the scheduling of the battery is optimised with a receding horizon control algorithm. The optimisation model is used on a Norwegian real-life case study to find the best possible configuration with an already existing battery. Although current Norwegian regulations challenge the possibility for shared metering and billing for a s-BESS configuration, the results show that the total system cost was reduced by 19.2% compared to no battery. The community peak was reduced by 17.8% compared to no battery and 6.22-17.5% compared to individual storage, which indicates that s-BESS is of value for the DSO as well.

Sets		$D_{h,b,s}^{cons}$	Consumption in hour h by building b
S	Set of scenarios	η	Battery (dis)charging efficiency
B	Set of buildings	π_s	Probability of scenario s
H	Set of hours	P^{peak}	Previously measured system power peak
Indices		$P_b^{building}$	Previously measured power peak for each building
s	A scenario s in set S		
h	An hour h in set H		
k	The final hour in the first stage problem	Decision variables	
b	A building in set B	$e_{h,s}$	Energy stored in the battery in hour h for scenario s
Parameters		Δp_s^{peak}	The additional power to reach new maximum total system peak
C_h^{spot}	Energy spot price in hour h	$\Delta p_{b,s}^{building}$	The additional power to reach new maximum peak for each building
C^{peak}	Peak power tariff	$p_{h,s}^{imp}, p_{h,s}^{exp}$	Total power imported/exported to grid in hour h for scenario s
C^{vol}	Volumetric costs	$y_{h,b,s}^{imp}, y_{h,b,s}^{exp}$	Power imported/exported in hour h by building b in scenario s
C^{fixed}	Fixed cost	$x_{h,s}^{cha}, x_{h,s}^{dch}$	Power to/from the battery at hour h in scenario s
E^{max}	Battery energy storage capacity		
K^{max}	Battery (dis)charge capacity		
δ_b	Battery connected to building {0,1}		
δ^{joint}	Joint metering for all buildings {0,1}		
$D_{h,b,s}^{prod}$	Production in hour h by building b		

*Corresponding author.

1. Introduction

The interest in battery energy storage systems (BESS) integration on the demand side is increasing due to the ability to handle the intermittency of renewable energy sources and the increasing power demand. This ability to provide location-specific services can in turn postpone costly grid investments [1]. Batteries can assist in peak-shaving which ensures that the grid will not experience the full effects of high energy demands [1]. In addition, other studies show that optimal operation of s-BESS between several residential buildings will result in higher energy efficiency and lower total system cost for the whole area compared to individual battery storage [2, 3]. It should, however, be noted that these studies typically include buildings with similar load and production patterns.

Due to the high consumption of commercial buildings and their varying consumption patterns and power peaks, this work will focus on the integration of a s-BESS between commercial buildings in urban areas, including a case study from Trondheim, Norway. There are already considerable volumes of work dedicated to the economic value of BESS implementation in commercial buildings under different grid tariffs [4, 5]. Work in Refs. [6, 7] considered the monetary benefits of peak shaving for commercial buildings with BESS and photovoltaics(PV), showing increased self-consumption and that costs can be efficiently reduced by peak shaving. Shared BESS between commercial buildings has been considered by [8, 9], but few others investigate the effects of s-BESS for commercial buildings with different production profiles and measured peak (MP) grid tariff.

Currently, Norwegian DSOs use MP grid tariffs for high demand commercial buildings, but regulations do not allow shared metering for more than one building or legal entity [10]. This challenges the s-BESS, as the economical benefits disappears with individual metering.

This paper investigates the monetary benefits of s-BESS and metering and compares this configurations to other configurations that are in line with current regulations. When optimising BESS operatio, a receding horizon control (RHC) approach is advantageous because of the ability to consider future uncertainties [11]. Therefore, a receding horizon optimisation model is developed to perform the analysis, with a stochastic linear program to consider future uncertainties. The contributions from this paper are:

- The development of an RHC model for shared commercial community under the influence of long-term capacity-based grid tariffs.
- Quantified gains of shared energy storage for urban area commercial buildings compared to configurations in line with regulatory regimes.

2. Methodology

The presented methodology aims at investigating the benefit of using a BESS as a shared asset in a community, or individually by a chosen building in the community. To be able to properly control the battery, while taking into account the long-term significance of the maximum power peak grid tariff, a receding horizon control (RHC) optimization algorithm has been developed. The RHC makes use of a stochastic LP problem to control the BESS optimally. Both the stochastic LP model and RHC is explained further in the following sections.

2.1. Stochastic linear program(LP) model formulation

The objective of the stochastic LP-formulation is to minimise the electricity costs by operating the BESS. The optimization model is divided into two stages; the first stage has deterministic information up until hour k , while the second stage has the problem split into three discrete stochastic scenarios for the rest of the month. The second stage allow the model to foresee the possible future peak levels and include the peak power grid tariff.

2.1.1. Objective function The objective function is dependent on whether the BESS is shared by the community or owned individually. For joint metering the binary variable δ^{joint} holds value 1, and 0 for individual metering, hence changing the objective function. As shown in Eq. (1), the objective function represents the cost from the energy spot price and the grid tariff that consists of volumetric costs, peak power costs and fixed costs from the DSO.

$$\begin{aligned} \min \quad z = & \delta^{joint} \sum_{s \in S} \pi_s \left(\sum_{h \in H} ((C_h^{spot} + C^{vol}) p_{h,s}^{imp} - C_h^{spot} p_{h,s}^{exp}) + C^{peak} (\Delta p_s^{peak} + P^{peak}) + C^{fixed} \right) \\ & + (1 - \delta^{joint}) \sum_{s \in S} \pi_s \left(\sum_{b \in B} \sum_{h \in H} ((C_h^{spot} + C^{vol}) y_{h,b,s}^{imp} \right. \\ & \left. - C_h^{spot} y_{h,b,s}^{exp}) + C^{peak} (\Delta p_{b,s}^{peak} + P_b^{building}) + C^{fixed} \right) \quad (1) \end{aligned}$$

2.1.2. Energy balance constraints The electric energy balance between the buildings and the grid is shown in Eq. (2), while the balance for each individual building is captured in Eq. (3). The BESS can be placed either in the community or with a specific building, based on the parameters δ^{joint} and δ_b . δ_b holds value 1 if it is placed with building b and 0 otherwise.

$$p_{h,s}^{imp} - p_{h,s}^{exp} + \delta^{joint} x_{h,s}^{dch} + \sum_{b \in B} y_{h,b,s}^{exp} = \sum_{b \in B} y_{h,b,s}^{imp} + \delta^{joint} x_{h,s}^{cha} \quad \forall h \in H, s \in S \quad (2)$$

$$y_{h,b,s}^{imp} - y_{h,b,s}^{exp} + D_{h,b,s}^{prod} + \delta_b x_{h,s}^{dch} = D_{h,b,s}^{cons} + \delta_b x_{h,s}^{cha} \quad \forall h \in H, b \in B, s \in S \quad (3)$$

2.1.3. Battery constraints The BESS has an upper and lower limit on how much energy the battery can store, shown in Eq. (5), and how much power can be charged and discharged within an hour, as shown in Eq. (4). Eq. (6) addresses the energy balance for the battery based on charging/discharging quantities.

$$0 \leq x_{h,s}^{cha}, x_{h,s}^{dch} \leq K^{max} \quad \forall h \in H, s \in S \quad (4)$$

$$0 \leq e_{h,s} \leq E^{max} \quad \forall h \in H, s \in S \quad (5)$$

$$e_{h,s} - e_{h-1,s} = \eta x_{h,s}^{cha} - \frac{x_{h,s}^{dch}}{\eta} \quad \forall h \in H, s \in S \quad (6)$$

2.1.4. Power peak constraints The maximum power peak grid tariff is based on the highest single-hour peak import level during a one month period, for the community or for the individual buildings. As shown in Eq. (7) for the community and Eq. (8) for the individual building, the peak power is based on previous peak levels, P^{Peak} , and the increase of peak levels during operation, Δp_s^{peak} , for each scenario.

$$\Delta p_s^{peak} + P^{peak} \geq p_{h,s}^{imp} \quad \forall h \in H, s \in S \quad (7)$$

$$\Delta p_{b,s}^{building} + P_b^{building} \geq y_{h,b,s}^{imp} \quad \forall h \in H, b \in B, s \in S \quad (8)$$

2.1.5. Non-anticipativity constraints The purpose of Eq. (9) is to ensure the first-stage problem has equal State-of-charge (SoC) until the stochastic second-stage problem has started.

$$e_{k,s} = e_{k,s+1} \quad \forall s \in S \quad (9)$$

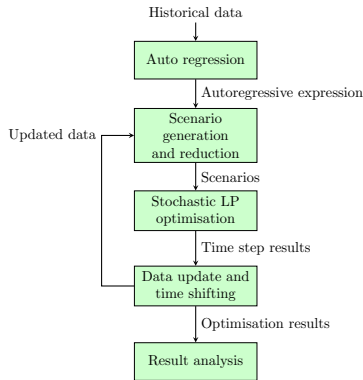


Figure 1: Flow chart showing the process of optimising with receding horizon control including scenario generation and data updates.

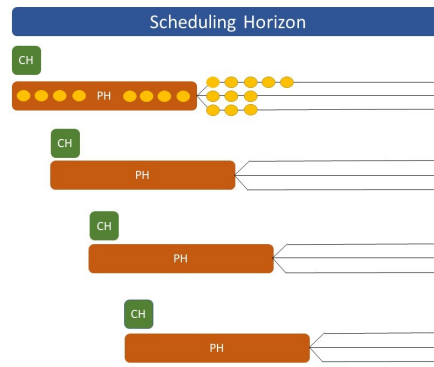


Figure 2: The iterative process of receding horizon control, showing how the scenario tree, control and prediction horizon is shifted through time.

2.2. Receding horizon control

The RHC has the following setup, as illustrated in Figure 1: First, scenarios are generated by finding an auto regressive expression for the stochastic time series, $D_{h,b,s}^{prod}$ and $D_{h,b,s}^{cons}$, used in the optimisation model. Historical data for production and consumption of the previous year is used for training the auto regressive process. Then, several scenarios are generated and later reduced to obtain a reasonable scenario tree that is representative of all the possible outcomes. These scenarios are used to solve the stochastic LP problem, and find the operational plan for the BESS within the control horizon (CH) time period. As seen in Figure 2, the CH and prediction horizon (PH) is considered deterministic, but the period beyond is stochastic with a given number of discrete scenarios to capture the uncertainty of operation. After solving the LP problem, time is shifted with a step equal to the CH, and the process is repeated with updated data concerning current battery storage and previous measured power peak. For every iteration new realistic, simulated scenarios are generated and used for solving the stochastic LP problem until the end of the scheduling horizon (SH).

3. Case studies

The presented RHC optimization algorithm has been tested for a real-life case study located in Trondheim, Norway for January 2020. The case study examines three consumers/prosumers (referred to as 1, 2 and 3). Building 1 and 2 are office buildings (where 1 has installed PV). Consumer 3 is a walking bridge with an integrated system for snow melting. The grid tariffs consist of volumetric cost $C^{vol} = 0.00687 \frac{EUR}{kWh}$, fixed cost $C^{fixed} = 881.78 EUR$, and peak cost $C^{peak} = 8.163 \frac{EUR}{kWh/h}$. A conversion factor at 10.00 NOK/EUR has been used.

The goal of the analysis is to see how an existing BESS with $K^{max} = 200$ kW and $E^{max} = 500$ kWh can benefit the community by reducing the total electricity cost with both peak-shaving and load-shifting. As the current Norwegian regulations do not allow shared metering for a community of commercial buildings and facilities [10], the cases will not only involve looking into s-BESS, but also individual metering and ownership of the battery.

The analysis is conducted for January 2020 when power peaks are on their highest during the year. However, due to minimal irradiation in Norway in January, the total PV-production is merely 260.8kWh, limiting impact from PV-production with joint metering and a s-BESS. The CH and PH have a 1 and 8 hour horizon, respectively, with hourly resolution and actual

measuring data. The scenario tree is made up of three scenarios from 100 generated scenarios for consumption and production for the buildings, which is updated for each operating hour. The number of scenarios were chosen to limit computational time. The presented optimization algorithm is programmed using the Python-based optimisation modeling language, Pyomo 5.7, with the GLPK solver. The simulations were run on a AMD Ryzen 5 4500 64-bit processor, with an average run time of 1 hour per case. The following cases are investigated:

3.1. Case 1: All buildings and the battery behind the meter

Case 1 consist of the community operating together behind a shared meter ($\delta^{joint} = 1$), with a s-BESS at their disposal ($\delta_b = 0, \forall b \in B$). The peak grid tariff is paid based on the accumulated import from all participants. With free float of power behind the meter, this configuration can be seen as a microgrid depending on a strong connection to the distribution grid.

3.2. Case 2: Individual metering and no battery

Case 2 let all three consumers being metered individually ($\delta^{joint} = 0$), and the BESS is not present in the system ($\delta_b = 0, \forall b \in B$). Each consumer pays electricity imported and their own separate peak grid tariff.

3.3. Case 3: Individual battery and metering

Case 3 is divided into three different sub-cases, where it is looked into how the BESS can assist each individual consumer behind their individual meter ($\delta^{joint} = 0$). Case 3.X depicts where the BESS is connected to consumer X ($\delta_X = 1, \delta_{b \neq X} = 0 \forall b \in B$). The BESS can assist in storing electricity to perform peak-shaving or load-shifting without extra costs only for consumer X.

4. Results and discussion

With the RHC optimization algorithm, the BESS can be operated to consider the short-term costs of operation, and the long-term effects of for instance peak-shaving. Based on the case depicting the location of the BESS, the value the BESS can offer to peak-shaving and load shifting changes. The performance of the three cases are presented in Table 1. The results show that the RHC model successfully manages to reduce total system costs and power peaks by considering the uncertainty of high power peaks even in the early stages of the SH.

With s-BESS, total system power peaks are reduced by 17.8%, while individual BESS power peaks are reduced by 0.4 – 12.4% compared to having no battery. This shows that s-BESS reduces the power peaks with 6.2 – 17.5% compared to individual batteries, resulting in a cost reduction of 19.2% and 13.9–18.3% compared to no battery and individual batteries respectively. The cost reduction obtained here supports the results displayed in References [8, 9], finding the s-BESS beneficial for the community. In addition, the findings show that the s-BESS promote cost reduction for buildings with different production profiles and an MP grid tariff.

The system still experiences such high power peaks with individual batteries, because only one consumer will benefit from the peak shaving effect of battery operation. This causes one consumer's reduced power peaks to possibly have little effect on total system peak reduction, if the consumers experience coinciding peak hours. While the RHC model optimises the total system costs, case 3 highlights that for the consumers without an integrated BESS, there are no incentives for importing power from the local battery rather than the grid as costs will be exactly the same. Case 1 shows that even with low PV-production, there is great potential for consumer cost reductions with joint metering and s-BESS as well as reduced system power peaks which in turn will benefit the DSOs. Even though this configuration is not in line with current Norwegian regulations, the results indicate that the introduction of means such as local grid tariffs or a local energy or flexibility market to get closer to the realisation of case 1, should be of interest.

Table 1: Total cost and peak power for the 3(5) cases.

	Case 1			Case 2			Case 3.1			Case 3.2			Case 3.3		
Total Peak [kW]	769			936			910			932			820		
Total Cost [EUR]	14 927.6			18 463.8			18 091.4			18 260.5			17 337.0		
Buildings	1	2	3	1	2	3	1	2	3	1	2	3	1	2	3
Building Peak [kW]	270	96	617	270	96	617	228	96	617	270	72	617	270	96	479

5. Conclusion

This paper presents a receding horizon control (RHC) model for optimal battery operation to minimise total system costs under a measured peak (MP) grid tariff. The MP tariff incentivises the reduction of power peaks to reduce costs, which is enabled by battery operation.

The RHC model is applied to a realistic case study in Norway to find the optimal placement of a 500kWh battery in an urban area. The case study shows that a shared battery energy storage system (s-BESS) can reduce total system costs by up to 17.8% and allow consumers to reduce their costs by not having to import all their power from the grid. s-BESS also reduce total power peaks more effectively than individually owned batteries, making the case for s-BESS for commercial buildings with varying consumption and production profiles.

An s-BESS where there is a free float of power behind the meter, is clearly the most energy efficient and monetary beneficial solution. However, as this is not in line with current Norwegian regulations, one should look at other shared storage solutions. As power peak and total system costs were significantly reduced, one can conclude that there are incentives for other solutions. Further work should investigate solutions such as implementing local grid tariffs or local energy and flexibility markets for s-BESS.

References

- [1] C. Jankowiak, A. Zacharopoulos, C. Brandoni, P. Keatley, P. MacArtain, and N. Hewitt, "Assessing the benefits of decentralised residential batteries for load peak shaving," *Journal of Energy Storage*, vol. 32, p. 101779, 2020.
- [2] A. Walker and S. Kwon, "Analysis on impact of shared energy storage in residential community: Individual versus shared energy storage," *Applied Energy*, vol. 282, p. 116172, 1 2021.
- [3] F. Boulaire, A. Narimani, J. Bell, R. Drogemuller, D. Vine, L. Buys, and G. Walker, "Benefit assessment of battery plus solar for customers and the grid," *Energy Strategy Reviews*, vol. 26, p. 100372, 11 2019.
- [4] P. H. Tiemann, A. Bensmann, V. Stuke, and R. Hanke-Rauschenbach, "Electrical energy storage for industrial grid fee reduction – a large scale analysis," *Energy Conversion and Management*, vol. 208, p. 112539, 3 2020.
- [5] C. J. Meinrenken and A. Mehmani, "Concurrent optimization of thermal and electric storage in commercial buildings to reduce operating cost and demand peaks under time-of-use tariffs," *Applied Energy*, vol. 254, 11 2019.
- [6] F. Berglund, S. Zaferanlouei, M. Korpås, and K. Uhlen, "Optimal operation of battery storage for a subscribed capacity-based power tariff prosumer—a norwegian case study," *Energies*, vol. 12, p. 4450, 2019.
- [7] S. B. Sepúlveda-Mora and S. Hegedus, "Making the case for time-of-use electric rates to boost the value of battery storage in commercial buildings with grid connected pv systems," *Energy*, vol. 218, p. 119447, 12 2020.
- [8] K. Rahbar, M. R. Vedady Moghadam, S. K. Panda, and T. Reindl, "Shared energy storage management for renewable energy integration in smart grid," in *2016 IEEE Power Energy Society Innovative Smart Grid Technologies Conference (ISGT)*, 2016, pp. 1–5.
- [9] E. Oh and S. Son, "Shared electrical energy storage service model and strategy for apartment-type factory buildings," *IEEE Access*, vol. 7, pp. 130 340–130 351, 2019.
- [10] NVE, "Norwegian energy regulatory authority, individuell måling." [Online]. Available: <https://www.nve.no/reguleringsmyndigheten/nettjenester/nettleie/individuell-maling/>
- [11] A. B. Forough and R. Roshandel, "Multi objective receding horizon optimization for optimal scheduling of hybrid renewable energy system," *Energy and Buildings*, vol. 150, pp. 583–597, 9 2017.

